Spring 3-4-2013

Batf3-Deficient Mice: Susceptibility to Toxoplasma gondii and Responses to IL-12 Treatment in vivo

Mona Mashayekhi
Washington University in St. Louis

WASHINGTON UNIVERSITY IN ST. LOUIS

Division of Biology and Biomedical Sciences

Immunology

Dissertation Examination Committee:
Kenneth Murphy, Chair
Brian Edelson
Robert Schreiber
Laurence Sibley
Herbert Virgin
Wayne Yokoyama

Batf3-Deficient Mice: Susceptibility to *Toxoplasma gondii* and Responses to IL-12 Treatment *in vivo*

by

Mona Mashayekhi

A dissertation presented to the
Graduate School of Arts and Sciences
of Washington University in
partial fulfillment of the
requirements for the degree
of Doctor of Philosophy

May 2013

St. Louis, Missouri

TABLE OF CONTENTS

LIST OF FIGURES

LIST OF ABBREVIATIONS

AIDS	Acquired Immuno-Deficiency Syndrome
AP-1	Activator Protein 1
APC	Antigen Presenting Cell
BATF	Basic Leucine Zipper Transcription Factor, ATF-like
BM	Bone Marrow
BMM	Bone Marrow-Derived Macrophages
CCL	Chemokine (C-C motif) Ligand
CCR	Chemokine (C-C motif) Receptor
CD	Cluster of Differentiation
cDC	Conventional Dendritic Cell
CFDA-SE	Carboxy-Fluorescein diacetate Succinimyidyl Ester
CFSE	Carboxy-Fluorescein Succinimyidyl Ester
CLEC9A	C-Type Lectin Domain Family 9A
CTL	Cytotoxic T Lymphocyte
CX3CR1	CX3C Chemokine Receptor 1
DC	Dendritic Cell
DT	Diphtheria Toxin
DTR	Diphtheria Toxin Receptor
ER	Endoplasmic Reticulum
FACS	Fluorescence Activated Cell Sorting
Flt3L	Fms-related Tyrosine Kinase 3 Ligand

GCET2	Germinal Center B-Cell Expressed Transcript 2
GFP	Green Fluorescence Protein
GM-CSF	Granulocyte Macrophage Colony-Stimulating Factor
ICS	Intracellular Cytokine Staining
IDO	Indoleamine Dioxygenase
IFNγ	Interferon gamma
IL	Interleukin
IL-12p35	IL-12 subunit p35
IL-12p40	IL-12 subunit p40
IL-12R	Interleukin 12 Receptor
IL-23p19	IL-23 subunit p19
iNOS	Inducible Nitric Oxide Synthase
IP	Intraperitoenal
IRF	Interferon Regulator Factor
IRG	Immunity-Related GTPases
IRGM3	Interferon-Gamma-Inducible GTPase
IV	Intravenous
L. monocytogenes	Listeria monocytogenes
LOD	Low Density
LysM	Lysozyme M
MHC	Major Histocompatibility Complex
MHCI	Major Histocompatiblity Complex Class I

MHCII	Major Histocompatibility Complex Class II
MyD88	Myeloid Differentation Primary Response Gene 88
NF-κB	Nuclear Factor Kappa-B
NK	Natural Killer
NO	Nitric Oxide
OVA	Ovalbumin
pDC	Plasmacytoid Dendritic Cell
PEC	Peritoneal Exudate Cell
PRU	Prugniaud
PV	Parasitophorous Vacuole
RAG	Recombination Activating Gene
RAC	Ras-Related C3 Botulinum Toxin Substrate
SCID	Severe Combined Immunodeficiency
SIRPα	Signal-Regulatory Protein Alpha
STAg	Soluble Tachyzoite Antigen
STAT	Signal Transducer and Activator of Transcription
T. gondii	Toxoplasma gondii
TAP	Transporter Associated with Antigen Processing
Th1	T Helper Cell 1
Th17	T Helper Cell 17
TLR	Toll-like Receptor
TNF	Tumor Necrosis Factor

ACKNOWLEDGEMENTS

I would like to thank many people for their contribution to this work and to my development as a scientist. First and foremost, I would like to thank Ken Murphy for teaching me new ways to think and ask questions over the last four years. Ken's ability to approach problems from various angles and overcome obstacles is awe-inspiring. I would also like to thank Theresa Murphy, who has been a second mentor and a friend, and is never frustrated by my daily barrage of questions. I would like to thank our collaborator David Sibley, who adopted me into his lab without hesitation, was extremely generous with reagents, and was an incredible mentor over the last two years.

I am extremely grateful for my colleagues in both the Murphy and the Sibley lab. They have inspired and supported me, and offered a helping hand or a shoulder to lean on throughout my graduate career. Michelle Sandau, Jennifer Gill, and Ellen Langer were always there to listen, give advice, critique, collaborate, and entertain me, and have truly made my time in lab memorable. I would also like to thank Brian Edelson, Wumesh KC, Ansu Satpathy, and Roxane Tussiwand for a number of collaborative efforts, without which this work would not have been completed. I would like to thank the entire Sibley lab for taking me in as one of their own, and helping me at every step along the way. I would especially like to thank Asis Khan for teaching me everything I know about *Toxoplasma gondii*.

In addition, I would like to thank my thesis committee for their continuous support and guidance: Dr. Wayne Yokoyama (Chair), Dr. Robert Schreiber, Dr. Herbert W. Virgin, Dr. Laurence David Sibley, Dr. Brian Edelson, and Dr. Deborah Lenschow.

I would also like to acknowledge the grants that funded this work: the National Research Science Award for the Medical Scientist through the NIH Institutional Research Training Grant, the Principles in Pulmonary Research Award through the NIH Institutional Research Training Grant, and the American Heart Association Midwest Affiliate Predoctoral Fellowship.

Finally, I would like to thank my friends and family for their continuing support through my endless graduate career: my mother, who always knows what to say; my best friend Nicole Maloney, who has been my companion and my other half throughout this journey; and my husband Gary, who puts up with me through my highs and lows and reminds me of the joys in life.

ABSTRACT OF THE DISSERTATION

Batf3-Deficient Mice: Susceptibility to *Toxoplasma gondii* and Responses to IL-12 Treatment *in vivo*

by

Mona Mashayekhi

Doctor of Philosophy in Biology and Biomedical Sciences

Immunology

Washington University in St. Louis, 2013

Professor Kenneth Murphy, Chairperson

CD8α^+ dendritic cells are important *in vivo* for cross-presentation of antigens derived from intracellular pathogens and tumors. Additionally, stimulation of IL-12 production by CD8α^+ DCs has suggested a role for these cells in response to *Toxoplasma gondii* antigens, although no experiments have yet shown an *in vivo* requirement for these cells against *T. gondii* infection. Towards this goal, we examined *T. gondii* infection of *Batf3*$^{-/-}$ mice, which selectively lack only lymphoid-resident CD8α^+ DCs and related peripheral CD103$^+$ DCs. *Batf3*$^{-/-}$ mice were extremely susceptible to *T. gondii* infection, with defective priming of CD8$^+$ T cells, and decreased production of IL-12 and IFNγ. IL-12 administration restored resistance in *Batf3*$^{-/-}$ mice, and mice in which IL-12 production was ablated only from CD8α^+ DCs failed to control infection. These results reveal that the function of CD8α^+ DCs extends beyond a role in cross-presentation and includes a critical role for activation of innate immunity through IL-12 production during *T. gondii*

infection.

While investigating the immune responses of *Batf3*$^{-/-}$ mice to *T. gondii* infection, we made the surprising discovery that IL-12 treatment of infected *Batf3*$^{-/-}$ mice resulted in re-appearance of the CD8α^+ DC population in the spleen. In addition, we show that IL-12-treatment alone in the absence of infection restored the CD8α^+ DC population in *Batf3*$^{-/-}$ mice. Analysis of the restored cells by microarray revealed very few differences in gene expression between wild-type and IL-12-induced *Batf3*$^{-/-}$ CD8α^+ DCs. Furthermore, IL-12 treatment of *Batf3*$^{-/-}$ mice restored their capacity for *in vivo* cross-presentation of necrotic cell-associated antigens. Finally, the restored CD8α^+ DCs primed CD8$^+$ T cells against *T. gondii*-derived antigen, and produced IL-12 *in vivo* in response to *T. gondii* infection. Thus, IL-12 can induce development of CD8α^+ DCs through a *Batf3*-independent mechanism, and these cells can function to both prime T cells as well as produce IL-12 during infection *in vivo*.

CHAPTER 1

Introduction

The innate immune response is the first line of defense against pathogens. Innate immune cells arrive first at the site of infection, limit immediate pathogen replication, and recruit other immune cells to mount an effective response. In addition, these cells have the crucial role of initiating and skewing the adaptive immune response, which is necessary in most cases for final elimination of the pathogen from the host. Dendritic cells (DCs) are antigen-presenting cells (APCs) of the innate immune system that serve the crucial function of activating T cells of the adaptive immune system.

Antigen presentation

The two main subsets of T cells, $CD4^+$ and $CD8^+$ T cells, are activated in different ways. $CD8^+$ T cells are traditionally thought to respond to endogenous antigens within the cytosol, such as viral proteins in an infected cell. These antigens are presented by DCs via the major histocompatibility complex class I (MHCI) pathway, in which antigens from the cytoplasm are degraded by the proteosome and transported into the ER by the TAP1/2 proteins and chaperones. Within the ER, peptides are loaded onto MHCI, and the MHCI:peptide complex is transported to the plasma membrane for $CD8^+$ T cell recognition.

Exogenous antigens, on the other hand, are processed through the MHC class II (MHCII) pathway and presented to $CD4^+$ T cells. In this pathway, exogenous antigens

such as extracellular bacteria are phagocytosed, sequentially processed within phagosomes into smaller peptide fragments, and loaded onto MHCII within the vesicle and transported to the surface.

Cross-presentation is the process by which exogenous antigens are presented to $CD8^+$ T cells on MHCI molecules. Although the precise mechanism is not yet known, cross-presentation is thought to require the transport of exogenous antigens from within phagosomes into the cytoplasm, followed by degradation of these antigens by the proteosome, and transport into the ER by TAP (Norbury et al., 1997; Vyas et al., 2008). Cross-presentation is thought to be important in inducing a robust $CD8^+$ T cell response when endogenous antigens are not produced in the professional antigen presenting cells: DCs, macrophages, and B cells. Non-professional APCs are incapable of effectively priming $CD8^+$ T cell responses. For example, viruses that do not directly invade and replicate in DCs fail to generate endogenous cytoplasmic antigens in these cells. Yet DCs are able to prime $CD8^+$ T cell responses to such viruses by phagocytosis of dead cells containing virus particles, export of viral antigens from the phagosomes into the cytoplasm, followed by cross-presentation of these peptides on MHCI (Villadangos and Schnorrer, 2007). Similarly, cross-presentation is also necessary for $CD8^+$ T cell priming to tumors (Huang et al., 1994).

Dendritic cell subsets in the mouse

Dendritic cells are the most efficient antigen presenting cells, and many DC subsets have now been described in both mice and humans, although the distinct

functions of these subsets are still under investigation. Mouse DCs in the spleen can be subdivided into two general groups, the plasmacytoid DCs (pDCs) and the conventional DCs (cDCs) (Satpathy et al., 2011). Plasmacytoid DCs express the cell surface markers CD11c, B220, Siglec-H and Bst2, and are thought to be important for the production of type I IFN during viral infection. Conventional DCs are currently divided into at least three subsets, namely CD8α^+ DCs, CD4$^+$ DCs, and double-negative DCs. Alternatively, the surface marker CD11b can be used to identify the CD4$^+$ DCs. The unique functions of CD4$^+$ DCs and double-negative DCs are not clearly understood, and will not be discussed further here.

CD8α^+ DCs were originally characterized based on the expression of MHCII$^+$, CD11c$^+$, and CD8α^+. A newly described CD8α^+ CX3CR1$^+$ steady-state DC population in the spleen has made it necessary to use additional markers when defining the "classical" CD8α^+ DCs. These markers include the C-type multilectin receptor DEC205 and the integrin CD103 (Bar-On et al., 2010). A unique function in antigen cross-presentation by CD8α^+ DCs, described in detail below, was first proposed by den Haan and colleagues, and has since been the focus of intense study (den Haan et al., 2000). However, there are a number of challenges in studying CD8α^+ DCs, such as their sparse numbers in the spleen, as well as challenges in extrapolating *in vitro*-generated data to the *in vivo* setting.

DCs can be generated from bone marrow *in vitro*, either by culturing in GM-CSF and IL-4 (Inaba et al., 1992), or in Flt3 ligand (Flt3L) (Brasel et al., 2000), although each system has certain limitations. First, GM-CSF-derived DCs have characteristics of inflammatory DCs, and not steady-state populations (Xu et al., 2007). Conversely, Flt3L-

derived DCs are more similar to *in vivo* steady-state populations, and can be divided into CD8α$^+$ and CD4$^+$ equivalent subsets (Naik et al., 2005). However, while these "equivalent" subsets resemble *in vivo* steady-state DCs in many respects, there are a number of discrepancies that make it difficult to reliably extrapolate *in vitro*-generated DC data to *in vivo* DC populations. For example, CD8α$^+$ DC-equivalents from Flt3L cultures were originally described to be as efficient at cross-presentation as their *in vivo*-generated counterparts (Naik et al., 2005). We had difficulty replicating this finding in our hands, and two recent papers have demonstrated that a maturation step is actually required to endow *in vitro*-generated DCs with cross-presentation ability (de Brito et al., 2011; Sathe et al., 2011). Thus, it is unclear if *in vitro*-generated DCs can serve as an accurate model for *in vivo* populations.

Batf3$^{-/-}$ mice as a tool to study CD8α$^+$ DCs

Due to the crucial function of DCs in the immune system, a number of tools have been generated to study these cells, such as mice genetically deficient in specific transcription factors involved in DC development. However, *in vivo* studies of DC subsets have also been limited up to this point, as all knockouts generated thus far exhibit multiple defects in a number of cells types, confounding any *in vivo* findings. For example, the transcription factor *Irf8* is crucial in the development of CD8α$^+$ DCs (Aliberti et al., 2003; Schiavoni et al., 2002), making it an attractive tool to study this subset. Yet the *Irf8*-deficient mice also lack plasmacytoid DCs (Tsujimura et al., 2003), and have reduced numbers of Langerhans cells (Schiavoni et al., 2004). Due to this

complexity, there are many gaps in our knowledge of DC function *in vivo*.

BATF3 is an AP-1 family member transcription factor, expressed almost exclusively in conventional DCs. The *Batf3*-knockout mouse, generated in our lab by Kai Hildner, is specifically deficient in the lymphoid-resident CD8α^+ DCs, and the related peripheral CD103$^+$ DCs, without other abnormalities (Hildner et al., 2008; Edelson et al., 2010). Thus, this mouse is an ideal tool to study the function of CD8α^+ DCs in *in vivo* immune responses where cross-presentation is thought to be important. For example, CD8$^+$ T cell priming to tumors requires DC cross-presentation of tumor antigens (Huang et al., 1994). Accordingly, *Batf3*-deficient mice fail to reject a fibrosarcoma cell line that is rapidly rejected by wild-type animals, highlighting the crucial role of CD8α^+ DCs in priming CD8$^+$ T cell responses to tumor antigen (Hildner et al., 2008). Cross-presentation is also important for initiation of CD8$^+$ T cell responses to intracellular pathogens, as demonstrated by a failure of *Batf3*$^{-/-}$ mice to prime CD8$^+$ T cell responses against West Nile and Sendai viruses *in vivo* (Hildner et al., 2008; Edelson et al., 2010). Thus, we investigated the response of *Batf3*$^{-/-}$ mice to another intracellular pathogen, *Toxoplasma gondii*.

The Apicomplexan Toxoplasma Gondii

The protozoan *Toxoplasma gondii* is a unicellular, obligate intracellular parasite that is the cause of the human and animal disease toxoplasmosis (Laliberte and Carruthers, 2008). The definitive host of *T. gondii* is the cat, wherein the parasite can undergo sexual reproduction. All other mammals can carry *T. gondii* and serve as

intermediate hosts. In humans, *T. gondii* infection is usually asymptomatic and self-limiting, with the actively dividing form of *T. gondii*, the tachyzoites, being cleared by the immune system. Tachyzoites will convert to bradyzoites, or the latent form of *T. gondii*, under pressure from the immune response. Bradyzoites form tissue cysts within the brain and striated muscles, including the heart, where they set up a chronic infection (Laliberte and Carruthers, 2008). These tissue cysts are not eradicated by the immune system or medications, but do not cause disease in healthy individuals because they are maintained in a latent state (Laliberte and Carruthers, 2008). However, individuals with congenital or acquired immunodeficiencies (AIDS, immunosuppression after organ transplantation, etc.), can experience reactivation of the parasite with conversion of bradyzoites to tachyzoites and active replication (Hunter et al., 1994). The most serious consequences of infection in immunocompromised individuals include toxoplasmic encephalitis, toxoplasmic myocarditis, disseminated toxoplasmosis and death. Perinatal infection with *T. gondii* is also a serious and potentially fatal problem, and can lead to significant birth defects ranging from severe mental retardation to ocular disease (Yap et al., 2006).

It is approximated that 25% of the world's population has the chronic (latent) form of *T. gondii*, and toxoplasmosis is the third leading cause of death due to food-born illness in the US (Laliberte and Carruthers, 2008; CDC, 2008). Thus, as a significant human pathogen, there is great interest in understanding *T. gondii* pathogenesis. In addition, there is much to be learned from the interaction between the parasite and the host immune system.

The Mouse Immune Response to Toxoplasma Gondii

The life cycle of *T. gondii* is very similar in humans and mice, and development of distinct acute and chronic phases of infection occurs in both species. In addition, similar immune effector functions are important for control of infection in both humans and mice, making analysis of these mechanisms in the mouse instrumental to understanding human immune responses. Cell-mediated immunity is critical for defense against *T. gondii,* although the precise cells responsible for initiating the protective responses have been difficult to identify. However, it has been clearly demonstrated that several immune effector mechanisms are vital in defense against *T. gondii* infection, including production of IL-12 and IFNγ, recruitment of inflammatory monocytes, and activation of *T. gondii*-specific $CD8^+$ T cells.

First, the effector cytokines IL-12 and IFNγ have been extensively studied in immune responses to *T. gondii*. Mice deficient in either cytokine rapidly succumb to infection by an avirulent strain of the parasite, dying within 9-13 days post infection, while 100% of wild-type animals survive at this dose (data not shown) (Scharton-Kersten et al., 1997a). A number of other cytokines such as TNFα and IL-1β have also been examined, but most have had a limited role in acute responses to this pathogen.

During *T. gondii* immune responses, IL-12 is thought to function exclusively by eliciting production of IFNγ from other cell types, such as NK cells and T cells (Scharton-Kersten et al., 1996). The cellular source of IL-12 has been greatly investigated and debated, as this cytokine is necessary for the initiation of IFNγ-dependent responses, and will be discussed in detail below. IFNγ, on the other hand, activates various cell-

intrinsic anti-parasitic defense pathways within infected cells (for review see (Yap et al., 2006)).

The major protective effects of IFNγ in mice are mediated through a group of genes collectively termed IRGs, or Immunity-Related GTPases (Taylor et al., 2000; Yap et al., 2006; Hunn et al., 2010). The expression of these genes is rapidly induced by IFNγ in all cell types, and the GTPases function by accumulating on the *T. gondii* parasitophorous vacuole (PV), which normally sequesters and protects the parasite within the host cell cytoplasm. The PV becomes ruffled and disrupted by the action of the IRGs, and the parasite is released into the cytoplasm, where it becomes moribund for unknown reasons (Zhao et al., 2009). Outside of the IRG family of proteins, IFNγ also induces NO production in certain cell types, which may function by limiting parasite respiration and replication (Scharton-Kersten et al., 1997b). Finally, the enzyme IDO is induced by IFNγ and depletes cellular tryptophan, which is an essential amino acid. Tryptophan starvation of *T. gondii* by IDO can also limit parasite replication and survival (Pfefferkorn, 1984; Fujigaki et al., 2002; Nagineni et al., 1996).

In addition to a crucial role for effector cytokines in *T. gondii* immune responses, inflammatory monocytes have also been shown to be necessary for defense against this parasite after oral infection (Dunay et al., 2008). $Gr1^{+}F4/80^{+}CCR2^{+}$ inflammatory monocytes are recruited to the site of infection by the chemokine CCL2. Mice deficient in either *Ccr2* or *Ccl2* succumb to oral infection with *T. gondii* due to a failure of inflammatory monocytes to home to the intestinal mucosa. The mechanism by which these monocytes protect the mouse against *T. gondii* is not known. Surprisingly, these

mice display normal serum levels of IFNγ and IL-12, suggesting a parallel but distinct requirement for inflammatory monocytes and effector cytokines (Dunay et al., 2008).

Finally, T cell mediated adaptive immune responses to *T. gondii* are necessary for clearance of the pathogen. SCID mice, in which both $CD4^+$ and $CD8^+$ T cells are absent, fail to control *T. gondii* infection and die after 2 weeks (Scharton-Kersten et al., 1996). The same results are observed in *Rag* knockout animals, which lack both B and T cells. In addition, the loss of $CD8^+$ T cells alone leads to comparable susceptibility, suggesting a crucial role for this cell type in the adaptive immune response to *T. gondii* (Goldszmid et al., 2007). Furthermore, Goldszmid et al. have demonstrated a requirement for the cross-presentation machinery for delivery of *T. gondii* antigens from within the parasite's parasitophorous vacuole into the cytoplasm, where it can enter the MHCI pathway, allowing for recognition of infected cells by $CD8^+$ T cells (Goldszmid et al., 2009).

Interleukin-12

Interleukin-12 (IL-12) is a pro-inflammatory cytokine that was first described as a potent NK-stimulating factor (Kobayashi et al., 1989; Chan et al., 1991). IL-12 has been extensively characterized for its ability to stimulate IFNγ production, and to skew T cell differentiation to the T helper 1 (Th1) pathway (Hsieh et al., 1993; Trinchieri, 2003). In addition, IL-12 regulates $CD8^+$ T cell expansion and contraction during infection (Takemoto et al., 2006; Curtsinger and Mescher, 2010). A number of cells are capable of producing IL-12 in different settings, including neutrophils, macrophages, and dendritic cells, as discussed below. IL-12-induced IFNγ mediates many of the pro-inflammatory

functions of IL-12, including the activation of anti-microbial functions in innate immune cells such as macrophages (Trinchieri, 2003). Thus, IL-12 is a critical cytokine that functions as both a potent stimulator of innate immune defense mechanisms, as well as a bridge between the innate and adaptive immune systems that is crucial in regulating T cell responses.

IL-12 is a heterodimeric protein composed of two chains, p40 and p35. IL-12p35 is expressed at low levels ubiquitously, while IL-12p40 expression is induced after cellular activation. The p40 chain is shared between IL-12 and IL-23, while the p35 chain is exclusive to IL-12. IL-12 is produced in response to toll-like receptor (TLR) engagement by microbial products (Ma and Trinchieri, 2001), and its production can also be enhanced by IFNγ, forming a positive-feedback loop in inflammatory settings (Ma et al., 1996). The IL-12 receptor (IL-12R) is composed of two chains, IL-12Rβ1 and IL-12Rβ2, and receptor engagement leads to activation of signal transducer and activator of transcription 4 (STAT4), and transcription of target genes. IL-12R is mainly expressed on naïve and activated NK cells, and activated Th1 cells (Trinchieri, 2003). Furthermore, IL-12R expression has been detected on dendritic cells, and IL-12 treatment of DCs *in vitro* has been shown to promote activation of the transcription factor NF-κB and prime DCs for both IL-12 production (Grohmann et al., 1998), and IFNγ production (Ohteki et al., 1999), suggesting additional positive-feedback loops. However, the significance of these results has not been determined in physiologic settings *in vivo*.

Potential sources of IL-12 in response to T. gondii infection

As mentioned above, the production of IFNγ in *T. gondii* infection is dependent on IL-12 (Gazzinelli et al., 1993). While a number of studies have identified cells capable of producing IL-12 in response to *T. gondii*, no study to date has unambiguously identified the cellular source of IL-12 in *T. gondii* infection relevant to protection *in vivo*. Several different cells have been proposed to be important sources of IL-12 during *T. gondii* infection, including neutrophils (Bliss et al., 1999; Bliss et al., 2000), macrophages (Gazzinelli et al., 1994; Robben et al., 2004), plasmacytoid dendritic cells (pDC) (Pepper et al., 2008), conventional dendritic cells (Liu et al., 2006), and the subset of conventional dendritic cells expressing CD8α (Reis e Sousa et al., 1997).

Neutrophils have been reported to produce IL-12 *in vitro* in response to *T. gondii* antigens, but it is unlikely that they are required for protective immunity to *T. gondi in vivo.* Neutrophils are rapidly recruited to the peritoneum after intraperitoneal infection with high doses of virulent strains of *T. gondii*, where they co-stain for IL-12 by microscopy (Bliss et al., 1999; Bliss et al., 2000). However, influx of neutrophils is not observed following oral infection with low virulence isolates, mimicking natural routes of infection (Dunay et al., 2008). Initial *in vivo* studies in which neutrophils were depleted using the Ly6C-specific antibody RB6-8C5 suggested a crucial function for neutrophils in protective immunity against *T. gondii* (Sayles and Johnson, 1996; Bliss et al., 2001; Scharton-Kersten et al., 1997b). However, inflammatory monocytes expressing the same marker Ly6C were later identified (Mordue and Sibley, 2003; Serbina and Pamer, 2006), and all studies conducted with RB6-8C5 were confounded by dual elimination of both

neutrophils and inflammatory monocytes. In a more recent study, Dunay et al. depleted only neutrophils *in vivo* using the Ly6G specific monoclonal antibody 1A8, and demonstrated that specific ablation of neutrophils does not increase the susceptibility of mice to *T. gondii* infection or alter serum levels of IL-12 (Dunay et al., 2010). These recent data would argue that neutrophils are less likely to be a critical *in vivo* source of IL-12 that is relevant to protection during *T. gondii* infection.

Several cells other than neutrophils are viable candidates as an important source of IL-12 in providing protective immunity to *T. gondii*, including monocytes and macrophages. Gazzinelli et al. first demonstrated that thioglycolate elicited peritoneal macrophages produce IL-12 in response to *in vitro* stimulation with soluble tachyzoite antigen (STAg) (Gazzinelli et al., 1994). In addition, IL-12 mRNA could be detected in peritoneal exudate cells (PEC) of mice infected with *T. gondii*, although individual cell types from the PEC were not distinguished in this study. Robben et al. further demonstrated that low density (LOD) splenocytes as well as bone marrow-derived macrophages (BMM) were also capable of producing IL-12 in response to *in vitro T. gondii* infection (Robben et al., 2004). These studies demonstrate that activated or *in vitro* derived macrophages can produce IL-12, but do not demonstrate an *in vivo* function for these cells. In a model of oral infection, Dunay et al. demonstrate that $Gr1^+$ inflammatory monocytes that are recruited to the intestine express IL-12 *in vivo* (Dunay et al., 2008), although a functional requirement for IL-12 production by these cells was not demonstrated. Plasmacytoid DCs can also produce IL-12 in response to *in vitro* infection by *T. gondii* (Pepper et al., 2008), although in this study, only *in vitro* generated bone-

marrow derived pDCs were examined, and an *in vivo* requirement for pDCs during *T. gondii* infection was not tested. Thus, while various monocyte, macrophage, and plasmacytoid DC populations can produce IL-12 in response to *T. gondii*, their importance as a source of IL-12 for *in vivo* protection against *T. gondii* infection has not been demonstrated and remains uncertain.

Several studies have suggested that conventional DCs are important as a source of IL-12 in *T. gondii* infection, but these studies do not exclude macrophages or identify the type of DC that might be responsible for protection. One study used a lineage ablation approach in which the Diphtheria toxin (DT) receptor was expressed under control of the *CD11c* gene promoter to ask whether dendritic cells were involved in protection against infection by *T. gondii* (Liu et al., 2006). DT administration in these mice caused the depletion of all CD11c-expressing cells and greatly increased susceptibility to *T. gondii* infection. Enhanced susceptibility was attributed to the depletion of IL-12-producing DCs, but could also result from loss of macrophages, since CD11c-DTR also depletes several subsets of splenic macrophages (Probst et al., 2005). Although transfer of wild-type DCs, but not IL-12-deficient DCs, did rescue susceptibility in DT-treated mice, this rescue does not exclude macrophages as the cell that normally provides protection againt *T. gondii* infection *in vivo*. A recent study used CD11c-Cre and LysM-Cre in an attempt to selectively delete the TLR-adaptor protein MyD88 from DCs and macrophages, respectively (Hou et al., 2011). Deletion of *myd88* by CD11c-Cre was sufficient to decrease early IL-12 production during *T. gondii* infection and led to increased susceptibility, suggesting that IL-12 production by a CD11c-expressing cell was critical

for resistance to *T. gondii* infection. However, as with the study by Liu et al. above, CD11c is expressed by certain macrophage populations, making it difficult to discern unambiguously which cell is protective *in vivo*.

A few studies have addressed the potential function of the CD8α^+ DC subset in resistance to *T. gondii.* Studies of *IRF8*-deficient mice have suggested a role for the CD8α^+ DC subset as a protective source of IL-12 in *T. gondii* infection (Scharton-Kersten et al., 1997a), but such studies are inconclusive because these mice harbor additional defects beyond the loss of CD8α^+ DCs. *IRF8*-deficient mice lack development of both CD8α^+ DCs as well as pDCs (Aliberti et al., 2003; Tsujimura et al., 2003), and additionally have defects in activation of IFNγ-inducible genes (Tamura and Ozato, 2002). Thus, the increased susceptibility of *IRF8*$^{-/-}$ mice to *T. gondii* infection (Scharton-Kersten et al., 1997a) could result from the absence of either CD8α^+ DCs or pDCs, or from a failure of IFNγ-induced effector mechanisms. Consistent with the latter, administration of IL-12 to *IRF8*$^{-/-}$ mice produces only a partial and temporary reduction in susceptibility to *T. gondii* (Scharton-Kersten et al., 1997a). In addition, CD8α^+ DCs are the major source of IL-12 after intravenous administration of STAg (Reis e Sousa et al., 1997), although the relevance of this IL-12 to protection against live *T. gondii* has not been shown. In summary, although several cell types have been shown to be capable of producing IL-12 in response to *T. gondii*, the important cell type required for *in vivo* production of IL-12 after *T. gondii* infection has not been established.

Summary of reported findings

In this study, we used *Batf3*$^{-/-}$ mice (Hildner et al., 2008) that are specifically defective in the generation of the CD8α^{+} dendritic cell subset to address the function of these cells during *T. gondii* infection. *Batf3*$^{-/-}$ mice exhibit defective priming of *T. gondii*-specific CD8^{+} T cells, decreased IL-12 and IFNγ production, and a dramatically increased susceptibility to *T. gondii*. Furthermore, this susceptibility in *Batf3*-deficient mice is reversed by administration of IL-12. Finally, we show that the CD8α^{+} dendritic cells are the only cells within the innate immune system whose IL-12 production is required for resistance to acute *T. gondii* infection.

We also describe a novel function of IL-12 in regulating CD8α^{+} DC development. Administration of IL-12 can rescue the development of CD8α^{+} DCs in *Batf3*$^{-/-}$ mice in an IFNγ-dependent manner. In addition, IL-12 produced endogenously during the course of *T. gondii* infection can also restore CD8α^{+} DCs in *Batf3*$^{-/-}$ mice. Restored CD8α^{+} DCs in *Batf3*$^{-/-}$ mice are capable of producing IL-12 *in vivo* during *T. gondii* infection, and are similar in global gene expression to their wild-type counterparts. Finally, IL-12 treatment of *Batf3*$^{-/-}$ mice restores *in vivo* cross-presentation to necrotic cell-associated antigens, as well as CD8^{+} T cell priming to *T. gondii*-derived antigens, suggesting that restored CD8α^{+} DCs are capable of cross-presentation and priming.

CHAPTER 2

Experimental Procedures

Mice. Wild-type 129S6/SvEv, BALB/c, C57BL/6, and B6.SJL mice were originally purchased from Taconic and then bred in-house for experimental use. C57BL/6 *Rag2*$^{-/-}$ mice were purchased from Taconic. *IL-12p35*$^{-/-}$ mice were purchased from Jackson Labs on both C57BL/6 and BALB/c backgrounds. Additional experimental C57BL/6 and B6.SJL mice were also purchased from Jackson Labs. Some experiments on the BALB/c background were done using C.Cg-*Foxp3*^{tm2Tch}/J purchased from Jackson Labs that express an IRES-EGFP downstream of the *Foxp3* gene; these mice were used as wild-type controls. *Batf3*$^{-/-}$ mice were previously generated in our laboratory (Hildner et al., 2008) on a 129S6/SvEv background, and subsequently backcrossed for 10 generations onto both C57BL/6 and BALB/c backgrounds. The following mouse was obtained through the NIAID Exchange Program, NIH: C57BL6-*Tg(OT-I)-RAG1*^{tm1Mom} 004175 (Mombaerts et al., 1992; Hogquist et al., 1994). *Kb*$^{-/-}$ *x Db*$^{-/-}$ *x β2-m*$^{-/-}$ mice (C57/BL6 background) were a gift from Herbert W. Virgin and Ted Hansen, Washington University, St. Louis (Lybarger et al., 2003).

Mice were age and sex-matched for each experiment, and were generally between 8-15 weeks old. All mice were maintained under specific-pathogen-free conditions according to institutional guidelines and with protocols approved by the Animal Studies Committee of Washington University.

Parasites and infections. The type II Prugniaud strain of *T. gondii* expressing a firefly luciferase and GFP transgene (PRU-FLuc-GFP) (provided by J. Boothroyd, Stanford University, Palo Alto, CA) was used in all tachyzoite experiments. The parasites were grown in culture in human foreskin fibroblasts as previously described (Robben et al., 2004). For infections, freshly egressed parasites were filtered, counted, and injected intraperitoneally into mice. C57BL/6, 129S6/SvEv, and BALB/c mice were infected with 100, 200, and 1,000 tachyzoites, respectively, for most experiments. BALB/c mice used for tetramer studies were infected with 5,000 tachyzoites. BALB/c bone marrow chimeras and controls were infected with 100 tachyzoites.

For oral infection of mice, both the PRU-FLuc-GFP strain and the type II ME49 strain of *T. gondii* expressing a firefly luciferase transgene (ME49-FLuc) (provided by Laura Knoll, University of Wisconsin, Madison, WI) were used. Outbred CD1 mice (Charles River Laboratories, Wilmington, MA) were infected ip with either 1,000 tachyzoites or 5-10 tissue cysts, and used as the source of tissue cysts for experiments 1-3 months after inoculation. To harvest cysts, animals were sacrificed, and the brains were removed and homogenized in 1mL of phosphate buffered saline (PBS). After counting, 5 ME49-FLuc cysts or 20 PRU-FLuc-GFP cysts were administered to experimental animals via oral gavage.

Luciferase imaging. Imaging was done as previously described (Saeij et al., 2005). Briefly, mice were given intraperitoneal injections of D-Luciferin (Biosynth AG, Switzerland) at 150mg/kg and allowed to remain active for 5 minutes. Animals were then

anesthetized with 2% isoflurane for 5 minutes, and then imaged using a Xenogen IVIS 200 machine (Caliper Life Sciences). Data was analyzed using the Living Image software (Caliper Life Sciences).

Histology. Mice were sacrificed on day 9 after infection, the spleen and ileum were harvested and fixed in 10% neutral buffered formalin. Tissues were dehydrates in ethanol, embedded in paraffin, and 5μm sections were stained with hematoxylin and eosin (H&E).

***In vitro* T cell re-stimulation**. 4 X 10^6 splenocytes from day 8 infected mice were incubated overnight in 100μL cIMDM with 100μg/mL GRA4 peptide (SPMNGGYYM). Brefeldin A at 1 μg/mL was added during the last 4 hours of incubation. Cells were then harvested and analyzed for IFNγ production using the intracellular cytokine staining protocol described above.

T cell transfer into *Rag*$^{-/-}$ mice. Wild-type T cells were purified using Miltenyi Thy1.2 microbeads and an LS cell separation column according to the manufacturer's protocol. 10 X 10^6 T cells were adoptively transferred into recipient animals one day prior to infection.

ELISA/CBA. IL-12p40 levels were measured from serum samples using the Mouse IL-12p40 OptEIA ELISA set (BD Bioscience). IFNγ serum levels were measured using the

BD CBA Mouse Inflammation Kit (BD Biosciences).

Cell preparation. For all experiments except tetramer analysis, spleens were digested in 5mL Iscove's Modified Dulbecco's Media (IMDM, Invitrogen) containing 10% fetal calf serum (HyClone) with 250μg/mL collagenase B (Roche) and 30 U/mL DNase I (Sigma-Aldrich) for 1 hour at 37 degrees with agitation using stir-bars. For experiments analyzing intracellular cytokines, brefeldin A was added at 1 μg/mL during collagenase B and DNase I treatment, after which the cells were incubated for an additional 3 hours in IMDM with brefeldin A. Red blood cells were lysed by incubation in ACK lysis buffer. Cells were filtered through 80-μm strainers and counted on an analyzer (Vi-CELL, Beckman Coulter). 1-5 X 10^6 cells were stained for flow cytometric analysis.

For T cell analysis using tetramers, spleens were disrupted in 2mL ACK lysis buffer, filtered through 80-μm strainers and counted on a Vi-CELL analyzer. 1-3 X 10^6 cells were stained for flow cytometric analysis.

For analysis of peritoneal cells, a peritoneal lavage was performed with 10mL Dulbecco's PBS (DPBS). Harvested cells were incubated in ACK buffer to lyse red blood cells, filtered, counted, and stained for flow cytometry.

Flow cytometry. Cells were incubated for 5 minutes at 4 degrees with Fc Block (clone 2.4G2, BD) in FACS buffer (DPBS + 0.5% BSA + 2mM EDTA). Dead cells were excluded using LIVE/DEAD Aqua Fixable Dead Cell Stain Kit (Invitrogen). Surface staining was done for 20 minutes at 4 degrees in FACS buffer. For tetramer staining, cells

were incubated in the presence of tetramer and surface antibodies for 45 minutes at 4 degrees. Absolute cell numbers were calculated using the total cell count multiplied successively by the percentages for the appropriate gates obtained through flow cytometry. Cells were analyzed on a BD FACSCantoII flow cytometer and data analyzed using FlowJo software (Tree star, Inc.).

Intracellular Cytokine Staining. For intracellular cytokine staining, cells were first surface stained, then fixed in 2% paraformaldehyde for 15 minutes at room temperature. Cells were then re-suspended in permeabilization buffer (DPBS + 0.1% BSA + 0.5% saponin) and stained with anti-IL-12p40 or anti-IFNγ for 30 minutes at 4 degrees.

Administration of IL-12. Recombinant murine IL-12 (Peprotech) was resuspended in pyrogen-free saline at a concentration of 2.5μg/mL, aliquoted and frozen at -80 degrees. For all *T. gondii* experiments, mice were injected ip with 0.5μg of IL-12 on days 0, 1, 2, 3, and 4 after infection. For all other experiments, mice were injected ip with 0.5μg of IL-12 either 3 times (days 0, 1, 2) or 1 time only (day 0), as specified in figure legends.

***In vitro* NK cell culture.** Splenocytes were incubated in 10ng/mL IL-12 and 50ng/mL IL-18 for 4 hours, with 1μg/mL brefeldin A added in for the last 3 hours. NK cells were identified using DX5 antibody, and stained for intracellular IFNγ.

BM Chimera generation. This experiment was performed once on mice on the C57BL/6

background, and once on mice on the BALB/c background. Bone marrow from femurs and tibias were harvested, red blood cells lysed in ACK lysis buffer, filtered through 80-μm strainers, and counted using the Vi-CELL analyzer (Vi-CELL, Beckman Coulter). Recipient mice were irradiated with 800 (BALB/c) or 1,200 (C57BL/6) rads of whole body irradiation. In the experiment using C57BL/6 mice, all recipients were WT C57BL/6 or B6.SJL. In the experiment using BALB/c mice, WT recipients were used for the WT donor BM condition, while *Batf3*$^{-/-}$ recipients were used for the *Batf*$^{-/-}$, WT + *Batf3*$^{-/-}$, and *IL-12p35*$^{-/-}$ + *Batf3*$^{-/-}$ donor BM conditions. The following day after irradiation, the recipients were injected intravenously with 2-4 million bone marrow cells from either a single donor or a 1:1 mixture from two donors. Mice were allowed to re-constitute for 10 (C57BL/6) to 18 (BALB/c) weeks after transfer, and subsequently bled to determine chimerism. In experiments using C57BL/6 mice, the congenic markers CD45.1 and CD45.2 were used to determine percent chimerism using flow cytometry. In experiments using BALB/c mice, male/female donors were mixed to allow for analysis of chimerism using the Y-chromosome. Peripheral blood from chimeras was lysed for genomic DNA and analyzed by quantitative real time PCR for the presence of the gene Zfy1 on the Y chromosome using the following primers: *Zfy1* (encoding zinc finger protein 1) Zfy1-forward, 5'-GCGTATCCTCATAAATGTGAC-3', and Zfy1-reverse, 5'-CATCTCTTACACTTGAATGG-3'. *Rag2* (encoding recombination activation gene 2) was used as a normalization control, Rag2-forward, 5'-GGGAGGACACTCACTTGCCAGTA-3', and Rag2-reverse, 5'-AGTCAGGAGTCTCCATCTCACTGA-3'.

***In vivo* blockade of IFNγ.** IFNγ-blocking antibody H22, and control antibody PIP were kindly provided by Robert Schreiber. For experiments performed with administration of IL-12, 250μg of PIP or H22 were administered ip on days -2 and +1, and 0.5μg of IL-12 was administered ip in a single dose on day 0. Mice were harvested for analysis on day 3.

For experiments performed with *T. gondii* infection, 250μg of PIP or H22 were administered ip on days -1 and +2. Mice were infected on day 0, and harvested on day 7 for analysis.

***In vivo* depletion of NK cells.** Anti-NK1.1 depleting antibody PK136, and control antibody MAR were kindly provided by Wayne Yokoyama. To deplete NK cells, 200μg of MAR or PK136 were administered ip on day -3, followed by 100μg or MAR or PK136 as a second dose on day 0. Mice were also given 0.5μg of IL-12 on day 0, and harvested for analysis on day 3. Depletion of NK cells on the day of harvest was confirmed using DX5 and NKp46 antibodies.

Microarray. For gene expression analysis $CD8\alpha^+$ DCs were isolated to greater than 99% purity from spleens using a FACSAria II (BD). $CD8\alpha^+$ DCs were identified as $MHCII^+$ $CD11c^+$ $B220^-$ $CD24^+$ $SIRP\alpha^-$ $CD8\alpha^+$ $DEC205^+$ cells. Total RNA was prepared with the RNAqueous-Micro Kit (Ambion). RNA was labeled using the 3' IVT Express Kit (Affymetrix), and the GeneChip Mouse Genome 430 2.0 Array (Affymetrix) was used as the platform. Expression data was analyzed using ArrayStar Software (DNASTAR).

***In vivo* cross-presentation assay.** The *in vivo* cross-presentation assay was previously described in detail (den Haan et al., 2000). Briefly, OT-I-Tg $CD8^+$ T cells were purified from OT-I-Tg *Rag1*$^{-/-}$ CD45.1 mice by positive selection using CD90.2 beads according to the manufacturer's protocol. The purity of the T cell population was >99%. T cells were labeled with CFSE (Sigma-Aldrich) by incubation with 1 μM CFSE for 9 min at RT at a density of 2 X 10^7/mL. Subsequently cells were incubated with an equal volume of FCS and washed 2X with media containing 10% FCS. Cells were washed 2X with PBS, and 2 X 10^5- 1 X 10^6 cells were injected ip into recipient mice.

Splenocytes from *Kb*$^{-/-}$ *x Db*$^{-/-}$ *x β2-m*$^{-/-}$ mice (gift from Herbert W. Virgin and Ted Hansen) were prepared in serum-free medium, and loaded with 10mg/mL ovalbumin (Calbiochem) by osmotic shock. 2.5 X 10^7 cells were incubated in 170μl of hypertonic medium (0.5M sucrose, 10% wt/vol polyethylene glycol 1000, and 10mM Hepes in RPMI 1640, pH 7.2) alone or in the presence of 10mg/mL ovalbumin for 10 minutes at 37 degrees. 2.2 mL of pre-warmed hypotonic medium (40% H2O, 60% RPMI 1640) was added followed by an additional 2 minutes of incubation at 37 degrees. The cells were washed 2X with cold PBS, irradiated at 1,350 rads, and injected IV 3 days after OT-I transfer. Mice were harvested 3 days after administration of antigen, and $CD45.1^+$ OT-I T cells analyzed for CFSE dilution.

Quantitative RT-PCR. For gene expression analysis various cell types were isolated to greater than 99% purity from spleens using a FACSAria II (BD). Total RNA and cDNA were prepared with the RNeasy Micro Kit (Qiagen) and Superscript III reverse

transcriptase (Invitrogen). For real-time PCR, StepOnePlus Real-Time PCR System (Applied Biosystems) was used according to the manufacturer's instructions, using the Quantitation, Standard-Curve method and SYBR Green PCR master mix. PCR conditions were 10 min at 95 °C, followed by 40 two-step cycles consisting of 15 s at 95 °C and 1 min at 60 °C.

For analysis of TLR11 expression, dendritic cells and neutrophils were identified using the following antibodies: PDCA, CD11c, B220, CD4, CD8, GR1 and CD11b. Listed are only the markers for which they express: CD4 DC = $CD11c^+$ $CD4^+$, CD8 DC = $CD11c^+$ $CD8^+$, Plasmacytoid DC = $CD11c^+$ $B220^+$ $PDCA^+$, Neutrophils = $GR1^+$ $CD11b^+$. Lymphoid cells were identified using the following antibodies: CD4, CD8, B220, CD11b and CD11c. Listed are only the markers for which they express: CD4 T cells = $CD4^+$, CD8 T cells = $CD8^+$, B cells = $B220^+$. Monocytes were isolated from bone marrow and expressed CD11b and Ly-6C.

For analysis of IL-23p19, IL-12p35 and IL-12/23p40 subunits, $CD8\alpha^+$ DCs were sorted based on the following markers: $PDCA^-$ $MHCII^+$ $CD11c^+$ $CD8\alpha^+$ $DEC205^+$. As a control, total splenic $CD11c^+$ cells were purified using Miltenyi microbeads to negatively select for cells expressing B220, Thy1.2, and DX5, followed by positive selection using CD11c (done according to the manufacturer's protocol). In addition, RNA was harvested from whole kidney lysate as well as from the macrophage cell line J774 to serve as positive and negative controls.

For analysis of *Batf3*, *Batf*, and *IRF-8*, $CD8\alpha^+$ DCs were sorted based on the following markers: $B220^-$ $CD3^-$ $NKp46^-$ $MHCII^+$ $CD11c^+$ $CD8\alpha^+$ $DEC205^+$. For positive

and negative controls for *Batf*, RNA from WT or *Batf*$^{-/-}$ B cells stimulated with LPS for 1 day was used. For positive and negative controls for *IRF-8*, RNA from *in vitro* cultured CD8α^+ or CD4$^+$ equivalent DCs was used.

Primers used to evaluate relative expression were as follows: *TLR11* (encoding toll-like receptor 11) TLR11-forward, 5'-TGATGTATTCGTGTCCCACTGC-3', and TLR11-reverse, 5'- CCACTCTTTCTCTCCTCTTCCTCG-3'. *IL-23p19* (encoding interleukin 23, alpha subunit p19) IL-23p19-forward, 5'-AGCGGGACATATGAATCTACTAAGAGA-3', and IL-23p19-reverse, 5'-GTCCTAGTAGGGAGGTGTGAAGTTG-3' (Uhlig et al., 2006). *IL-12p35* (encoding interleukin 12A) IL-12p35-forward, 5'-TACTAGAGAGACTTCTTCCACAACAAGAG-3', and IL-12p35-reverse, 5'-TCTGGTACATCTTCAAGTCCTCATAGA-3' (Uhlig et al., 2006). *IL-12/23p40* (encoding interleukin 12B) IL-12/23p40-forward, 5'-GACCATCACTGTCAAAGAGTTTCTAGAT-3', and IL-12/23p40-reverse, 5'-AGGAAAGTCTTGTTTTTGAAATTTTTTAA-3' (Uhlig et al., 2006). *Batf3* (encoding basic leucine zipper transcription factor, ATF-like 3) Batf3-forward, 5'-GCTCAGAGGAGCCGGAAGA-3', and Batf3-reverse, 5'-CTGCGCAGCACAGAGTTCTC-3'. *Batf* (encoding basic leucine zipper transcription factor, ATF-like) Batf-forward, 5'-CGACAGCAGTGACTCCAGCTT-3', and Batf-reverse, 5'-CTCTGAACTTTCCTCACATCATCAG-3'. *Irf8* (encoding interferon regulator factor 8) IRF-8-forward, 5'-TGCCACTGGTGACCGGATAT-3', and IRF-8-reverse, 5'-GACCATCTGGGAGAAAGCTGAA-3'. *Hprt1* (encoding hypoxanthine

guanine phosphoribosyl transferase) was used as a normalization control, HPRT-forward, 5'-TCAGTCAACGGGGGACATAAA-3', and HPRT-reverse, 5'-GGGGCTGTACTGCTTAACCAG-3'.

Antibodies. The following antibodies were purchased from BD: PE-Cy7 anti-CD11b (M1/70); PE-Cy7 anti-CD4 (RM4-5); APC anti-CD3e (145-2C11); PerCP-Cy5.5 anti-CD8a (53-6.7); V450 anti-CD8a (53-6.7); APC anti-CD8a (53-6.7); PE-Cy7 anti-CD8a (53-6.7); PE anti-Thy1.2 (30-H12); V450 anti-Ly-6C (AL-21); APC anti-IFNg (XMG1.2); PE-Cy7 anti-IFNg (XMG1.2); APC anti-IL-12p40/p70 (C15.6); Rat IgG_1, κ APC (R3-34); V450 anti-Gr1 (RB6-8C5)

The following antibodies were purchased from eBioscience: eFluor 450 anti-MHCII I-A/I-E (M5/114.15.2); APC-eFluor 780 anti-CD11c (N418); APC-eFluor 780 anti-CD4; PE-Cy7 anti-B220 (RA3-6B2); APC-eFluor 780 anti-B220 (RA3-6B2); PE anti-CD103 (2E7); eFluor 450 anti-CD317 (PDCA) (eBio927); eFluor 450 anti-CD335 (NKp46) (29A1.4);

The following antibodies were purchased from Miltenyi: PE anti-DEC205 (NLDC-145); APC anti-DEC205 (NLDC-145); PE anti-Ly-6G (1A8)

Statistics. For analyses of survival data the log-rank test was used. For analyses of all other data, an unpaired, two-tailed Student's *t* test with a 95% confidence interval was used (Prism; GraphPad Software, Inc.). All data are represented as means $^{+}$/- SD.

CHAPTER 3

Batf3$^{-/-}$ Mice are Highly Susceptible to *T. gondii* Infection

We first compared the survival of wild-type and *Batf3*$^{-/-}$ mice to infection with *T. gondii* (Fig. 1). Intraperitoneal (ip) infection by tachyzoites of the type II avirulent Prugniaud (Pru) strain of *T. gondii* revealed a significantly increased susceptibility of *Batf3*$^{-/-}$ mice relative to wild-type mice (Fig. 1 A). While wild-type mice were resistant to *T. gondii* infection, infection of *Batf3*$^{-/-}$ mice was uniformly lethal in all genetic backgrounds tested and led to death within 9 to 10 days after infection. Using a *T. gondii* strain harboring a firefly luciferase transgene reporter, we observed approximately 100-fold increased parasite burden within 5 days following infection in *Batf3*-deficient mice compared to wild-type mice (Fig. 1, B and C). This exponential parasite growth continued in the *Batf3*$^{-/-}$ mice throughout the course of infection.

To extend our findings, we challenged wild-type and *Batf3*$^{-/-}$ mice with *T. gondii* cysts by oral gavage, which simulates the natural route of infection. Oral challenge of *Batf3*$^{-/-}$ mice demonstrated a similar susceptibility of these animals to *T. gondii* infection, with acute lethality and a failure to control parasite replication (Fig. 2, A and B). In addition, histological analysis of the spleen and ileum revealed extensive inflammation and destruction of tissue architecture in *Batf3*$^{-/-}$ mice 9 days after infection (Fig. 2 C).

In summary, *Batf3*$^{-/-}$ mice are highly susceptible to *T. gondii* infection compared with wild-type mice using both the ip route of tachyzoite challenge (Fig. 1), as

well as the oral route of tissue cyst challenge (Fig. 2). However, the underlying mechanism following oral challenge is likely to be complex and distinct from the underlying mechanism following tachyzoite challenge, and will be the focus of future studies. Specifically, gut $CD103^{+}$ DCs are also absent in the *Batf3*$^{-/-}$ mice (Edelson et al., 2010), and may play a role during oral challenge where the parasite's initial site of infection and replication is the small intestine. All other experiments in this work were performed following intraperitoneal tachyzoite challenge.

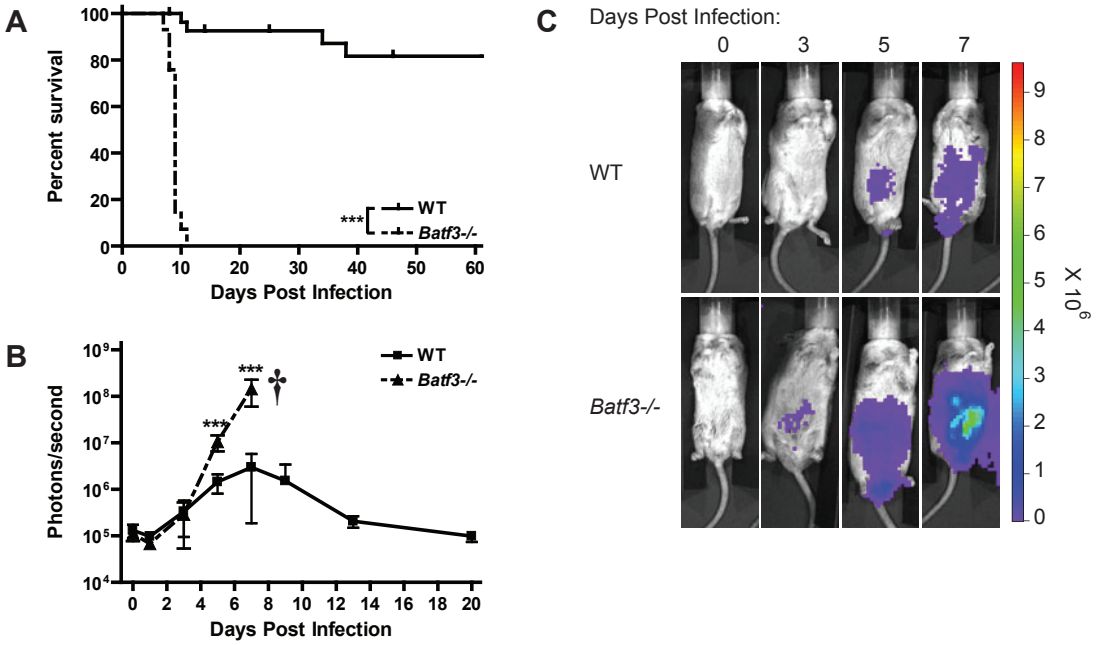

Figure 1. *Batf3*$^{-/-}$ mice rapidly succumb to infection with an avirulent strain of *Toxoplasma gondii*. Mice were infected with *T. gondii* tachyzoites ip, monitored for survival (A) and parasite burden (B and C). (A) Combined survival data from infected C56BL/6, 129S6/SvEV and BALB/c wild-type (solid line, n=30) and *Batf3*$^{-/-}$ (dashed line, n=29) mice from 8 independent experiments. (B) Infected wild-type (squares) and *Batf3*$^{-/-}$ (triangles) mice underwent whole body *in vivo* imaging throughout the course of infection to measure bioluminescence. Data shown is combined parasite burden from infected 129S6/SvEV mice from 2 independent experiments (n=5-8 at each time-point, representative of 6 independent experiments). Data are represented as mean +/- standard deviation. (C) Representative bioluminescence images of infected 129S6/SvEV mice throughout the course of infection. ***: P<0.001.

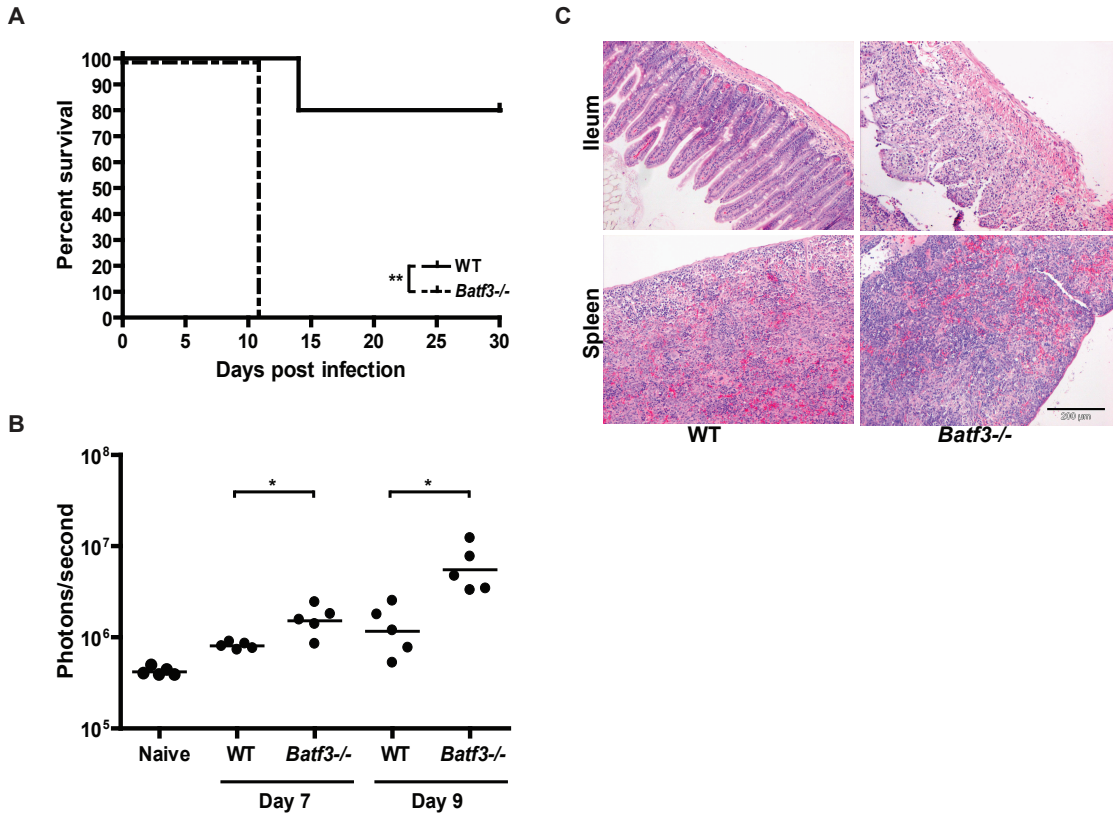

Figure 2. *Batf3*$^{-/-}$ mice are highly susceptible to oral infection with *T. gondii* cysts and cannot control parasite replication. Mice were infected with 5 ME49-FLuc tissue cysts by oral gavage, and monitored for survival (A) and parasite burden (B). (A) BALB/c wild-type (solid line) and *Batf3*$^{-/-}$ (dashed line) mice were monitored for survival over the course of the experiment (n=5, representative of 2 independent experiments). (B) Infected wild-type and *Batf3*$^{-/-}$ mice were monitored by whole body *in vivo* bioluminescence imaging on day 7 and 9 after infection (n=5, representative of 2 independent experiments). Horizontal lines represent the geometric mean. (C) 129S6/SvEV wild-type and *Batf3*$^{-/-}$ mice were infected with 20 PRU-FLuc-GFP tissue cysts and sacrificed on day 9 after infection for H&E analysis of the spleen and ileum. (C) was performed by Ildiko Dunay. *: 0.01<P<0.05, **: 0.001<P<0.01.

CHAPTER 4

CD8α$^+$ DCs are Required for CD8$^+$ T Cell Priming to Endogenous *T. gondii* Antigens

Priming of CD8$^+$ T cells in the acute phase of infection is defective in Batf3$^{-/-}$ mice

CD8$^+$ T cells are required for effective control of *T. gondii* infection (Goldszmid et al., 2007), and priming of CD8$^+$ T cell responses to *T. gondii* requires the unique mechanism of cross-presentation (Goldszmid et al., 2009). In order to determine if CD8$^+$ T cell priming to this parasite is diminished in the absence of the main cross-presenting cells, the CD8α$^+$ DCs, we utilized *T. gondii* specific tetramers (kindly provided by Dr. Hidde Ploegh). Tetramers are a chemically linked group of four MHCI molecules containing specific peptides that are recognized by CD8$^+$ T cells. The tetramers are linked to a fluorescent dye, and used to detect T cells that express a T-cell receptor specifically recognizing the given peptide. We used two MHCI tetramers to measure the expansion of CD8$^+$ T cells specific for peptides derived from the GRA4 and GRA6 dense granule proteins of *T. gondii* (Frickel et al., 2008). Tetramer positive CD8$^+$ T cells were significantly increased 8 days after infection with *T. gondii* in the spleen of wild-type mice, but not in *Batf3*$^{-/-}$ mice (Fig. 3 D). Tetramer staining in the peritoneum suggested a similar trend, although the data did not reach significance due to substantial variability in the observed response in wild-type mice (Fig. 3 A-C). Total splenic CD8$^+$ T cell numbers were comparable between wild-type and *Batf3*$^{-/-}$ mice both before and after infection (Fig. 4 B), consistent with a normal T cell compartment in *Batf3*$^{-/-}$ mice (Hildner et al.,

2008). However, the total number of peritoneal $CD8^+$ T cells appeared to be highest in infected wild-type mice (Fig. 4 A), suggesting local proliferation or recruitment of activated cells, although again this increase did not reach significance as compared to *Batf3*$^{-/-}$ numbers.

In addition, using the GRA4 peptide to activate splenic antigen-specific $CD8^+$ T cells harvested 8 days after infection, we observed a significant increase in peptide induced IFNγ production from wild-type $CD8^+$ T cells, but not from *Batf3*$^{-/-}$ $CD8^+$ T cells (Fig. 3 E). Thus, *Batf3*$^{-/-}$ mice have reduced priming of IFNγ-producing $CD8^+$ T cells after infection by *T. gondii*, suggesting that $CD8\alpha^+$ DCs contribute to the priming of $CD8^+$ T cells against this intracellular pathogen.

Although priming of *T. gondii*-specific $CD8^+$ T cells is reduced in infected *Batf3*$^{-/-}$ mice (Fig. 3), the rapid lethality of *T. gondii* infection in *Batf3*$^{-/-}$ mice suggests a defect in an innate rather than adaptive immune response. To further exclude a role for *Batf3* in T cells in the acute lethality observed, we transferred wild-type purified T cells into *Rag*-deficient mice that were either wild-type or deficient for *Batf3*. *Rag*$^{-/-}$ mice cannot generate T or B cells due to a failure to recombine and express the required receptors, and therefore the only T cells present in these mice will be the transferred wild-type cells. *Batf3/Rag*-double deficient animals that were given wild-type T cells are indistinguishable from *Batf3*$^{-/-}$ mice when examined for parasite burden after *T. gondii* infection (Fig. 5), suggesting that the defect observed in *Batf3*$^{-/-}$ mice is restricted to the innate compartment. Therefore, we next focused on identifying the innate function of $CD8\alpha^+$ DCs necessary for protection against *T. gondii* infection.

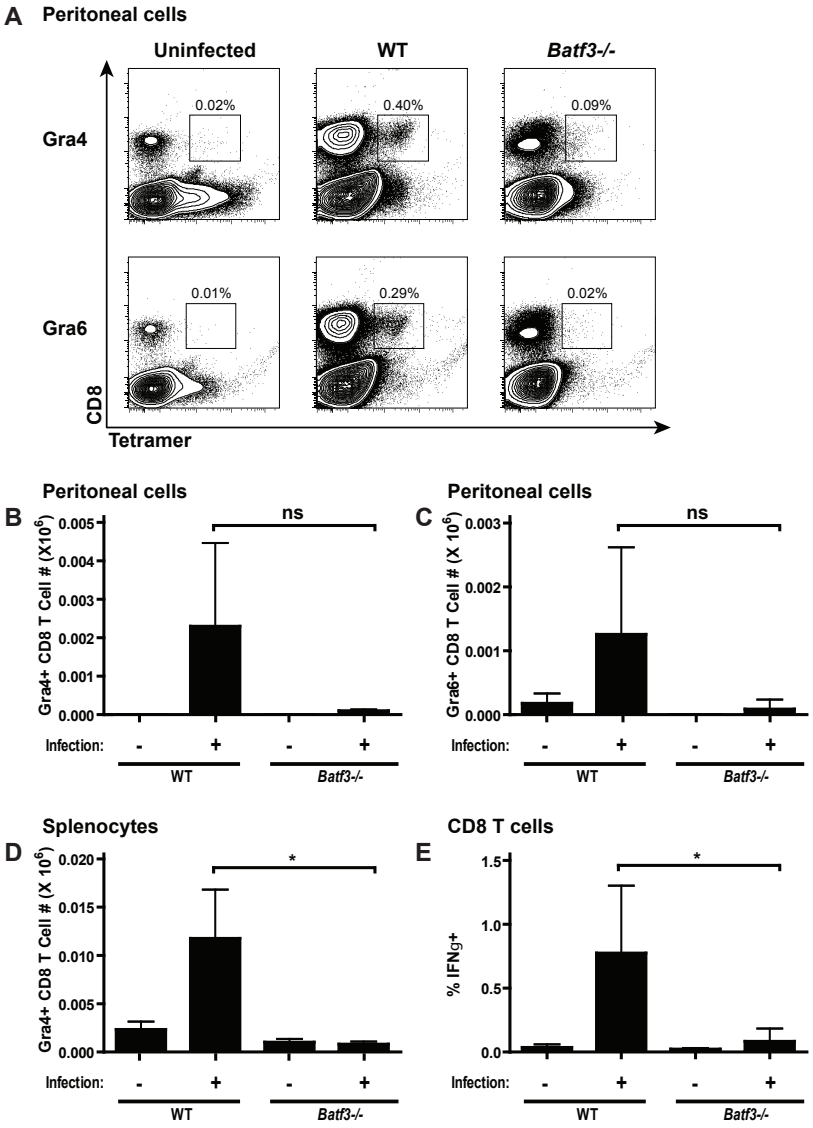

Figure 3. CD8$^+$ T cell priming to *T. gondii* is defective in *Batf3*-deficient mice. BALB/c wild-type and *Batf3*$^{-/-}$ mice were infected with *T. gondii*, sacrificed on day 8 after infection, and analyzed for CD8$^+$ T cell priming by tetramer staining *ex vivo* (A-D) and intracellular cytokine staining following peptide re-stimulation *in vitro* (E). (A) Representative plots of L^d-GRA4 and L^d-GRA6 tetramer staining in the peritoneum, with percentage of total peritoneal cells that are tetramer positive shown. (B-D) Absolute numbers of CD8$^+$ tetramer-positive cells in the peritoneum (B and C) or spleen (D) specific for GRA4 (B and D) or GRA6 (C) on day 8 after infection (n=3, representative of 2 independent experiments). (E) Absolute numbers of IFNγ-positive CD8$^+$ T cells as measured by intracellular cytokine staining after overnight re-stimulation of whole splenocytes with the GRA4 peptide (n=5). (B-E) Data are represented as mean +/- standard deviation. Not significant (ns): P>0.05, *: 0.01<P<0.05.

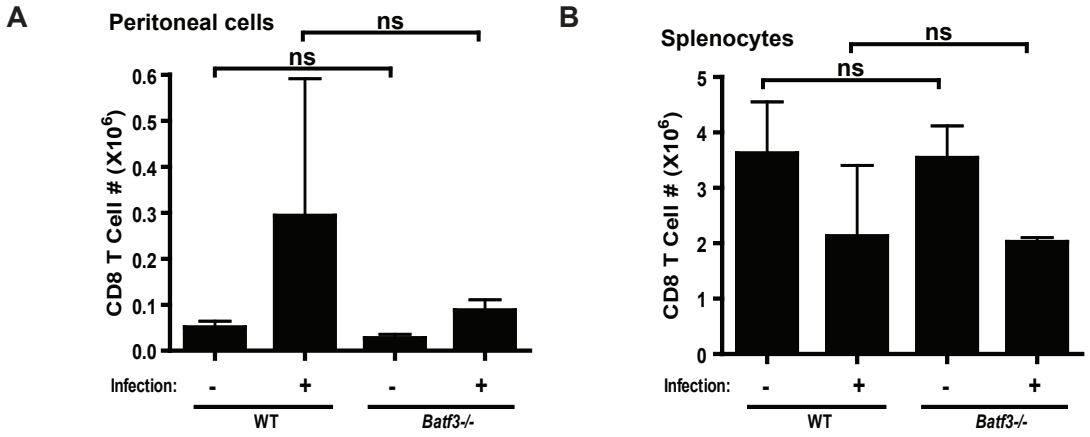

Figure 4. CD8$^+$ T cell compartment is normal in *Batf3*$^{-/-}$ mice. (A and B) BALB/c wild-type and *Batf3*$^{-/-}$ mice were infected with *T. gondii*, sacrificed on day 8 after infection, and analyzed for total numbers of CD8$^+$ T cells in the spleen (B) and peritoneum (A) (n=3). Data are represented as mean +/- standard deviation. Not significant (ns): P>0.05.

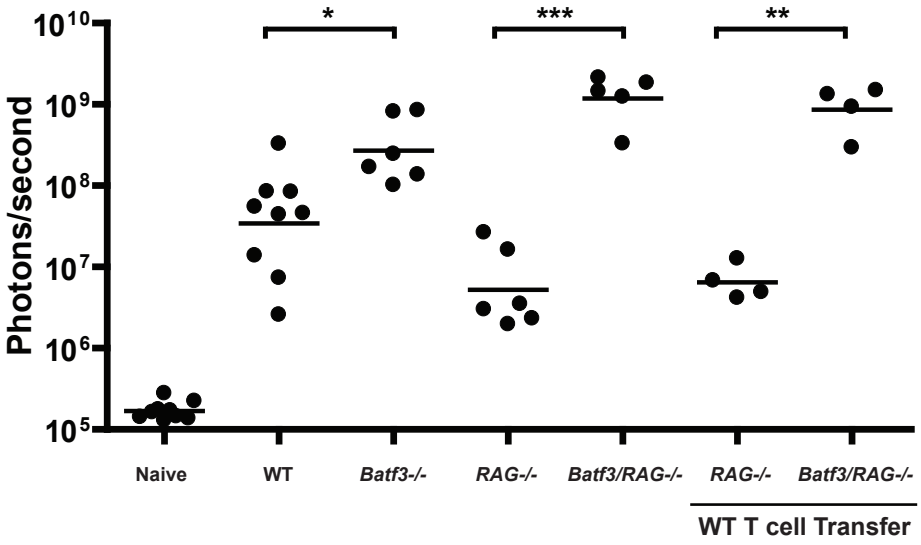

Figure 5. The presence of wild-type T cells in *Batf3*$^{-/-}$ mice does not change their susceptibility to *T. gondii* infection. C57BL/6 wild-type, *Batf3*$^{-/-}$, *Rag*$^{-/-}$, or *Batf3/Rag*$^{-/-}$ mice were infected with *T. gondii* and parasite burden measured by *in vivo* bioluminescence imaging on day 7 or 8 after infection. In two groups, wild-type T cells were adoptively transferred into the recipient mice one day before infection. Horizontal lines represent the geometric mean. *: $0.01<P<0.05$, **: $0.001<P<0.01$, ***: $P<0.001$.

CHAPTER 5

IL-12 Production by CD8α$^+$ DCs is Required for Protection Against Acute *T. gondii* Infection

IL-12 and IFNγ production are defective in T. gondii-infected Batf3$^{-/-}$ mice.

To determine if the crucial effector cytokines IL-12 and IFNγ were being produced normally in *Batf3*$^{-/-}$ mice, we next examined the serum levels of these cytokines. The IL-12 subunit p40, which is shared with the cytokine IL-23, is used as the readout for IL-12 in all cases, since IL-23 plays no role in acute *T. gondii* infection in the mouse (Lieberman et al., 2004). IL-12p40 levels in serum were markedly reduced in *Batf3*$^{-/-}$ mice relative to wild-type mice infected with *T. gondii* (Fig. 6 A). In wild-type mice, serum IL-12p40 began to increase on day 3 after infection, and increased until 7 days after infection. In contrast, IL-12p40 remained at basal levels in *Batf3*$^{-/-}$ mice until day 5 after infection, at which point its increase was significantly reduced relative to wild-type mice for the remainder of infection. The decrease in IL-12p40 production in *Batf3*$^{-/-}$ mice correlated with significantly reduced levels of serum IFNγ (Fig. 6 B). In wild-type mice, IFNγ production began to increase after 4 to 5 days of infection, reaching a peak at day 8. By contrast, IFNγ showed no increase in *Batf3*$^{-/-}$ mice for 5 days after infection, and showed only a slight increase on day 7, when it was significantly reduced relative to wild-type mice.

CD8α$^+$ DCs increase in early infection by T. gondii and are the major producers of IL-12.

In uninfected wild-type mice, the CD8α$^+$ subset of conventional dendritic cells comprises approximately 5-10% of the total DC compartment in the spleen, depending on the mouse strain (Hildner et al., 2008). CD8α$^+$ DCs also express several surface markers such as CD103, CD24 and DEC205 that distinguish it from the newly described CX3CR1$^+$ CD8α$^+$ DC subset that is distinct from classical CD8α$^+$ DCs (Bar-On et al., 2010), and one of these additional markers is used in every experiment to ensure exclusion of the CX3CR1-expressing subset. The remainder of conventional DCs are distributed between those expressing high levels of CD11b, or low levels of CD11b. After infection by *T. gondii*, we observed that the percentage of CD8α$^+$ DCs in wild-type mice increased to represent approximately 20% of the total dendritic cell compartment in the spleen by 7 days after infection (Fig. 7 A). By contrast, *Batf3*$^{-/-}$ mice lacked CD8α$^+$ DCs as previously reported (Hildner et al., 2008) and showed no increase at any time after infection. Beyond this increase in their percentage, CD8α$^+$ DCs also increased in absolute numbers in the spleens of wild-type mice after *T. gondii* infection (Fig. 7 B). By contrast, CD11b$^+$ DCs were present in similar numbers during all times after *T. gondii* infection in both wild-type and *Batf3*$^{-/-}$ mice (Fig. 8, A and B).

Increased numbers of CD8α$^+$ DCs after *T. gondii* infection suggests a role in protection against this parasite. Therefore, production of IL-12p40 by various cell types was measured in wild-type and *Batf3*$^{-/-}$ mice after infection by *T. gondii* (Fig. 9 and 10). We examined day 3 after infection specifically, since we were interested in cells

producing IL-12p40 early enough after infection that could control the exponential growth of *T. gondii* observed as early as day 4 in *Batf3*$^{-/-}$ mice (Fig. 1 B). We used intracellular cytokine staining (ICS) to quantify IL-12p40 production by CD8α^+ DCs, CD11b$^+$ DCs, plasmacytoid DCs, inflammatory monocytes and neutrophils. The percentage of CD8α^+ DCs producing IL-12p40 was increased from basal levels in uninfected mice to approximately 25-30% at day 3 after infection (Fig. 9). By contrast, the percentage of CD11b$^+$ DCs that produced IL-12p40 was not significantly altered by infection, being approximately 2 to 3% in both infected and uninfected mice (Fig. 9). Furthermore, inflammatory monocytes, neutrophils and plasmacytoid DCs displayed no induction of IL-12p40 by *T. gondii* infection (Fig. 10). Accordingly, CD8α^+ DCs express the highest levels of the *T. gondii* profilin sensor TLR11 as compared with a variety of immune cell types (Fig. 11), suggesting that this cell is optimally poised for sensing *T. gondii* and producing initial IL-12 during early infection. In addition, since the IL-12p40 chain is shared between the cytokines IL-12 and IL-23, we formally excluded a role for IL-23 in our system by examining CD8α^+ DC induction of the IL-23-specific subunit p19 and the IL-12-specific subunit p35 upon infection. Uninfected and infected CD8α^+ DCs express the IL-12p40 subunit (Fig. 12 A), as shown above, in conjunction with the IL-12p35 subunit (Fig. 12 B), but not the IL-23p19 subunit (Fig. 12 C), clearly showing production of IL-12 and not IL-23 by these cells. In addition, expression of IL-12p40 is significantly increased in these cells on day 3 after infection (Fig. 12 A). In summary, our data demonstrates that CD8α^+ DCs are the major IL-12-producing cells in the spleen 3 days after infection by *T. gondii*.

IL-12 administration to Batf3$^{-/-}$ mice restores IFNγ production and controls T. gondii infection.

If susceptibility of *Batf3*$^{-/-}$ mice to *T. gondii* results from decreased IL-12 production caused by the absence of CD8α^{+} DCs, then administration of IL-12 to *Batf3*$^{-/-}$ mice should restore their resistance to infection. Administration of recombinant murine IL-12 to wild-type mice had no impact on their susceptibility to infection by *T. gondii* (Fig. 13 A). In contrast, administration of IL-12 to *Batf3*$^{-/-}$ mice during the first 5 days of infection dramatically reversed their susceptibility, promoting their survival after infection for more than 60 days. Moreover, IL-12 treatment of *Batf3*$^{-/-}$ mice reduced their pathogen burden compared to untreated *Batf3*$^{-/-}$ mice, bringing parasite loads to levels in wild-type mice (Fig. 13, B and C).

Since reduced IL-12 in *Batf3*$^{-/-}$ mice may cause susceptibility to *T. gondii* by lowering early IFNγ production, and since NK cells are a significant source of IFNγ in response to IL-12, we asked if *Batf3*$^{-/-}$ NK cells could produce IFNγ *in vitro.* After culture with IL-12 and IL-18, wild-type and *Batf3*$^{-/-}$ NK cells produce equivalent amounts of IFNγ as measured by intracellular cytokine staining (Fig. 14). We next asked whether IL-12 administration to *Batf3*$^{-/-}$ mice also restored normal IFNγ production during infection (Fig. 15 A-D). IL-12 administration to wild-type mice did not influence serum IFNγ levels at day 4 after infection (Fig. 15 A). However, IL-12 administration to *Batf3*$^{-/-}$ mice significantly increased serum IFNγ on day 4, which approximated levels found in infected wild-type mice. The IFNγ induced by IL-12 in *Batf3*$^{-/-}$ mice appeared to arise from several cell types (Fig. 15 B-D). NK, CD4^{+} and CD8^{+} T cells from infected wild-

type mice produced IFNγ by ICS on day 3 when examined immediately *ex vivo*, but NK, $CD4^+$ and $CD8^+$ T cells from infected *Batf3*$^{-/-}$ mice were devoid of IFNγ at this time. However, administration of IL-12 to *Batf3*$^{-/-}$ mice infected with *T. gondii* substantially restored levels of IFNγ production by all three cell types. In summary, IL-12 administration to *Batf3*$^{-/-}$ mice reverses their susceptibility to *T. gondii* infection, decreases pathogen burden, and increases IFNγ production by natural killer cells and T lymphocytes.

CD8α$^+$ DCs are the only cell whose IL-12 production is required to control acute T. gondii infection.

The fact that $CD8\alpha^+$ DCs are a major source of IL-12 during acute *T. gondii* infection does not prove that they are the only source of IL-12 capable of controlling infection, and their requirement for protection against acute infection may derive from different, unknown functions. To test whether IL-12 production by $CD8\alpha^+$ DCs is relevant for resistance to acute *T. gondii* infection, we generated mixed chimeras using bone marrow (BM) derived from *IL-12p35*$^{-/-}$ and *Batf3*$^{-/-}$ mice. $CD8\alpha^+$ DCs can develop from *IL-12p35*$^{-/-}$ BM, but not *Batf3*$^{-/-}$ BM. This protocol allows the generation of chimeras in which $CD8\alpha^+$ DCs now develop but are unable to produce IL-12, while all other immune cell types can produce IL-12. If $CD8\alpha^+$ DCs are solely required for providing an early source of IL-12, then the mixed chimeras will remain susceptible to infection.

For this experiment, several other chimeras are necessary as controls. We

generated chimeras receiving only wild-type, *Batf3*$^{-/-}$, or *IL-12p35*$^{-/-}$ BM, as well as mixed chimeras receiving wild-type BM with either *Batf3*$^{-/-}$ or *IL-12p35*$^{-/-}$ BM (Fig. 16 and 17). This experiment was performed once using BALB/c mice (Fig. 16) and once using C57BL/6 mice (Fig. 17); both experiments are shown as the data are complementary. Chimeras were in general more susceptible to death following infection as compared with non-chimeric controls, potentially due to long-term effects of lethal irradiation. To allow for analysis of survival kinetics following infection, the dose of *T. gondii* was reduced in the BALB/c experiment from 1,000 tachyzoites to 100 tachyzoites. This was not possible in the C57BL/6 experiment, since the LD50 in this strain is much lower than in BALB/c mice, and C57BL/6 mice are routinely infected with only 100 tachyzoites; reduction of the dose below 100 tachyzoites could not be performed reproducibly. On the other hand, the experiment performed on C57BL/6 mice was more complete overall, as two additional controls were added to measure the response in chimeras re-constituted with *IL-12p35*$^{-/-}$ BM alone, or with wild-type plus *IL-12p35*$^{-/-}$ BM.

Chimeras of all 6 types were infected with *T. gondii* and analyzed along with non-chimera controls for survival and parasite burden (Fig. 16 and 17). First, chimeras reconstituted with wild-type BM controlled parasite numbers as expected, with burden equivalent to wild-type non-chimeric mice. The majority of these mice also survived acute infection. Chimeras reconstituted either with *Batf3*$^{-/-}$ or *IL-12p35*$^{-/-}$ BM succumbed to acute infection as expected and showed high parasite burdens, each approximately 100-fold higher that wild-type, reflecting the phenotype of the respective mutant non-chimeric mice.

We next examined mixed bone marrow chimeras. Mixed chimeras reconstituted with wild-type plus *Batf3*$^{-/-}$ BM or *IL-12p35*$^{-/-}$ BM showed low parasite burdens, equivalent to wild-type mice and chimeras reconstituted with wild-type BM. In both of these mixed chimeras, only half of the cells would harbor a defect, and the other half would be normal. Thus, a half cell complement of normal cells appears sufficient for normal control of parasite burden.

Finally, we analyzed chimeras reconstituted with a mixture of *Batf3*$^{-/-}$ and *IL-12-p35*$^{-/-}$ BM. In these chimeras, CD8α^+ DCs develop only from *IL-12p35*$^{-/-}$ BM, whereas all other cells develop from both IL-12-sufficient and *IL-12p35*$^{-/-}$ BM. Thus, in these chimeras, the CD8α^+ DCs uniformly lack the capacity to produce IL-12, whereas all other cell types retain the capacity to produce IL-12. These mixed chimeras are highly susceptible to infection and have extremely high parasite burden, comparable to levels in *Batf3*$^{-/-}$ mice. These results indicate that the CD8α^+ DCs are the only cell whose IL-12 production is sufficient for controlling parasite burden and maintaining resistance to acute *T. gondii* infection.

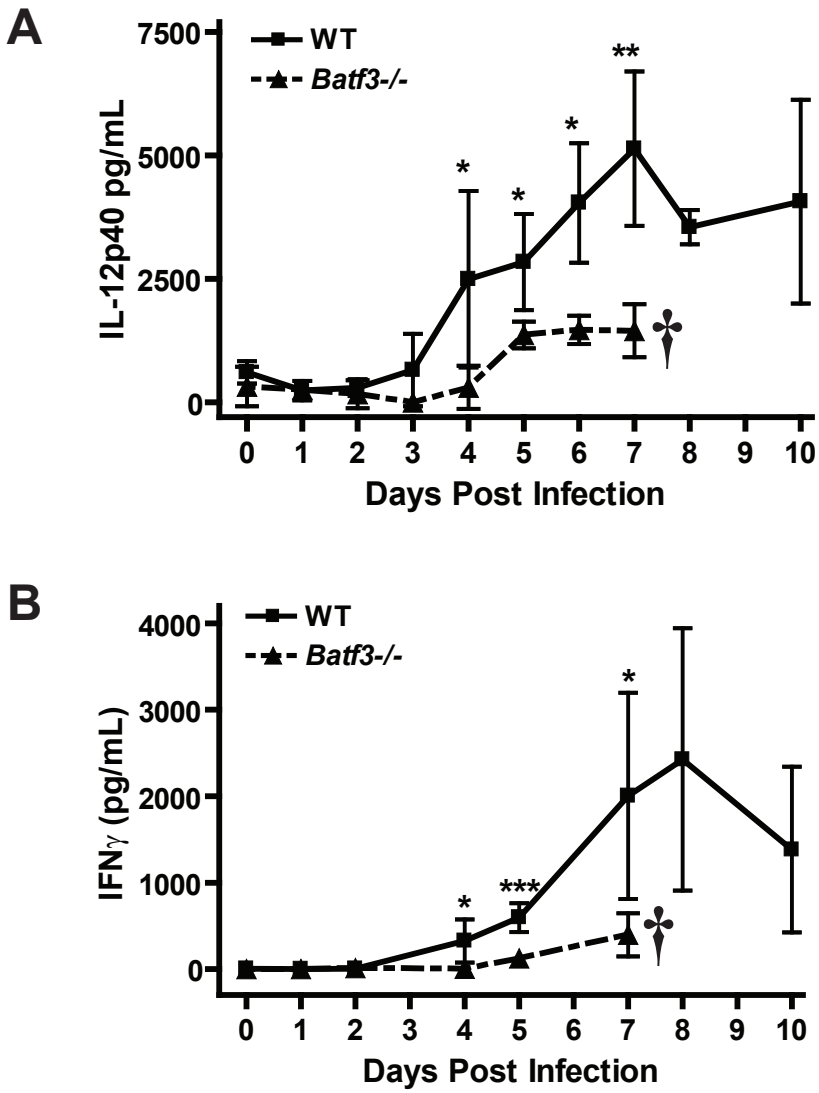

Figure 6. *Batf3*$^{-/-}$ mice have reduced serum IL-12 and IFNγ during *Toxoplasma gondii* infection. Infected 129S6/SvEV wild-type (squares) and *Batf3*$^{-/-}$ (triangles) mice were bled at various time-points after infection, and serum analyzed for cytokine levels. Data represents combined serum levels of IL-12p40 (A) and IFNγ (B) through the course of infection from 2-3 independent experiments (n=3-5 at each time-point). Data are represented as mean +/- standard deviation. *: 0.01<P<0.05, **: 0.001<P<0.01, ***: P<0.001.

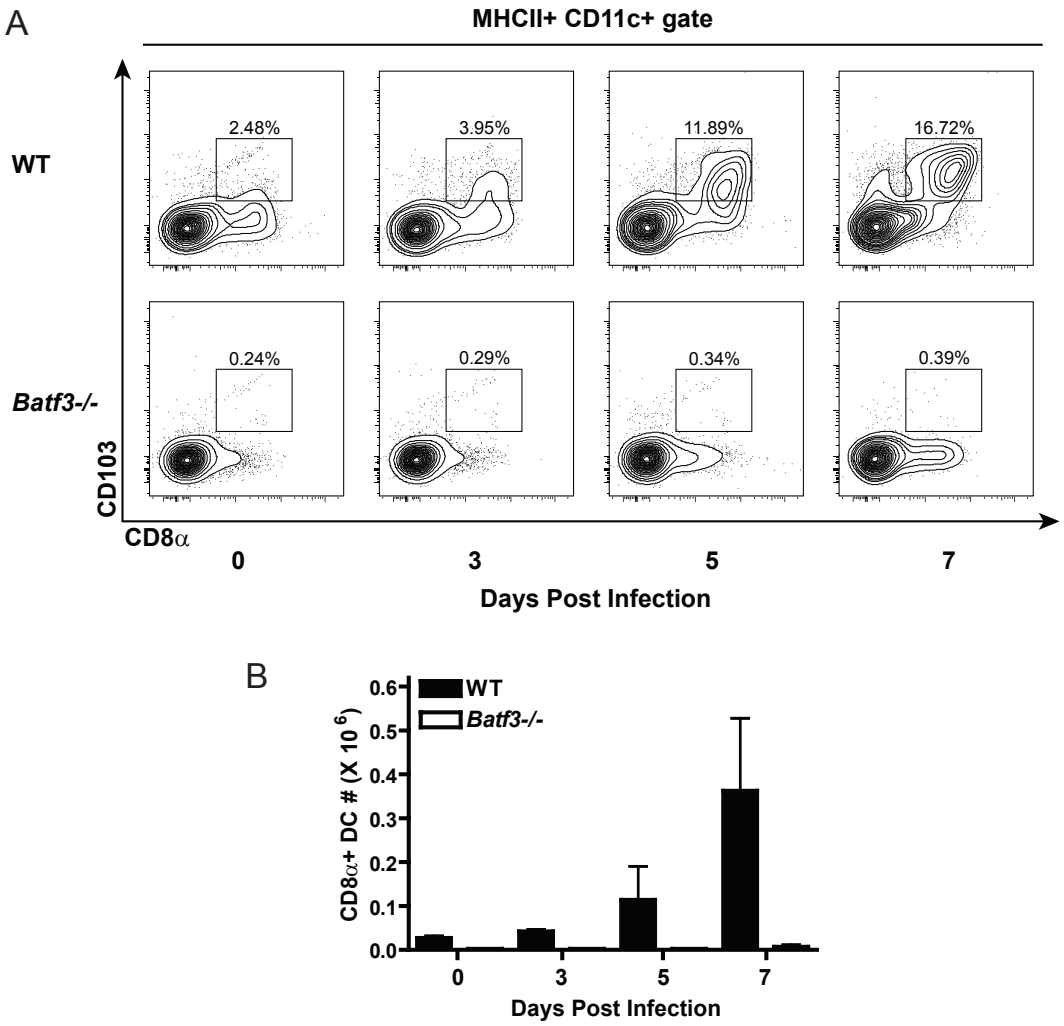

Figure 7. Splenic CD8α$^+$ dendritic cells expand after *T. gondii* infection in wild-type mice. 129S6/SvEV wild-type and *Batf3*$^{-/-}$ mice were infected with *T. gondii*, sacrificed on days 0, 3, 5 and 7 after infection, and analyzed for changes in dendritic cell subsets by flow cytometry. (A) Representative FACS plots gated on Aqua-negative, MHCII$^+$, CD11c$^+$ conventional dendritic cells. (B) Absolute numbers of CD8α$^+$ CD103$^+$ DCs in the spleen of wild-type (black bars) and *Batf3*$^{-/-}$ (white bars) mice throughout the course of infection (n=3, representative of 2 independent experiments). Data are represented as mean +/- standard deviation.

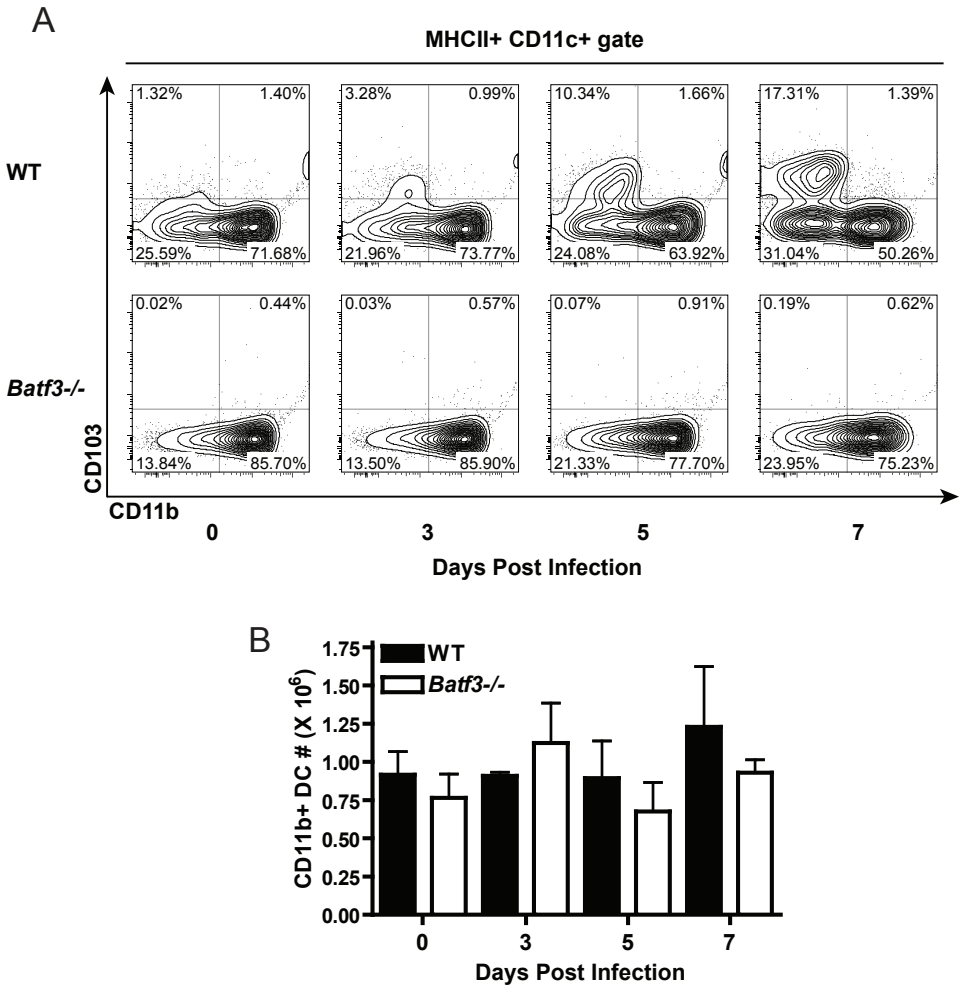

Figure 8. CD11b$^+$ DC percentages or numbers do not change during *T. gondii* infection. 129S6/SVeV wild-type and *Batf3*$^{-/-}$ mice were infected with *T. gondii* tachyzoites ip, and harvested on days 0, 3, 5 and 7 after infection. (A) Representative FACS plots gated on MHCII$^+$ CD11c$^+$ cells. (B) Absolute numbers of CD11b$^+$ DCs in the spleen of wild-type (black bars) and *Batf3*$^{-/-}$ (white bars) mice throughout the course of infection (n=3, representative of 2 independent experiments). Data are represented as mean +/- standard deviation.

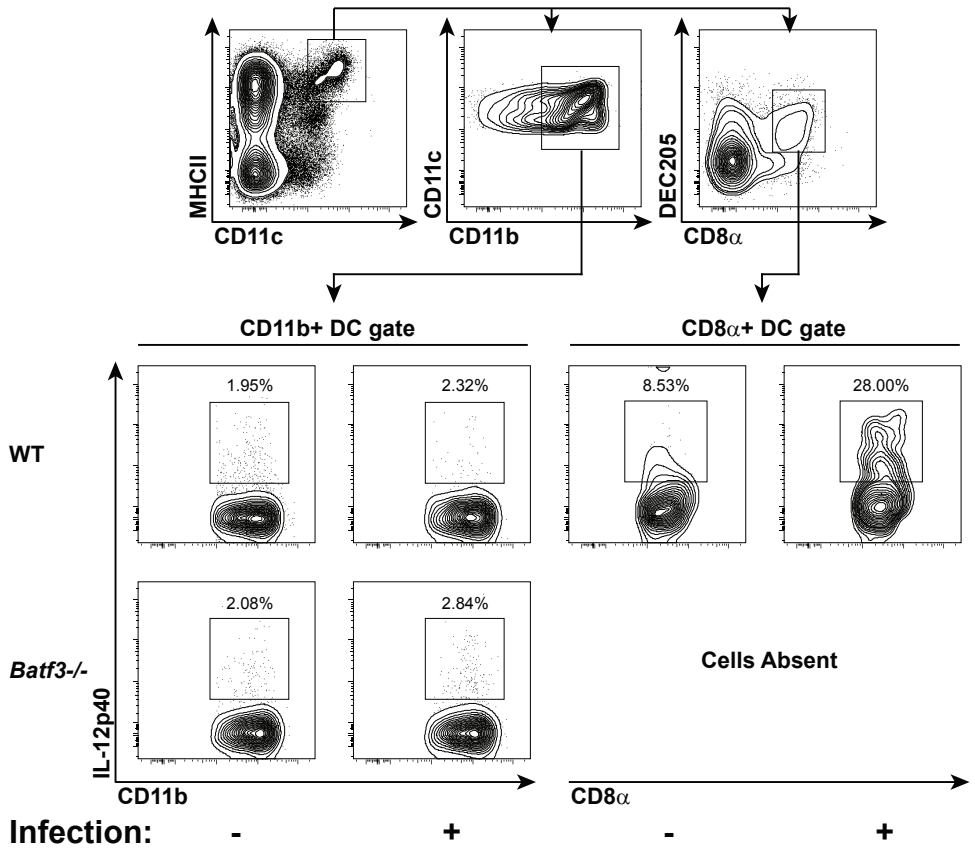

Figure 9. CD8α$^+$ dendritic cells are the major producers of IL-12 after *T. gondii* infection in wild-type mice. 129S6/SvEV wild-type and *Batf3*$^{-/-}$ mice were infected with *T. gondii*, sacrificed on day 3 after infection, and analyzed for the cellular source of IL-12 by intracellular cytokine staining. Representative FACS plots gated on MHCII$^+$ CD11c$^+$ expressing CD11b$^+$ DCs or CD8α$^+$ DEC205$^+$ DCs are shown. (n=3, representative of 3 independent experiments).

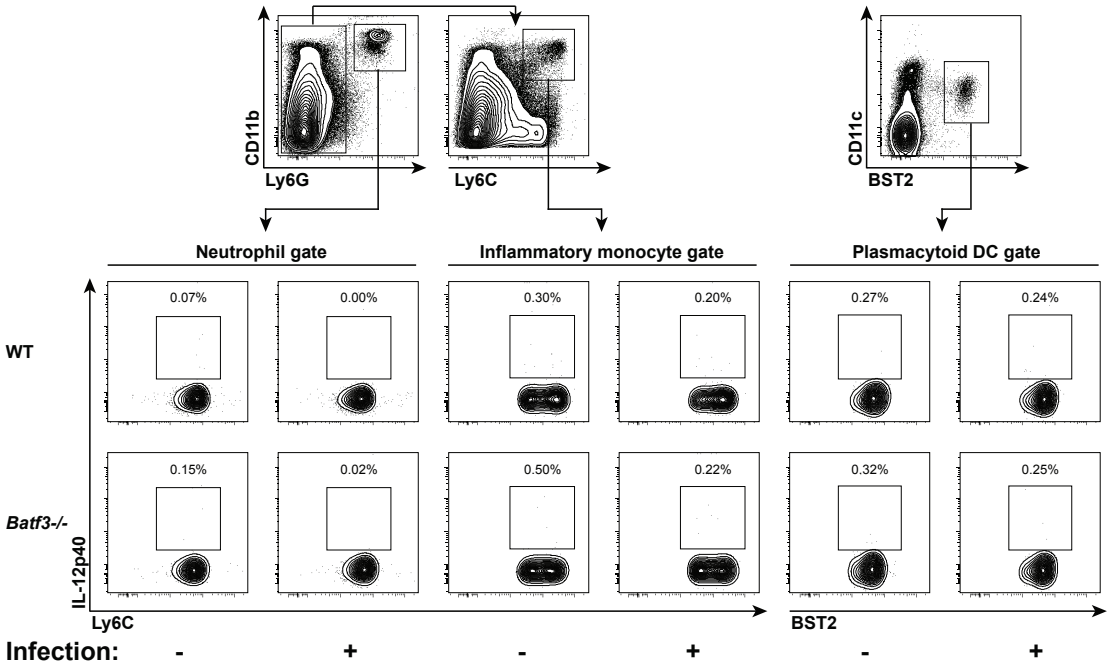

Figure 10. Neutrophils, inflammatory monocytes and plasmacytoid DCs do not produce IL-12p40 upon *T. gondii* infection. 129S6/SvEV wild-type and *Batf3*$^{-/-}$ mice were infected with *T. gondii*, sacrificed on day 3 after infection, and analyzed for the cellular source of IL-12 by intracellular cytokine staining. Representative FACS plots gated on Ly-6G^{+} CD11b^{+} neutrophils, Ly-6G^{-} Ly-6C^{+} CD11b^{+} inflammatory monocytes, or CD11c^{+} Bst2^{+} plasmacytoid DCs are shown. (n=3, representative of 3 independent experiments).

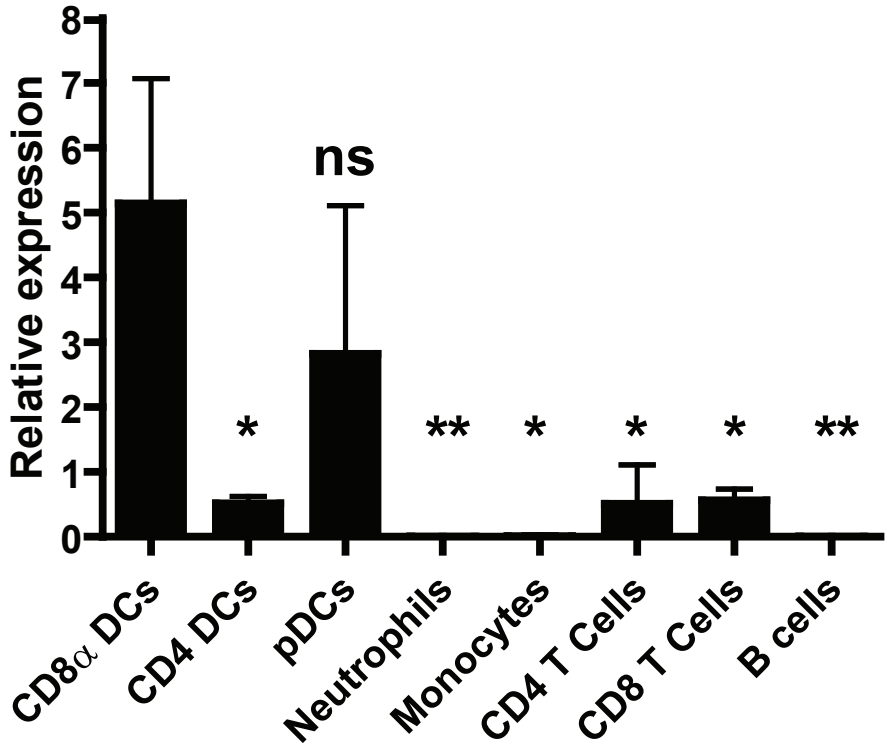

Figure 11. CD8α^+ DCs express the highest level of the *T. gondii* sensor TLR11. Listed immune cells were sort-purified from 129S6/SvEV wild-type mice, harvested for RNA, and analyzed for the expression of TLR11 by quantitative RT-PCR (n=3). All P-values compare CD8α^+ DCs to indicated population. Data are represented as mean +/- standard deviation. Not significant (ns): $P>0.05$, *: $0.01<P<0.05$, **: $0.001<P<0.01$.

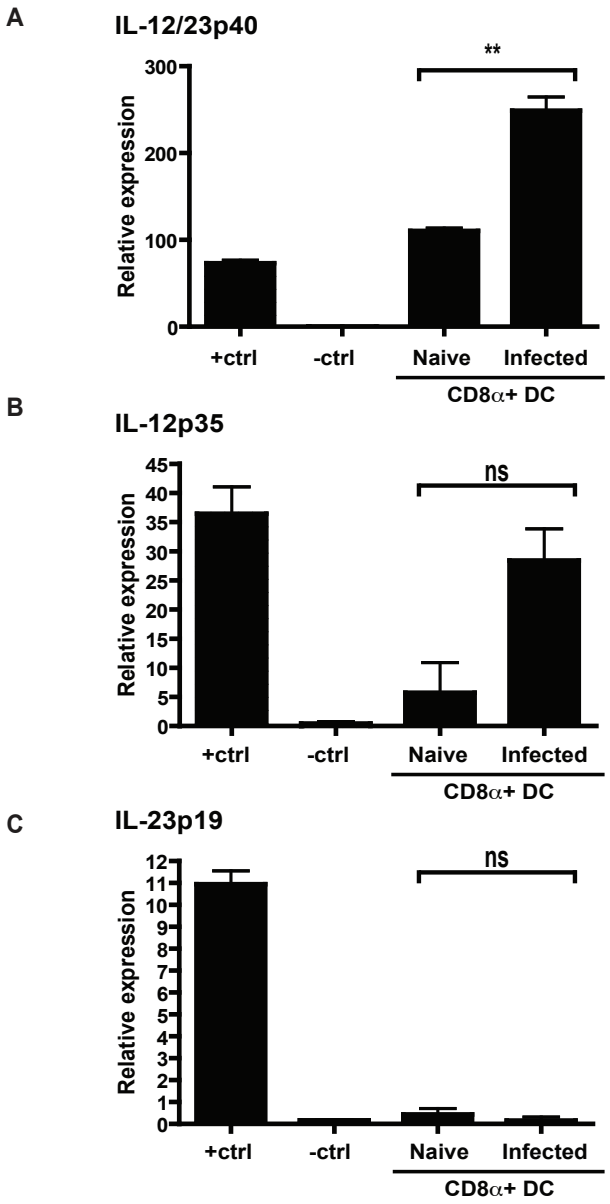

Figure 12. CD8α^+ DCs produce IL-12, but not IL-23, in response to *T. gondii* infection. (A-C) CD8α^+ DCs were sort-purified from *T. gondii* infected 129S6/SvEV wild-type mice on days 0 and 3 after infection, harvested for RNA, and analyzed for the expression of cytokine chains by qRT-PCR. Two uninfected and three infected spleens were pooled prior to the sort. As positive and negative controls for qRT-PCR, cDNA from total splenic CD11c$^+$ cells, the macrophage cell line J774, and total kidney lysate were also analyzed. IL-23p19 +ctrl = J774 cDNA, -ctrl = Kidney cDNA; IL-12p35 +ctrl = CD11c$^+$ cDNA, -ctrl = J774 cDNA; IL-12/23p40 +ctrl = CD11c$^+$ cDNA, -ctrl = J774 cDNA. Data are represented as mean +/- standard deviation. Not significant (ns): $P>0.05$, **: $0.001<P<0.01$.

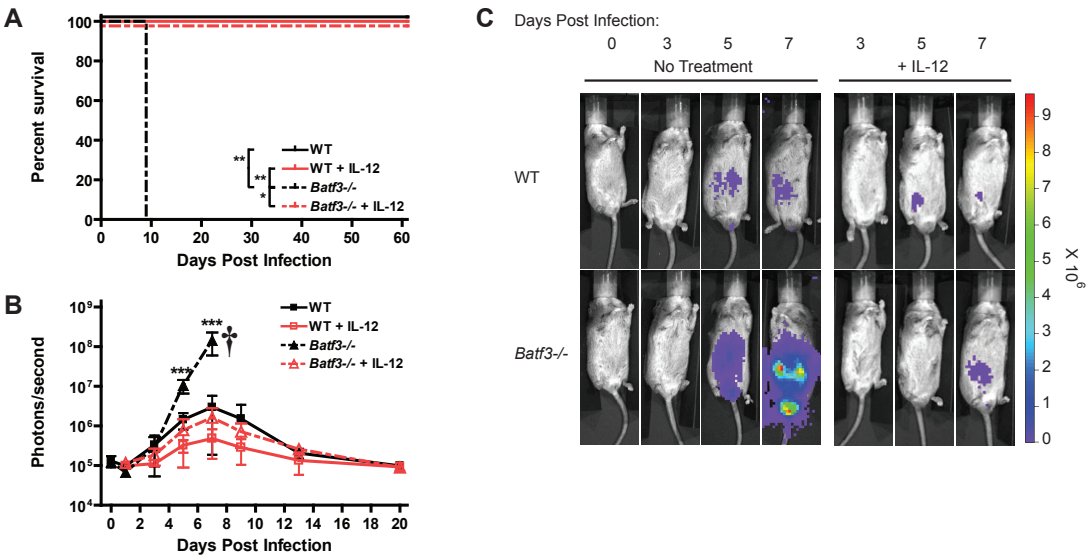

Figure 13. Administration of IL-12 rescues *Batf3*-deficient mice during *T. gondii* infection. 129S6/SvEV mice were infected with *T. gondii* and injected with saline or 0.5µg of recombinant murine IL-12 on days 0, 1, 2, 3, and 4 after infection. (A) Survival data from infected mice (WT: solid black line; WT + IL-12: solid red line; *Batf3*$^{-/-}$: dashed black line; *Batf3*$^{-/-}$ + IL-12: dashed red line) (n=3-5, representative of 3 independent experiments). (B) Combined parasite burden from whole body *in vivo* bioluminescence imaging of infected mice (WT: black squares; WT + IL-12: red squares; *Batf3*$^{-/-}$: black triangles; *Batf3*$^{-/-}$ + IL-12: red triangles) from 2 independent experiments (n=3-8 at each time-point, representative of 4 independent experiments). Data are represented as mean +/- standard deviation. (C) Representative bioluminescence images of infected mice throughout the course of infection. *: 0.01<P<0.05, **: 0.001<P<0.01, ***: P<0.001.

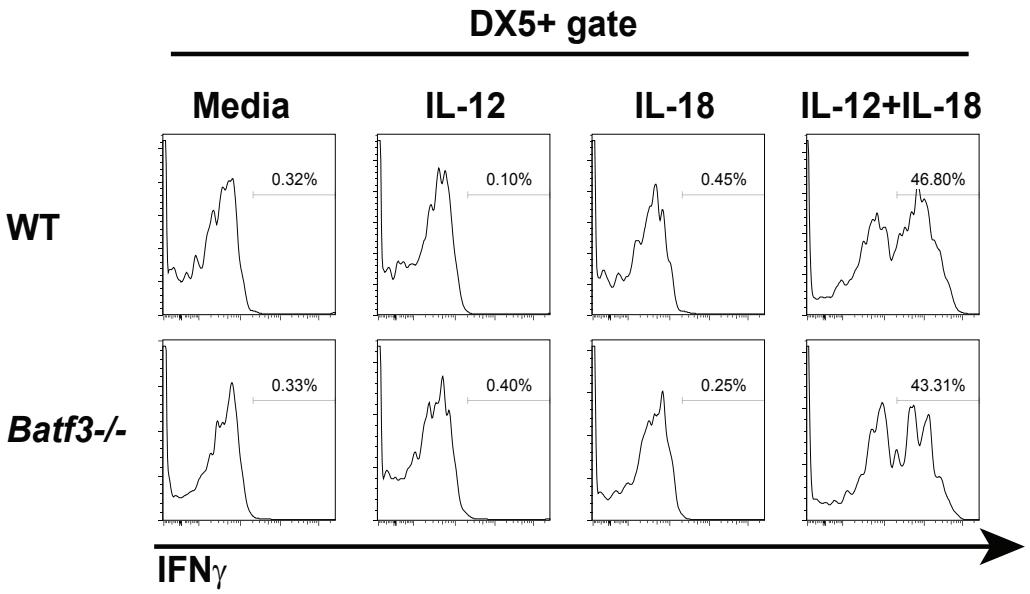

Figure 14. *Batf3*$^{-/-}$ NK cells can produce IFNγ *in vitro* in response to IL-12 and IL-18. 129S6/SvEV wild-type and *Batf3*$^{-/-}$ spleens were incubated in IL-12 and IL-18 for 4 hours. NK cells were identified using DX5 staining, and stained for intracellular IFNγ.

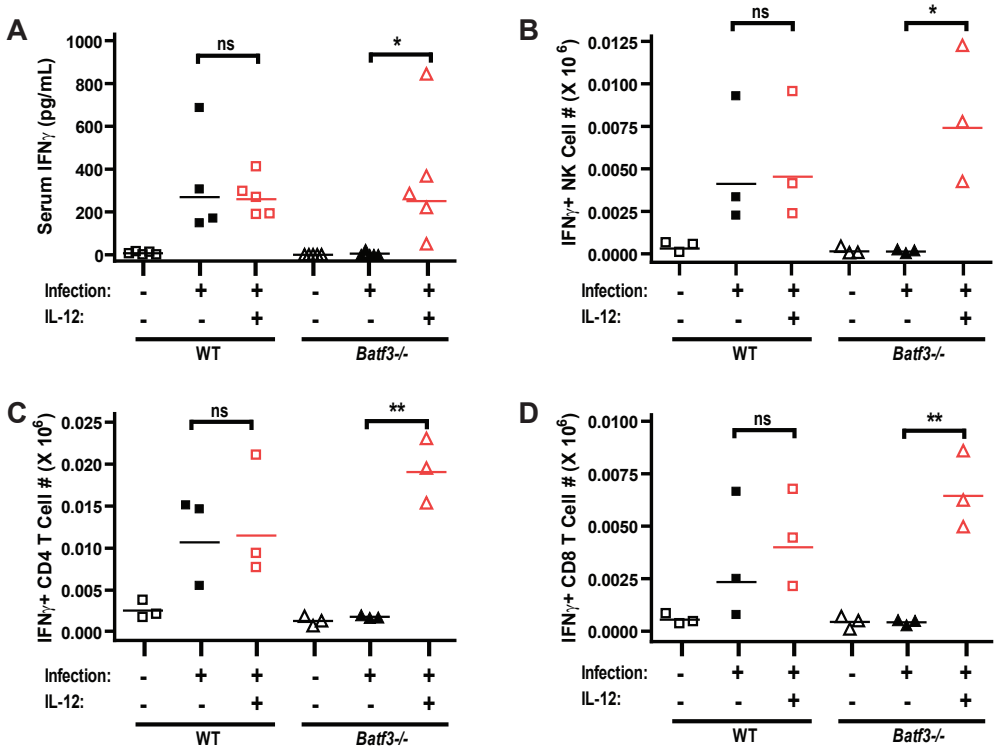

Figure 15. Administration of IL-12 restores IFNγ production in *Batf3*-deficient mice during *T. gondii* infection. 129S6/SvEV mice were infected with *T. gondii* and injected with saline or 0.5µg of recombinant murine IL-12 on days 0, 1, 2, 3, and 4 after infection. (A) Serum levels of IFNγ on day 4 after infection (n=4-5). (B-D) Absolute numbers of IFNγ-positive NK (B), $CD4^+$ T (C), and $CD8^+$ T (D) cells in the spleen directly *ex vivo* on day 3 after infection as measured by intracellular cytokine staining (n=3). (A-D) Horizontal lines represent the geometric mean. Not significant (ns): $P>0.05$, *: $0.01<P<0.05$, **: $0.001<P<0.01$, ***: $P<0.001$.

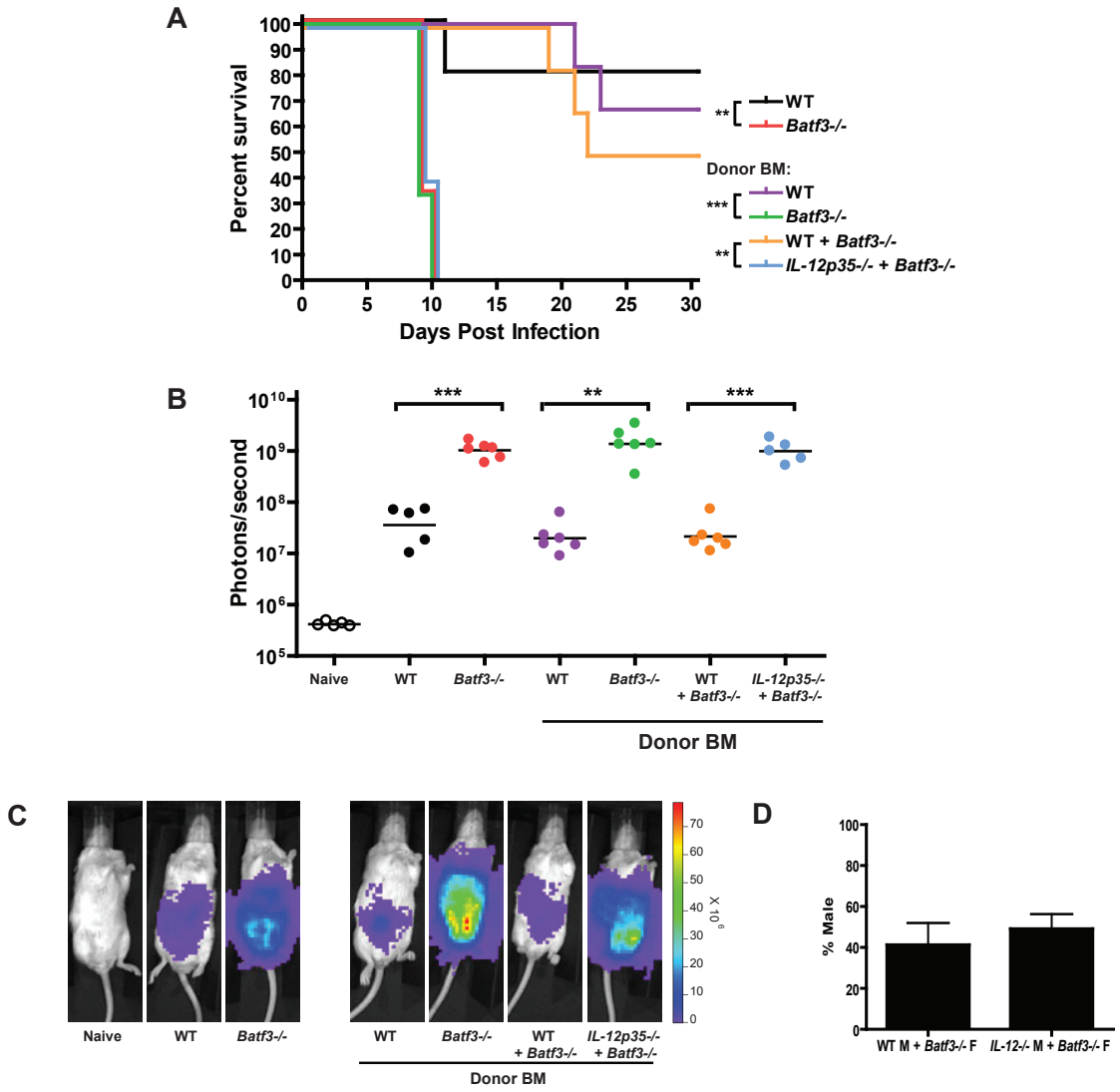

Figure 16. CD8α$^+$ dendritic cells are the only cells whose IL-12 production is protective against acute *T. gondii* infection. BALB/c chimeras and control non-chimeric mice were infected with *T. gondii* and monitored for survival (A) and parasite burden (B-C). (A) Survival data from non-chimeric wild-type (black line) and *Batf3*$^{-/-}$ (red line) mice were compared to lethally irradiated recipients which received only wild-type (purple line) or *Batf3*$^{-/-}$ (green line) BM, or a 1:1 mixture of wild-type with *Batf3*$^{-/-}$ BM (orange line) or *IL-12p35*$^{-/-}$ with *Batf3*$^{-/-}$ BM (blue line) (n=5-6, representative of 2 independent experiments). Parasite burden (B) and representative images (C) on day 7 after infection from the groups in (A). (B) Horizontal lines represent the geometric mean. (D) Mixed BM chimeras were analyzed after re-constitution to determine chimerism. Blood from BALB/c BM chimeras was analyzed by quantitative RT-PCR. The contribution from different donor BM was determined using the male Y chromosome gene *Zfy* as a marker. Data are represented as mean +/- standard deviation. **: 0.001<P<0.01, ***: P<0.001.

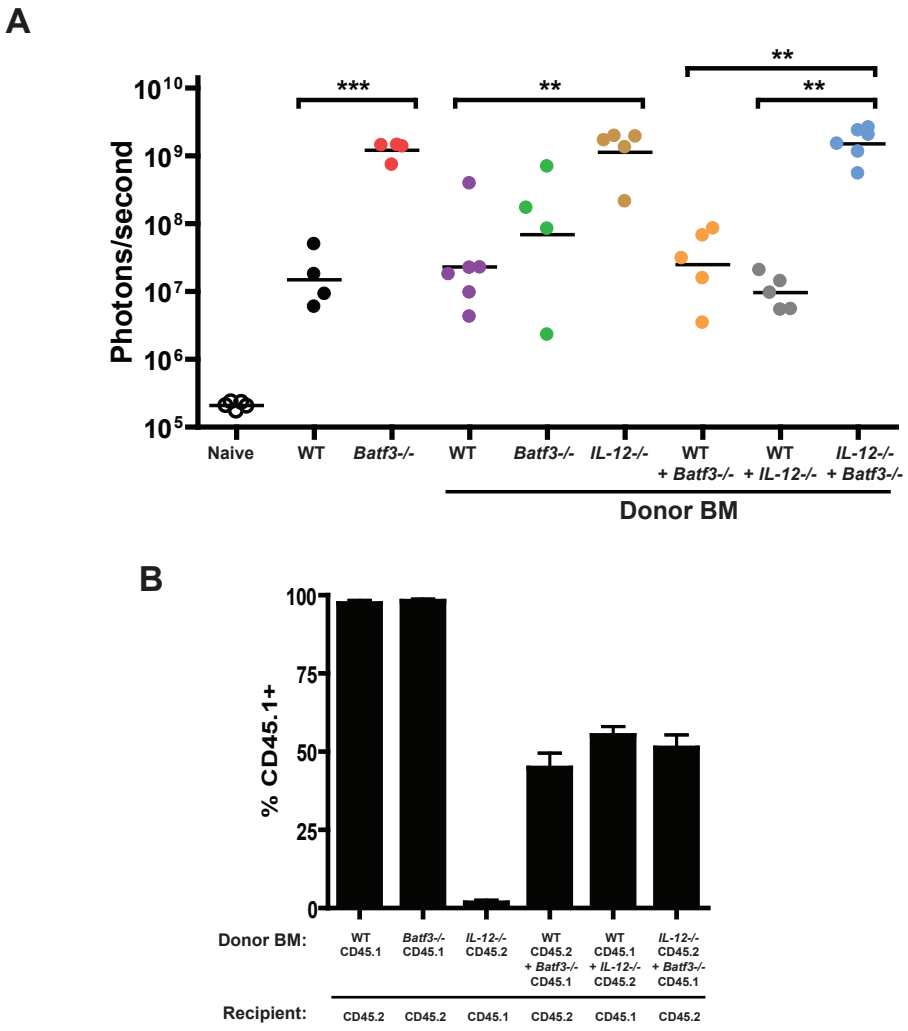

Figure 17. Mice re-constituted with a 1:1 mixture of *Batf3*$^{-/-}$ plus *IL-12p35*$^{-/-}$ bone marrow are unable to control *T. gondii* burden. (A) Parasite burden from C57BL/6 BM chimera experiment is shown. Non-chimeric C57BL/6 WT and *Batf3*$^{-/-}$ mice were compared with lethally irradiated WT C57BL/6 recipients who were given either WT, *Batf3*$^{-/-}$, or *IL-12p35*$^{-/-}$ BM, or a 1:1 mixture of WT plus *Batf3*$^{-/-}$, WT plus *IL-12p35*$^{-/-}$, or *Batf3*$^{-/-}$ plus *IL-12p35*$^{-/-}$ BM. Whole body *in vivo* bioluminescence imaging was done on day 7 after infection (n=4-6, data representative of 2 independent experiments). Horizontal lines represent the geometric mean. (B) Mixed BM chimeras were analyzed after re-constitution to determine chimerism. Blood from C57BL/6 BM chimeras was analyzed by flow cytometry. The contribution from different donor BM was determined using the congenic markers CD45.1 and CD45.2. **: 0.001<P<0.01, ***: P<0.001.

CHAPTER 6

IL-12 Bypasses the Block in CD8α$^+$ DC Development in *Batf3*$^{-/-}$ Mice

Administration of IL-12 to T. gondii infected Batf3$^{-/-}$ *mice restores CD8α*$^+$ *DCs*

While further characterizing the expansion of CD8α$^+$ DCs in *T. gondii*-infected wild-type animals, we made the surprising discovery that exogenous IL-12 could rescue the development of CD8α$^+$ DCs in *Batf3*$^{-/-}$ mice (Fig. 18). In this experiment, wild-type and *Batf3*$^{-/-}$ animals were infected with *T. gondii*, and half the animals were treated with IL-12 for the first five days of infection. As shown previously, CD8α$^+$ DCs expanded in wild-type animals in response to infection, while they were absent in *Batf3*$^{-/-}$ mice before and during infection (Fig. 18 A). Administration of IL-12 increased the percentage and absolute numbers of CD8α$^+$ DCs in wild-type mice on day 3 after infection. Surprisingly, infected *Batf3*$^{-/-}$ mice that received exogenous IL-12 now acquired a splenic DC subset that displayed hallmarks of the CD8α$^+$ DC on both day 3 and 7 after infection (Fig. 18, A and B). It is important to note that the markers used for identification of CD8α$^+$ DCs in this experiment were CD103 and CD8α. In contrast, CD11b$^+$ DC numbers were comparable in all mice, and remained unchanged (Fig. 18 C). Thus, IL-12 administration during *T. gondii* infection bypasses the block in development of CD8α$^+$ DCs in *Batf3*$^{-/-}$ mice.

IL-12 administration in the absence of T. gondii infection can restore CD8α$^+$ DCs in Batf3$^{-/-}$ mice

In order to determine if the restoration of CD8α$^+$ DCs could be achieved by IL-12 administration alone, or required both IL-12 and *T. gondii* infection, we treated uninfected wild-type and *Batf3*$^{-/-}$ mice with IL-12 for 3 days, and analyzed the spleens by flow cytometry. IL-12 administration in the absence of *T. gondii* infection was sufficient to restore the CD8α$^+$ DC subset in *Batf3*$^{-/-}$ mice (Fig. 19, A and B). This finding was independent of the genetic background, as it occurred in all strains tested, namely BALB/c, C57BL/6 and 129S6/SvEV. Moreover, the effect was specific for the CD8α$^+$ DC compartment, since CD11b$^+$ DC numbers were unaffected by treatment (Fig. 19 C).

To further confirm the identity of the restored cells as CD8α$^+$ DCs, we added an additional antibody against DEC205. By comparing the different strains of mice, we found a discrepancy in antibody staining of CD8α$^+$ DCs using DEC205 versus CD103 (Fig. 19 A). Both markers are thought to be expressed exclusively on classic CD8α$^+$ DCs, as opposed to the newly described CD8α$^+$ CX3CR1$^+$ subset (Bar-On et al., 2010). However, in our hands, CD8α$^+$ DCs uniformly expressed the multilectin receptor DEC205, but not the integrin CD103. IL-12 administration consistently increased CD103 expression on the DEC205$^+$ CD8α$^+$ DCs, while untreated DEC205$^+$ CD8α$^+$ DCs expressed a range of CD103 that varied from experiment to experiment and between the different strains of mice. Therefore, DEC205 was chosen as a more specific surface marker to positively identify CD8α$^+$ DCs for future experiments, and any reference to CD8α$^+$ DCs will specifically delineate CD8α$^+$ DEC205$^+$ cells.

In addition, we formally ruled out the possibility that another cell type was acquiring these "DC markers" and falling within the CD8α$^+$ DC gate upon IL-12 treatment. Restored CD8α$^+$ DCs in *Batf3*$^{-/-}$ mice were negative for the B cell marker B220, the T cell marker CD3, and the NK cell marker NKp46 (Fig. 20), suggesting that these cells were not B, T, or NK cells that had acquired "DC markers" upon IL-12 treatment.

CD8α$^+$ DCs are present in normal numbers in IL-12-deficient mice

Based on this novel finding that IL-12 may play a role in CD8α$^+$ DC development, we examined CD8α$^+$ DCs during steady state conditions in *IL-12p35*$^{-/-}$ mice. These mice have not been reported to have a defect in the dendritic cell compartment, although we could not find a published report specifically analyzing DCs subsets. Wild-type and *IL-12p35*$^{-/-}$ mice had comparable percentages of CD8α$^+$ DCs in the spleen (Fig. 21), suggesting that IL-12 is not required for normal development or maintenance of this population in the steady state.

The restoration of Batf3$^{-/-}$ CD8α$^+$ DCs by IL-12 is IFNγ-dependent

IL-12 is known to induce IFNγ production, and many of its effects are mediated by IFNγ (Trinchieri, 2003). Therefore, in order to understand the underlying mechanism for the reappearance of CD8α$^+$ DCs, we evaluated a requirement for IFNγ by using the IFNγ-blocking antibody H22. H22 treatment completely blocked the IL-12-induced development of CD8α$^+$ DCs in *Batf3*$^{-/-}$ mice *in vivo* (Fig. 22, A and B). In contrast,

CD11b$^+$ DC numbers were not significantly altered by H22 treatment (Fig. 22 C). Thus, IL-12 induces the development of CD8α^+ DCs in *Batf3*$^{-/-}$ mice via IFNγ.

NK, B and T Cells are not required for the restoration of CD8α^+ DCs in Batf3$^{-/-}$ mice after IL-12 treatment

IFNγ can be produced by a number of cell types, although NK cells are thought to be the major producers of IFNγ in response to IL-12 (Trinchieri, 2003). In order to determine if NK cells were required for the IL-12/IFNγ-mediated generation of CD8α^+ DCs in *Batf3*$^{-/-}$ mice, we treated the mice with the anti-NK1.1 antibody PK136 to deplete NK cells *in vivo*. NK cell depletion was confirmed using the NK-specific antibodies DX5 and NKp46. PK136 effectively depleted NK cells by approximately 10-fold on day 6 after antibody treatment (Fig. 23, A and B). However, the IL-12-induced restoration of CD8α^+ DCs in *Batf3*$^{-/-}$ mice was unaffected by NK cell depletion (Fig. 24, A and B).

T cells and B cells can also produce IFNγ in response to inflammation as well as antigen encounter (Lertmemongkolchai et al., 2001; Harris et al., 2005). We therefore hypothesized that T and/or B cells could be the source of "by-stander" antigen-independent IFNγ in the *Batf3*$^{-/-}$ mice following IL-12 treatment. To test this hypothesis, we used RAG-deficient mice that are missing both B and T cells due to a developmental block in the antigen-receptor recombination machinery. IL-12-induced CD8α^+ DC restoration was not abrogated in the absence of B and T cells in *Rag/Batf3*$^{-/-}$ mice (Fig. 24, A and C), suggesting that B and T cells are dispensable for this effect.

Finally, considering that all lymphocytes are able to produce IFNγ, we wanted to

exclude the possibility that one subset, meaning B, T, or NK cells, could compensate for the absence of the other. Therefore, we combined NK depletion with the use of RAG-deficient mice. NK cell depletion was again confirmed on the day of harvest using DX5 and NKp46 antibodies (Fig. 23, A and C). IL-12 treatment could restore CD8α^+ DC development in *Rag/Batf3*$^{-/-}$ animals treated with PK136 (Fig. 24, A and C), suggesting that NK cells, B cells, and T cells are not required. This result leaves a few hypotheses open. First, NK cell depletion was not 100% efficient, especially in mice that received exogenous IL-12 (Fig. 23). It is possible that the remaining NK cells are producing sufficient amounts of IFNγ for restoration of CD8α^+ DCs after IL-12 treatment. Alternatively, it is possible that other cells belonging to the innate compartment can respond to IL-12 treatment and produce IFNγ *in vivo* (Ohteki et al., 1999; Puddu et al., 1997; Munder et al., 1998). These questions will be addressed in future work.

Time-course of CD8α^+ DC reappearance in response to IL-12 treatment in vivo

To understand the effect of IL-12 on CD8α^+ DC development in *Batf3*$^{-/-}$ mice, we performed a time-course experiment, evaluating how quickly CD8α^+ DCs appear in the spleen, and how long they remain. CD8α^+ DCs have a relatively short half-life in the periphery, and are constantly replenished from precursors present in the spleen and bone marrow (Kamath et al., 2000; Kamath et al., 2002). Mice were treated with a single dose of IL-12, and analyzed from day one to seven by flow cytometry. Absolute numbers of CD8α^+ DCs in wild-type mice were fairly constant throughout the course of the experiment (Fig. 25). In *Batf3*$^{-/-}$ mice, CD8α^+ DCs began to appear on day 2 after IL-12

treatment, reaching the peak numbers on day 4, with a few CD8α^+ DCs still detectable as late as day 7. This quick wave of appearance in the spleen suggests that IL-12 may be acting on a local progenitor population, such as the splenic pre-cDCs.

Analysis of CD8α^+ DC precursors in the spleen

For this reason, we decided to carefully analyze splenic progenitors in terms of the percentage and absolute numbers of pre-cDCs following IL-12 administration. Pre-cDCs are the immediate precursors of cDCs, and can be identified as MHCII$^-$ CD11c$^+$ B220$^-$ cells that are positive for Flt3 and intermediate for SIRPα (Fig. 26) (Naik et al., 2006). In the steady state, splenic pre-cDC numbers were comparable between wild-type and *Batf3*$^{-/-}$ mice. IL-12 treatment did not substantially alter pre-cDC numbers, although this experiment needs to be repeated with larger groups of mice to perform statistical analysis. From this preliminary experiment, it appears that the percentage of pre-cDCs is slightly reduced by IL-12 treatment (Fig. 26 A), while the absolute numbers tended to be increased (Fig. 26 B). However, IL-12 administration increases the cellularity of the spleen in wild-type and *Batf3*$^{-/-}$ mice, making it difficult to interpret data where percentages are unchanged or reduced, while absolute numbers are increased. Therefore, it is important to normalize pre-cDC cell numbers based on the spleen size, and determine the number of pre-cDCs per million splenocytes (Fig. 26 C). Using this analysis, it appears as though IL-12 treatment is not preferentially causing expansion of pre-cDCs in wild-type or *Batf3*$^{-/-}$ mice.

We next used an additional marker, CD24, to monitor CD8α^+ DC maturation in

the presence of IL-12. CD24 can be used to identify CD8α$^+$ DCs both *in vivo* and *in vitro*. When CD24$^+$ cells were analyzed for expression of DEC205, we saw that this population was in fact heterogenous for DEC205 staining (W KC, unpublished) and (Fig. 27). Using DEC205 as a marker of maturation, we could discern roughly 3 subpopulations: DEC205 low and intermediate expressing cells, which are presumably immediate CD8α$^+$ DC precursors, and DEC205 high expressing cells, which correspond to the mature CD8α$^+$ DCs. Treatment of wild-type mice with IL-12 shifted all the CD24$^+$ DCs to the subset expressing high levels of DEC205, which suggests that IL-12 is causing maturation of the pre-CD8α$^+$ DCs in the spleen. In *Batf3*$^{-/-}$ mice, very few cells fall within the CD24$^+$ gate, and most are low or intermediate for DEC205, consistent with a very late block in CD8α$^+$ DC development in these mice (W KC, unpublished). IL-12 treatment substantially increased the percentage of cells within the CD24$^+$ gate, and induced their maturation as measured by high expression of DEC205. Thus, it seems as though IL-12 is acting on the very late stage of CD8α$^+$ DC development to cause maturation of splenic progenitors in *Batf3*$^{-/-}$ mice.

Candidate transcription factors Batf and IRF-8 are not induced in Batf3$^{-/-}$ *IL-12-treated CD8α*$^+$ *DCs*

Batf and *Batf3* are members of the AP-1 transcription factor family. *Batf*-deficient mice have defects in Th17 differentiation and in B cell class-switch recombination (Schraml et al., 2009; Ise et al., 2011). However, these two AP-1 transcription factors are likely paralogous, and share significant homology. In addition, *in vitro* experiments have

shown that *Batf* and *Batf3* are interchangeable in CD8α$^+$ DC development, Th17 generation, and B cell class-switch recombination (W Ise, W KC, T Murphy, unpublished data). Thus, we hypothesized that *Batf* could complement for *Batf3* in CD8α$^+$ DC development *in vivo*, and we are in the process of generating *Batf/Batf3*-double deficient mice to directly ask this question. In the interim, we asked if *Batf* was up-regulated in IL-12-restored CD8α$^+$ DCs in *Batf3*$^{-/-}$ mice (Fig. 28).

Batf3 is highly expressed in wild-type untreated and IL-12-treated CD8α$^+$ DCs, as expected, and is absent from the IL-12-treated *Batf3*$^{-/-}$ CD8α$^+$ DCs (Fig. 28 A). In addition, the *Batf3* paralog *Batf* is expressed at comparable levels in all three DC populations, which is approximately 2-fold less than activated B cells, and is not induced by IL-12 treatment (Fig. 28 B).

We also looked for induction of the transcription factor *IRF-8*, which is important in CD8α$^+$ DC development as discussed in the introduction (Aliberti et al., 2003). *IRF-8* appears to be induced upon IL-12-treatment of wild-type CD8α$^+$ DCs, but is comparable between untreated wild-type and IL-12-treated *Batf3*$^{-/-}$ CD8α$^+$ DCs (Fig. 28 C). From this data, it was still unclear if either *Batf* or *IRF-8* could be compensating for the absence of *Batf3* in CD8α$^+$ DC development. Thus, we moved from this candidate-based approach to global expression analysis using microarrays.

Microarray analysis of restored CD8α$^+$ DCs from Batf3$^{-/-}$ mice

The restored CD8α$^+$ DCs in *Batf3*$^{-/-}$ mice correctly expressed a number of surface markers used to identify these cells. Nevertheless, we are only beginning to understand

the unique capabilities of CD8α$^+$ DCs and the host of genes required for their development and function. We therefore performed microarray analysis of IL-12-restored CD8α$^+$ DCs from *Batf3*$^{-/-}$ animals to determine the expression profile of these cells and compare them to wild-type CD8α$^+$ DCs.

Global comparison of genes expressed in CD8α$^+$ DCs from IL-12-treated wild-type and *Batf3*$^{-/-}$ mice revealed very few differences (Fig. 29 A), with only 206 genes displaying a greater than 4-fold difference between the samples. This high degree of similarity suggests that the restored CD8α$^+$ DCs in *Batf3*$^{-/-}$ mice are comparable to their wild-type counterparts in global gene expression. There were a few genes, such as germinal center B-cell expressed transcript 2 (GCET2), that seemed to be strictly *Batf3*-dependent and could not be restored with IL-12 treatment. However, none of these genes have yet been characterized in CD8α$^+$ DCs. In addition, wild-type CD8α$^+$ DCs from untreated and IL-12-treated mice were nearly identical in gene expression (Fig. 29 B), with only 70 genes displaying a greater than 4-fold difference between the samples. The few genes that significantly varied between wild-type untreated and IL-12-treated CD8α$^+$ DCs were X- or Y-chromosomes specific, which could be attributed to the sex of the mice used for the microarray analysis. Finally, we compared *Batf3*$^{-/-}$ IL-12-restored CD8α$^+$ DCs to wild-type CD8α$^-$ DCs (Fig. 29 C). Over fourteen-hundred genes displayed a greater than 4-fold difference between these samples, clearly demonstrating that these two population were disparate. Overall, the microarray data strongly suggests that the restored CD8α$^+$ DCs in *Batf3*$^{-/-}$ mice are extremely similar to wild-type CD8α$^+$ DCs in global gene expression.

CD8α$^+$ DCs are restored by T. gondii infection in Batf3$^{-/-}$ mice

As shown in Figure 6 A, significant levels of IL-12 are induced in *T. gondii*-infected wild-type mice as measured in the serum starting at day 4 after infection. In addition, intracellular IL-12p40 can be measured within CD8α$^+$ DCs as early as 3 days after infection in wild-type mice (Fig. 9), and is necessary for protective immunity against *T. gondii* as demonstrated in chapter 5. However, other cell types are capable of producing IL-12 in *Batf3*$^{-/-}$ mice, and IL-12p40 can be detected in the serum starting at day 5 after infection (Fig. 6 A). Although this delayed and reduced production of IL-12 is not sufficient to protect mice against *T. gondii*, we reasoned that it may be sufficient to restore the CD8α$^+$ DC population in *Batf3*$^{-/-}$ mice, similar to exogenous IL-12. However, the data in Figure 7 shows an absence of CD8α$^+$ DCs in infected *Batf3*$^{-/-}$ mice at all time-points examined. Yet upon closer inspection of Figure 7, we discerned an expansion of CD8α$^+$ CD103$^-$ DCs, especially by day 7 after infection. At that time, we were using the surface marker CD103 to distinguish classic CD8α$^+$ DCs from the CD8α$^+$ CX3CR1$^+$ subset. As mentioned above, we later determined that DEC205 is a more faithful marker of CD8α$^+$DCs, while CD103 expression can be variable. Therefore, we repeated the experiment using DEC205 as an additional marker to test if endogenous IL-12 could restore classic CD8α$^+$ DCs in infected *Batf3*$^{-/-}$ mice.

Wild-type and *Batf3*$^{-/-}$ mice were infected with *T. gondii* and examined for the development of CD8α$^+$ DCs in the spleen on day 7 (Fig. 30). A similar trend, as observed with exogenous IL-12 treatment (Fig. 19), could be seen following *T. gondii* infection. CD8α$^+$ DCs expanded in response to *T. gondii* infection in 129S6/SvEV wild-type mice

(Fig. 30), as seen in Figure 7. In addition, CD8α$^+$ DCs expanded in infected C57BL/6 wild-type mice, but not in BALB/c wild-type mice, although the groups in each case were not large enough to determine statistical significance. In *Batf3*$^{-/-}$ mice, CD8α$^+$ DCs, as identified by co-expression of DEC205, were restored on all three genetic strains tested upon *T. gondii* infection (Fig. 30). Infection also restored absolute numbers of CD8α$^+$ DCs in *Batf3*$^{-/-}$ mice, although to varying degrees depending on the strain (Fig. 30 B). In addition, if we only consider CD103 expression, the data from Figure 7 and Figure 30 would be consistent: there is no CD8α$^+$ CD103$^+$ DC subset in infected 129S6/SvEV *Batf3*$^{-/-}$ mice in either Figure 7 or Figure 30. Thus, by adding the more faithful marker DEC205 to our analysis, we were able to demonstrate restoration of CD8α$^+$ DCs by *T. gondii* infection in *Batf3*$^{-/-}$ mice.

T. gondii-mediated restoration of CD8α$^+$ DCs in Batf3$^{-/-}$ mice is IFNγ-dependent

To further prove that infection-mediated restoration of CD8α$^+$ DCs is due to IL-12 and IFNγ produced during the course of infection, we treated mice with the IFNγ-blocking antibody H22 (Fig. 31). H22 treatment effectively blocked the restoration of CD8α$^+$ DCs in *T. gondii*-infected *Batf3*$^{-/-}$ mice, demonstrating a requirement for IFNγ in this process *in vivo*. Future experiments using IL-12-blocking antibody will more definitively demonstrate a role for endogenous IL-12 in CD8α$^+$ DC restoration in infected *Batf3*$^{-/-}$ mice.

In lieu of that, we tested the response of BALB/c *IL-12p35*$^{-/-}$ mice to *T. gondii* infection. We hypothesized that if endogenous IL-12 produced in the course of infection

was causing expansion of the CD8α$^+$ DCs in wild-type mice, then perhaps this response would be absent in *IL-12p35*$^{-/-}$ animals (Fig. 32). However, the result of this experiment was difficult to interpret. While the percentage of CD8α$^+$ DCs increased with infection in both wild-type and *IL-12p35*$^{-/-}$ mice, the absolute numbers of these cells appeared to be unchanged. This can be attributed to the genetic background of the mice used. As discussed above, CD8α$^+$ DCs do not expand in response to infection in wild-type BALB/c mice, unlike their 129S6/SvEV and C57BL/6 counterparts (Fig. 30). Therefore, we could not conclude if endogenous IL-12 is required for CD8α$^+$ DC expansion in wild-type mice during *T. gondii* infection. One possible approach is to breed *Batf3*$^{-/-}$ mice to *IL-12p35*$^{-/-}$ mice, and test the re-appearance of CD8α$^+$ DCs in response to infection. As seen in Figure 30, the restoration of CD8α$^+$ DCs in *Batf3*$^{-/-}$ mice is consistently seen in all genetic backgrounds tested. Thus, if CD8α$^+$ DCs are not restored with *T. gondii* infection in *Batf3/IL-12p35*-double deficient mice, we would be able to conclude that endogenous IL-12 is required for restoration of CD8α$^+$ DCs during infection.

Restored Batf3$^{-/-}$ CD8α$^+$ DCs can cross-present necrotic cell antigens in vivo

CD8α$^+$ DCs possess an enhanced ability to cross-present exogenous antigen on MHCI molecules to prime CD8$^+$ T cell responses *in vivo* (Hildner et al., 2008). Extensive research on CD8α$^+$ DCs has been focused on understanding the cellular components that allow this particular cell to excel at cross-presentation, and we are only beginning to understand the underlying mechanisms (Lin et al., 2008). To determine if the IL-12-restored CD8α$^+$ DCs were capable of cross-presentation, we examined their ability to

cross-present necrotic-cell associated antigens *in vivo* (Fig. 33).

OT-I transgenic T cells were CFSE labeled and injected into wild-type or *Batf3*$^{-/-}$ mice intra-peritoneally. OT-I T cells are specific for the model antigen OVA, and are used as the responder cells in this assay. Carboxy-Fluorescein diacetate Succinimyidyl Ester (CFDA-SE) is a highly permeable compound that enters cells and is converted to a green fluorescent dye (CFSE). CFSE-labeling of cells is routinely used to follow cell proliferation by flow cytometry, since the amount of CFSE within cells is halved with each division.

Antigen was provided to the recipient wild-type and *Batf3*$^{-/-}$ animals three days later in the form of OVA-pulsed irradiated *MHCI*$^{-/-}$ splenocytes. *MHCI*$^{-/-}$ splenocytes were used to ensure that direct presentation of OVA to OT-I T cells cannot occur. *MHCI*$^{-/-}$ splenocytes were OVA-loaded by osmotic shock and subsequently irradiated to induce cell death. Thus, in order to prime CD8^{+} T cell responses, exogenous OVA must be taken up and processed by the recipient's MHCI-sufficient DCs via cross-presentation. Antigen delivery within the context of dead/dying cells mimics more physiologic conditions likely to occur during cross-presentation, such as virally infected cells dying in the course of infection. The recently identified CLEC9A, which is exclusively expressed on CD8α^{+} DCs, is most likely responsible for the uptake of dead/dying *MHCI*$^{-/-}$ splenocytes (Sancho et al., 2009).

Finally, recipient mice were harvested 3 days after antigen administration and analyzed by flow cytometry. As a negative control, un-pulsed *MHCI*$^{-/-}$ splenocytes were injected. OT-I T cells in these control mice did not proliferate, as demonstrated by a

failure to dilute CFSE (Fig. 33 A). OT-I T cells injected into wild-type recipients given OVA-pulsed *MHCI*$^{-/-}$ splenocytes completely diluted CFSE, indicating that all the cells had proliferated (Fig. 33 A). In addition, the absolute number of OT-I T cells recovered increased, also indicating proliferation (Fig. 33 B).

Batf3$^{-/-}$ mice cannot cross-present necrotic-cell associated antigen due to the absence of CD8α^+ DCs, as previously shown *in vitro* (Hildner et al., 2008). We now extend this finding to *in vivo* cross-presentation. OT-I T cells injected into *Batf3*$^{-/-}$ mice and given antigen did not proliferate as measured by CFSE dilution and absolute cell numbers (Fig. 33 A). Interestingly, high doses of antigen can induce OT-I T cell proliferation in *Batf3*$^{-/-}$ mice *in vivo* (Fig. 34 B), suggesting that at high doses of antigen, other cells that are less efficient at cross-presentation can compensate for the absence of CD8α^+ DCs. However, such high doses of antigen are unlikely to occur in physiologic settings, highlighting the importance of CD8α^+ DCs in CD8$^+$ T cell priming.

Since IL-12 treatment restores the CD8α^+ DC population in *Batf3*$^{-/-}$ mice, we asked if *in vivo* antigen cross-presentation was also restored with IL-12 treatment (Fig. 33). To ensure that IL-12 alone was not sufficient to cause antigen-independent OT-I T cell proliferation, we treated mice given unpulsed *MHCI*$^{-/-}$ splenocytes with IL-12. IL-12 treatment in the absence of antigen did not cause proliferation of OT-I T cells (Fig. 33 A). In addition, OT-I proliferation was comparable between wild-type untreated and IL-12 treated mice. However, IL-12 treated *Batf3*$^{-/-}$ mice now re-gained the ability to induce OT-I proliferation in response to exogenous OVA *in vivo*. This result suggests that the restored CD8α^+ DCs in IL-12 treated *Batf3*$^{-/-}$ mice were functional and could cross-

present exogenous necrotic-cell associated antigen as efficiently as their wild-type counterparts. However, it is still possible that IL-12 is having additional effects *in vivo* that could confound these conclusions. For example, IL-12 could be enhancing the ability of other cells to cross-present. An *in vitro* cross-presentation assay performed with sorted CD8α$^+$ DCs from IL-12 treated *Batf3*$^{-/-}$ mice must be done to completely rule out these possibilities, and to demonstrate the cross-presentation ability of the restored CD8α$^+$ DCs on a per cell basis.

Restored Batf3*$^{-/-}$ *CD8α*$^+$ *DCs can produce IL-12 in response to T. gondii infection in vivo

To determine if restored CD8α$^+$ DCs in *Batf3*$^{-/-}$ mice could function in the context of *T. gondii* infection, we examined intracellular IL-12p40 levels in these cells on days 3 and 7 after infection (Fig. 35). As discussed above, wild-type CD8α$^+$ DCs express IL-12p40 as early as day 3 after infection, and continue to express this cytokine on day 7. IL-12 treated wild-type CD8α$^+$ DCs, on the other hand, do not express significant levels of IL-12p40 on day 3 after infection, but begin to express IL-12p40 on day 7. As seen in Figure 34, IL-12-treated wild-type mice have lower parasite burden as compared to untreated wild-type mice, which could account for the delayed kinetics of IL-12p40 production by the CD8α$^+$ DCs in IL-12-treated mice.

We next examined IL-12-treated *Batf3*$^{-/-}$ CD8α$^+$ DCs in *T. gondii*-infected mice (Fig. 35). Three days after infection, there is no IL-12p40 being produced by the restored *Batf3*$^{-/-}$ CD8α$^+$ DCs, similar to their IL-12 treated wild-type counterparts. However, on

day 7 after infection, approximately 25% of CD8α$^+$ DCs in both wild-type and *Batf3*$^{-/-}$ mice are positive for IL-12p40. In summary, while the kinetics of endogenous IL-12 production by CD8α$^+$ DCs is slower in IL-12-treated *T. gondii* infected mice, both wild-type and *Batf3*$^{-/-}$ CD8α$^+$ DCs produce IL-12 7 days after infection.

Restored Batf3*$^{-/-}$ *CD8α*$^+$ *DCs can prime CD8*$^+$ *T cells to T. gondii-specific antigens in vivo

In addition to producing IL-12, CD8α$^+$ DCs are required for priming *T. gondii*-specific CD8$^+$ T cells during *in vivo* infection (Fig. 3). Therefore, we next asked if the IL-12-restored CD8α$^+$ DCs in *Batf3*$^{-/-}$ mice could prime CD8$^+$ T cells *in vivo* (Fig. 36). Wild-type and *Batf3*$^{-/-}$ animals were infected with *T. gondii* and treated with IL-12 during the first five days of infection, then harvested on day 7 for analysis. To test if T cells were primed *in vivo*, we cultured splenocytes from the infected animals overnight with peptide from the *T. gondii*-derived protein GRA4. After re-stimulation, T cells were analyzed for IFNγ production by intracellular cytokine staining. Wild-type T cells could produce IFNγ in response to the peptide from both untreated and IL-12 treated mice (Fig. 35). *Batf3*$^{-/-}$ T cells from mice that did not receive IL-12 could not produce IFNγ after *in vitro* re-stimulation, consistent with Figure 3. However, T cells from *Batf3*$^{-/-}$ IL-12 treated mice now regained the ability to produce IFNγ in response to the GRA4 peptide. This data suggests that IL-12-restored CD8α$^+$ DCs in *Batf3*$^{-/-}$ mice can present *T. gondii*-derived antigen to CD8$^+$ T cells and prime the adaptive immune response. However, as with the *in vivo* cross-presentation assay above, the priming ability of the IL-12-restored CD8α$^+$

DCs needs to be tested on a per cell basis *in vitro* to rule out other effects of IL-12 treatment during *in vivo* priming.

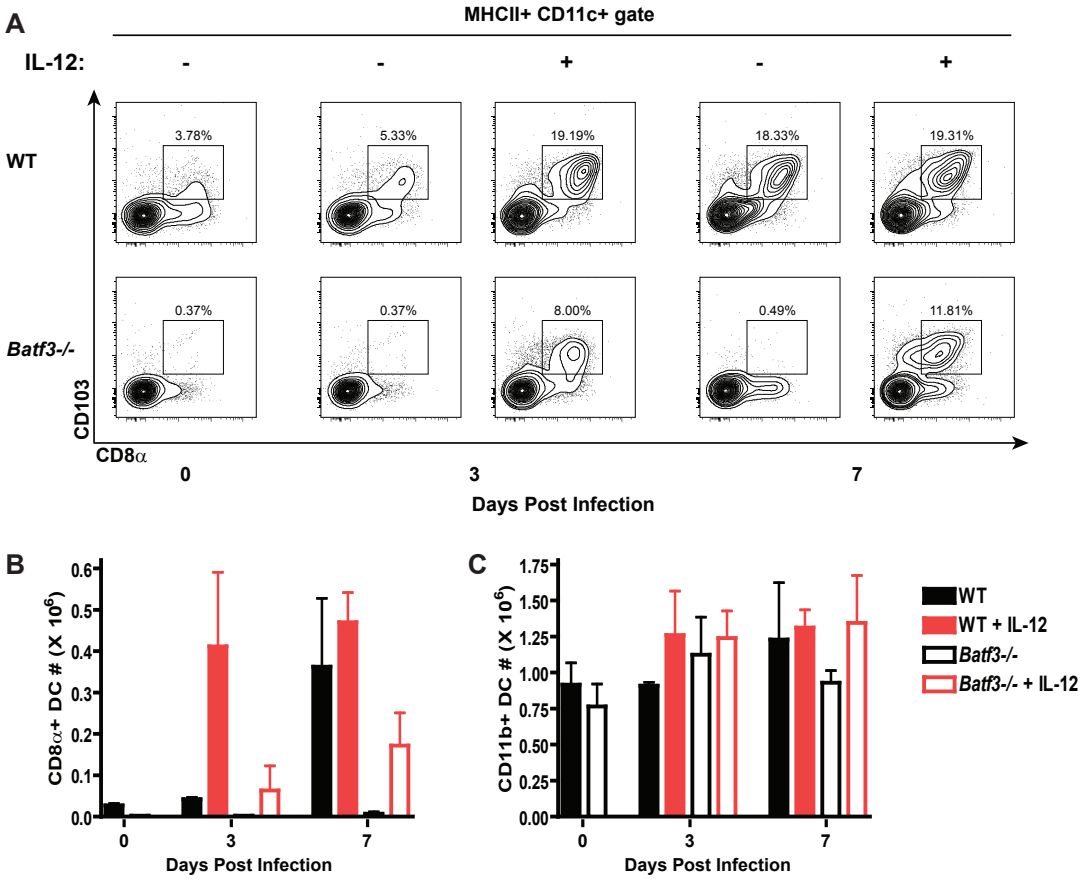

Figure 18. IL-12 administration rescues CD8α$^+$ DC development in infected *Batf3*$^{-/-}$ mice. 129S6/SvEv wild-type and *Batf3*$^{-/-}$ mice were infected with *T. gondii* and injected with saline or 0.5µg of recombinant murine IL-12 on days 0, 1, 2, 3, and 4 after infection. Animals were sacrificed on days 3 and 7 after infection, and analyzed by flow cytometry (n=3). (A) Representative FACS plots gated on Aqua-negative, MHCII$^+$, CD11c$^+$ conventional dendritic cells. (B and C) Absolute numbers of CD8α$^+$ CD103$^+$ DCs (B) and CD11b$^+$ DCs (C) in the spleen of wild-type and *Batf3-/-* mice on days 3 and 7 of infection. (B, C) Data are represented as mean +/- standard deviation.

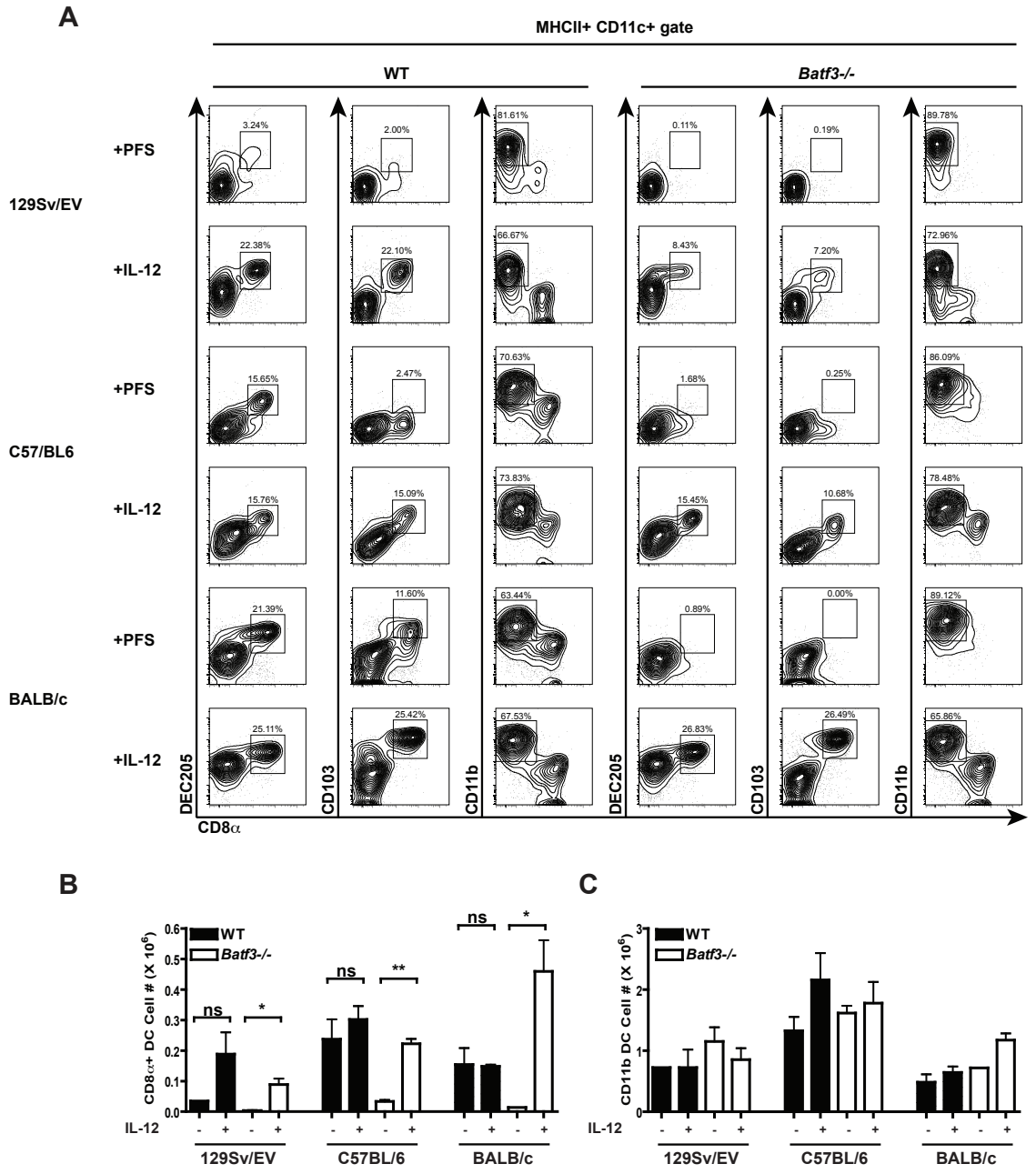

Figure 19. IL-12 treatment restores CD8α$^+$ DC development in *Batf3*$^{-/-}$ mice. Wild-type (black bars) and *Batf3*$^{-/-}$ (white bars) mice were given exogenous IL-12 and harvested for analysis of the splenic conventional DC compartment. 129S6/SvEV and C57BL/6 mice were treated on days 0, 1, and 2, and harvested on day 3. BALB/c mice were treated on days 0, 1, 2, 3 and 4, and harvested on day 5. (A) Representative FACS plots of the MHCII$^+$ CD11c$^+$ DCs. (B and C) Absolute numbers of CD8α$^+$ DCs (B) and CD11b$^+$ DCs (C). Data are represented as mean +/- standard deviation. Not significant (ns): P>0.05, *: 0.01<P<0.05, **: 0.001<P<0.01.

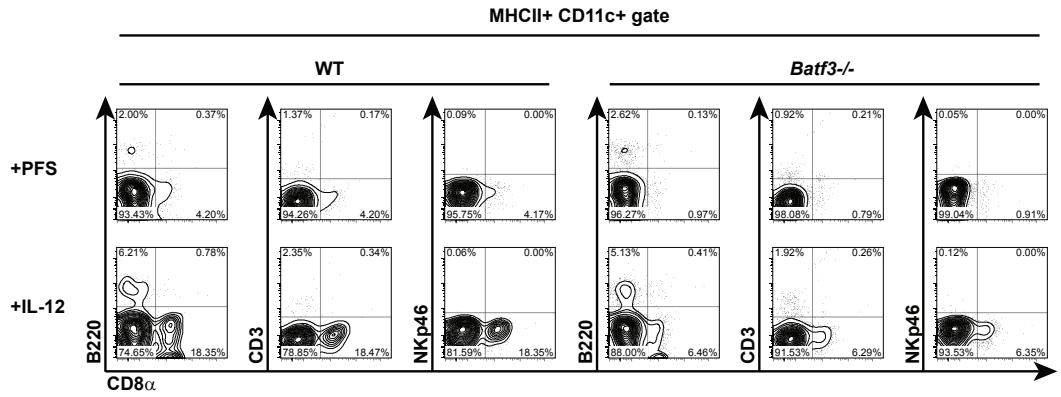

Figure 20. CD8α$^+$ DCs in the spleen of IL-12-treated *Batf3*$^{-/-}$ mice do not express the B cells marker B220, the T cell marker CD3, or the NK cell marker NKp46.
129S6/SvEV wild-type and *Batf3*$^{-/-}$ mice were treated with IL-12 on days 0, 1, and 2, and harvested on day 3 for FACS analysis. Representative FACS plots gated on MHCII$^+$ CD11c$^+$ DCs are shown.

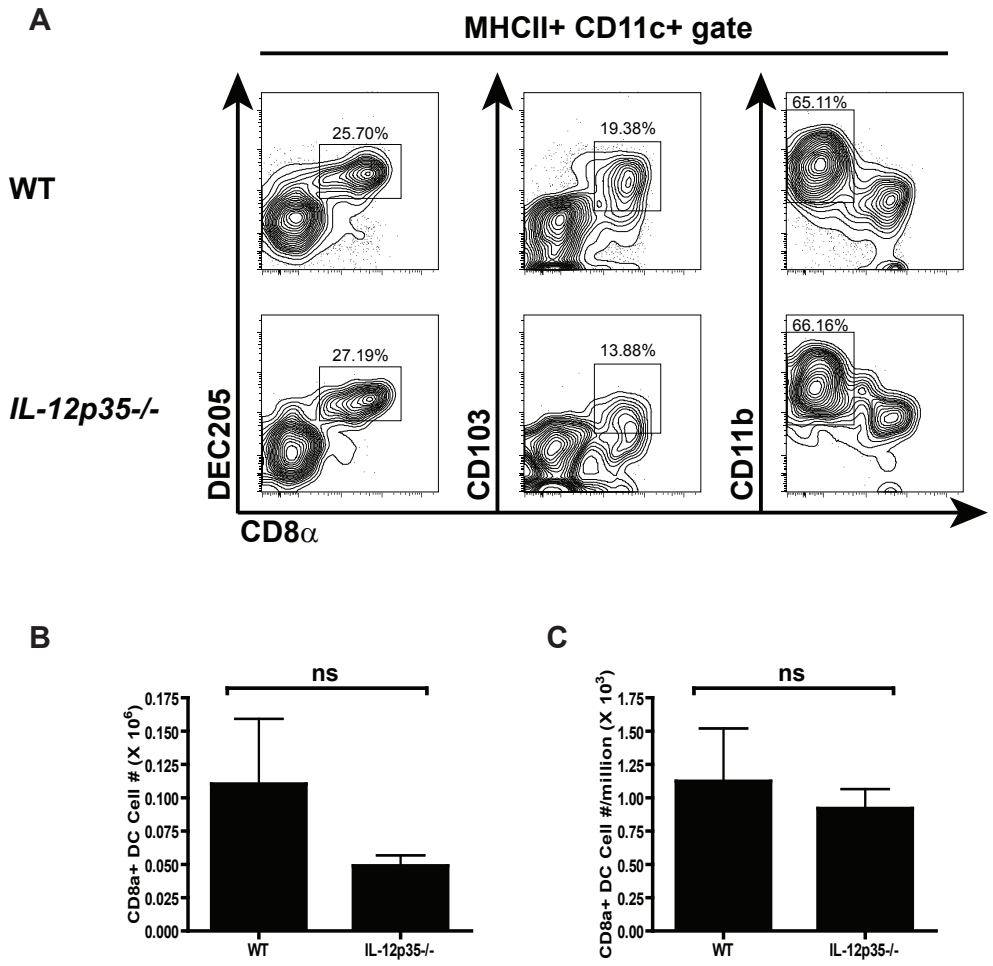

Figure 21. Mice deficient in IL-12 can develop splenic CD8α$^+$ DCs in the steady state. BALB/c wild-type and *IL-12p35*$^{-/-}$ mice were harvested for analysis of the splenic conventional DC compartment. (A) Representative FACS plots gated on MHCII$^+$ CD11c$^+$ cells are shown. (B and C) Absolute numbers of CD8α$^+$ DCs (B), or the number of CD8α$^+$ DC per million splenocytes (C). Data are represented as mean +/- standard deviation. Not significant (ns): P>0.05.

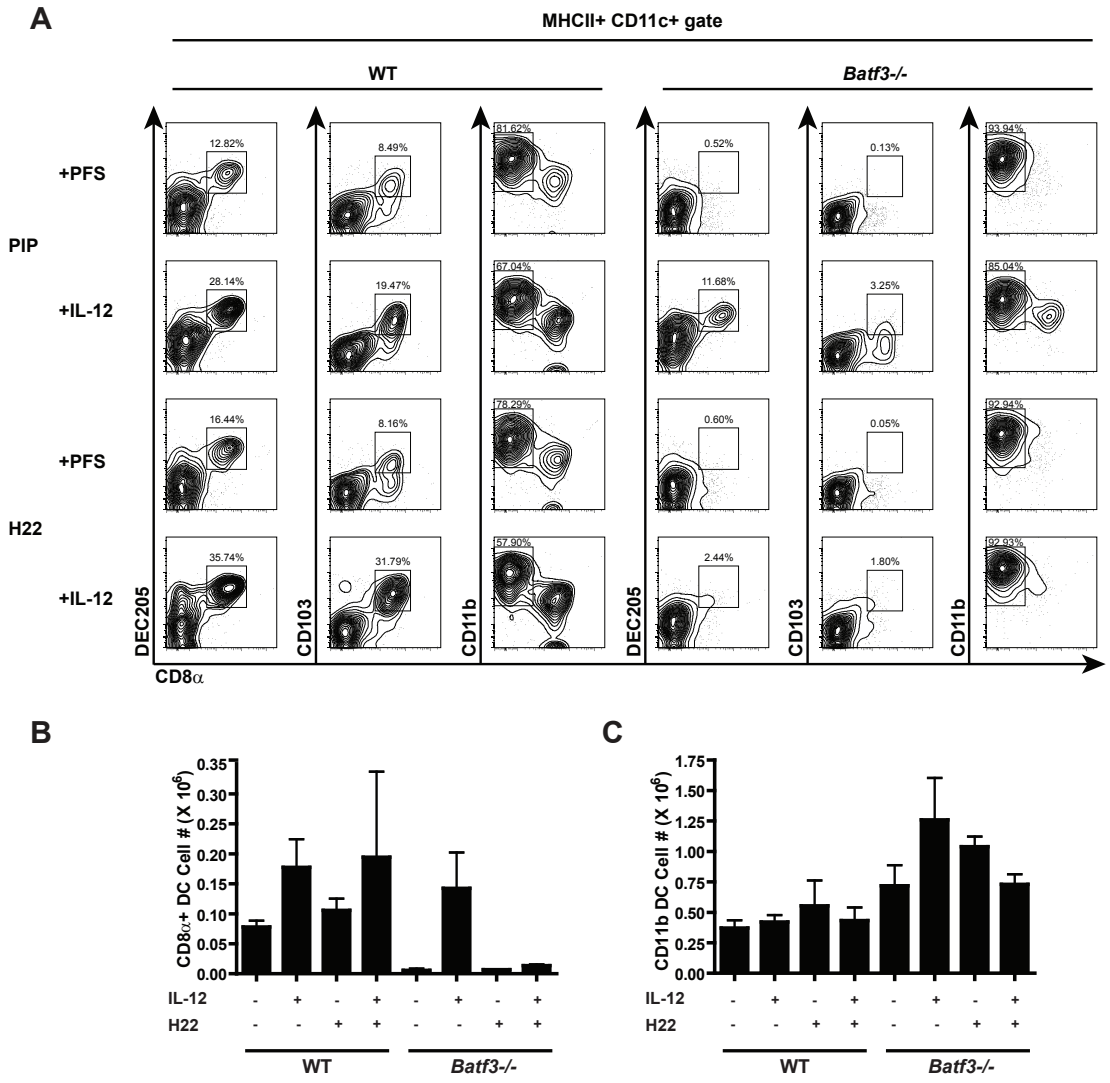

Figure 22. IL-12-mediated restoration of CD8α$^+$ DCs in *Batf3*$^{-/-}$ mice is IFNγ-dependent. BALB/c wild-type and *Batf3*$^{-/-}$ mice were treated with control PIP or anti-IFNγ blocking antibody H22 on days -2 and +1, given IL-12 on day 0, and harvested on day 3 for analysis of the splenic conventional DC compartment. (A) Representative FACS plots of MHCII$^+$ CD11c$^+$ DCs. (B and C) Absolute numbers of CD8α$^+$ DCs (B) and CD11b$^+$ DCs (C). Data are represented as mean +/- standard deviation.

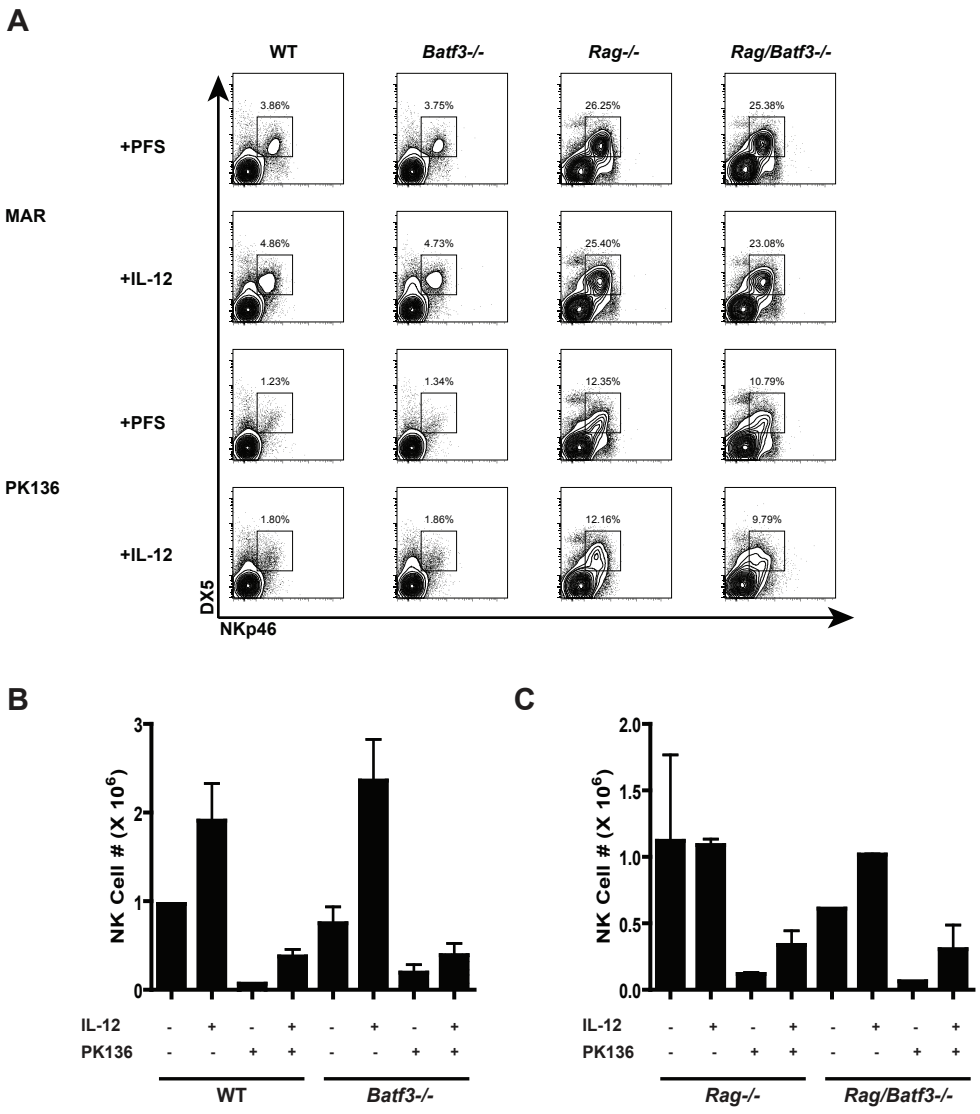

Figure 23. Efficiency of NK cell depletion using anti-NK1.1 PK136 antibody. C57BL/6 wild-type, *Batf3*$^{-/-}$, *Rag*$^{-/-}$, and *Rag/Batf3*$^{-/-}$ mice were treated with 200µg of NK cell depleting antibody PK136 on day -3, followed by 100µg on day 0, and in addition were treated with IL-12 on day 0. All mice were harvested on day 3 and analyzed for NK cell depletion efficiency. (A) Representative FACS plots of splenocytes. (B and C) Absolute numbers of NK cells in all mice. Data are represented as mean +/- standard deviation.

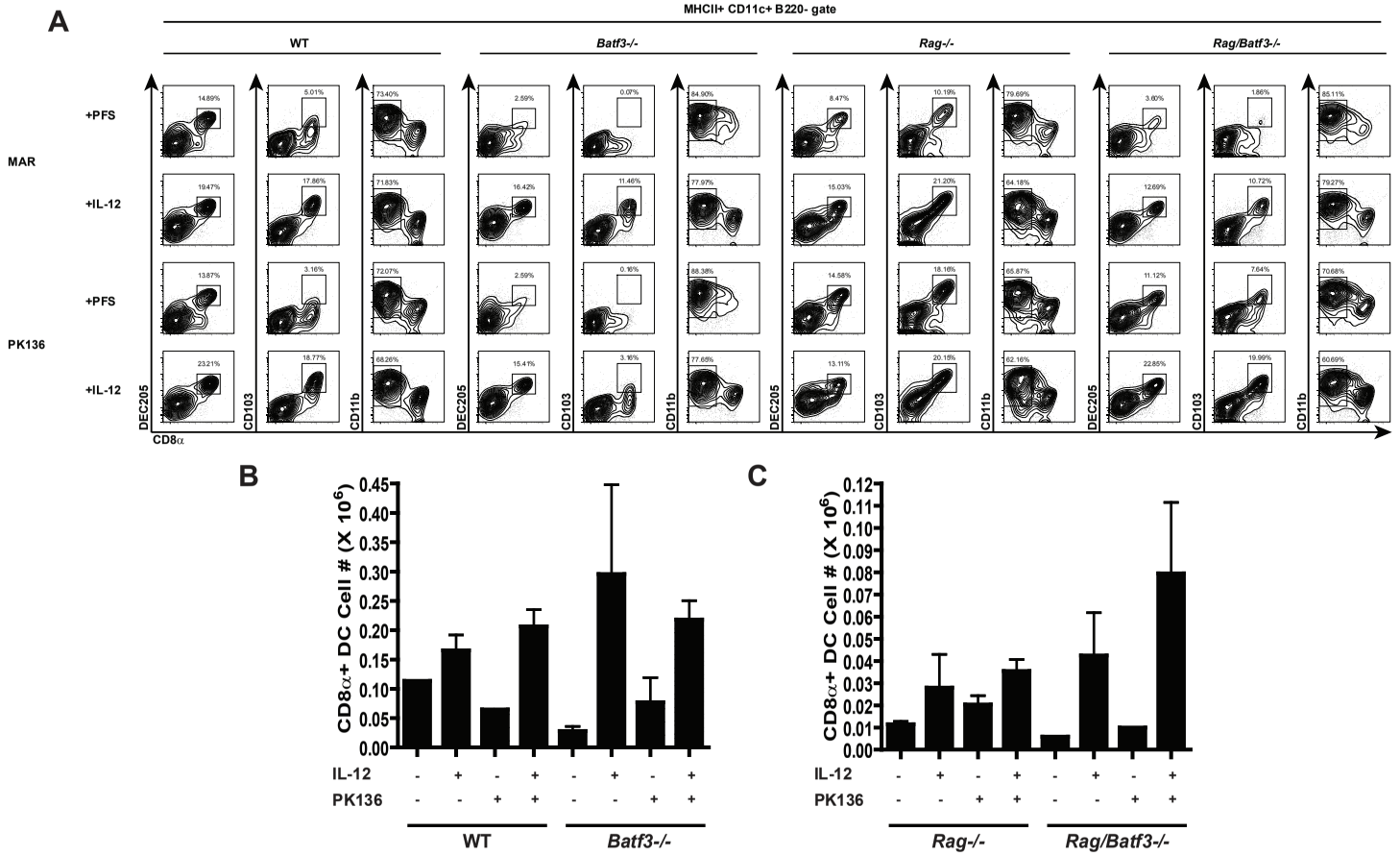

Figure 24. IL-12 can restore CD8α$^+$ DCs in *Batf3*$^{-/-}$ mice in the absence of B, T and NK cells. C57BL/6 wild-type, *Batf3*$^{-/-}$, *Rag*$^{-/-}$, and *Rag/Batf3*$^{-/-}$ mice were treated with 200μg PK136 on day -3, 100μg PK136 on day 0, and IL-12 on day 0. Mice were harvested on day 3 for analysis of the conventional DC compartment. (A) Representative FACS plots gated on MHCII$^+$ CD11c$^+$ B220$^-$ cells. (B and C) Absolute numbers of CD8α$^+$ DCs in all mice. Data are represented as mean +/- standard deviation.

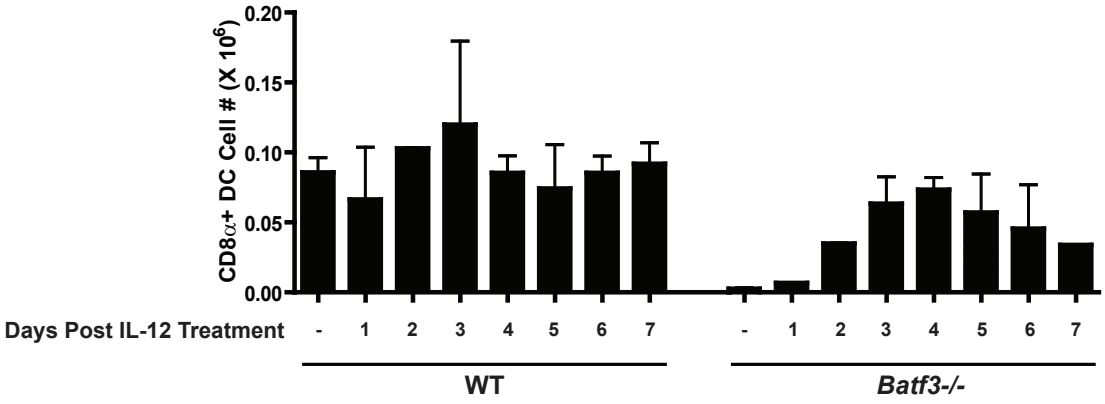

Figure 25. Time course of CD8α^+ DC development in IL-12-treated *Batf3*$^{-/-}$ mice. BALB/c wild-type and *Batf3*$^{-/-}$ mice were treated with a single dose of IL-12, and harvested 1 to 7 days later for analysis of spleen DCs. Absolute numbers of CD8α^+ DCs are shown. Data are represented as mean +/- standard deviation.

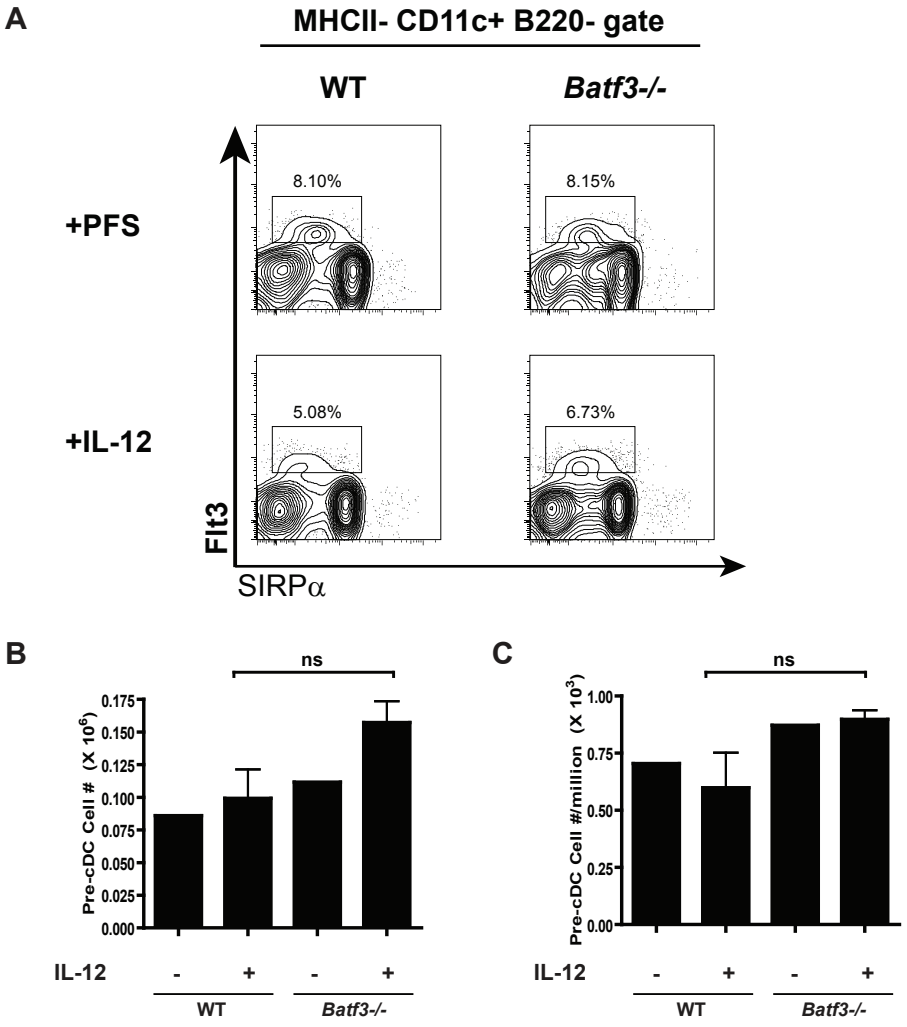

Figure 26. Pre-cDC numbers in the spleen are unchanged with IL-12 treatment. C57BL/6 wild-type and *Batf3*$^{-/-}$ mice were treated with a single dose of IL-12 on day 0, and sacrificed on day 3 for analysis of the pre-cDC in the spleen. (A) Representative FACS plots gated on MHCII^{+} CD11c^{+} B220^{-} cells are shown. (B and C) Absolute numbers of pre-cDCs (B), or the number of pre-cDCs per million splenocytes. Data are represented as mean +/- standard deviation.

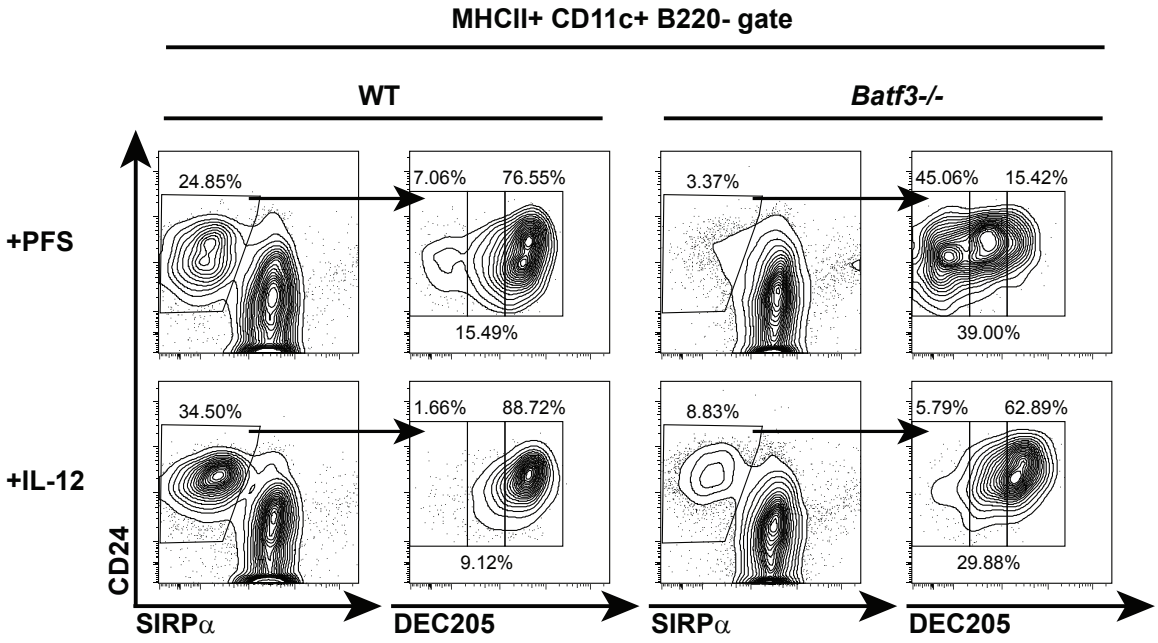

Figure 27. IL-12 treatment causes upregulation of DEC205 on CD8α$^+$ DC precursors in both wild-type and *Batf3*$^{-/-}$ mice. C57BL/6 wild-type and *Batf3*$^{-/-}$ mice treated on day 0 with IL-12 were analyzed for various CD8α$^+$ DC markers. Representative FACS plots gated on MHCII$^+$ CD11c$^+$ B220$^-$ cells are shown.

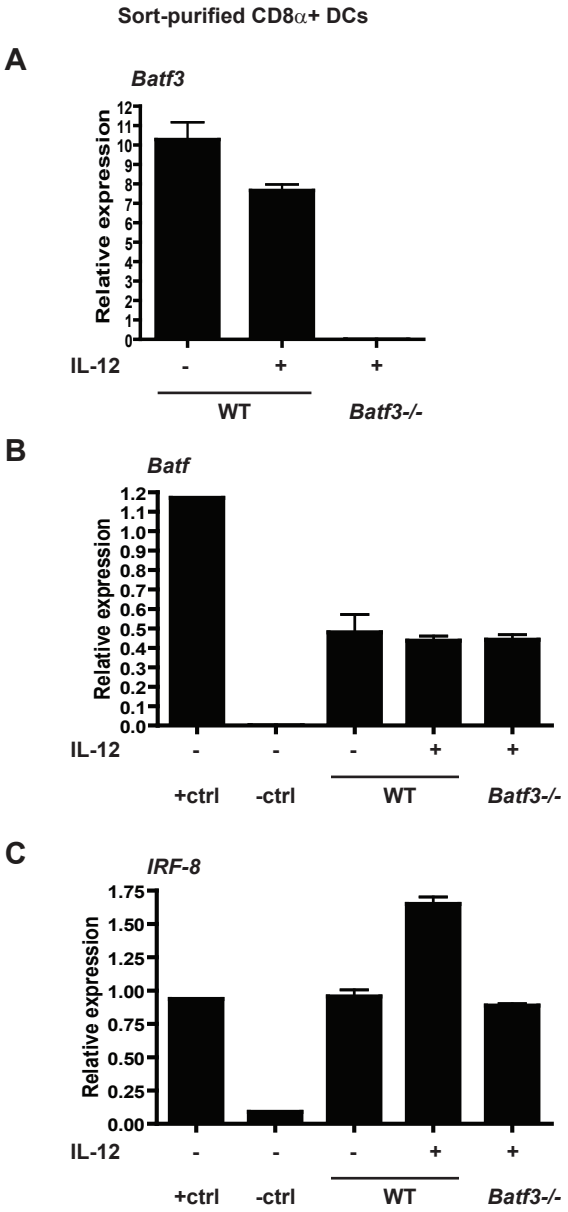

Figure 28. *Batf3*$^{-/-}$ IL-12-restored CD8α^{+} DCs express normal levels of the transcription factors *Batf* and *IRF-8*. C57BL/6 wild-type and *Batf3*$^{-/-}$ mice were treated with IL-12 on days 0, 1, and 2, and harvested on day 3 for sort purification of CD8α^{+} DCs. Shown is relative expression of *Batf3* (A), *Batf* (B), and *IRF-8* (C), as normalized against *HPRT*. Controls were as follows: *Batf*: +ctrl = WT LPS activated B cells, -ctrl = *Batf-/-* LPS activated B cells; *IRF-8*: +ctrl = *in vitro* Flt3L-cultured CD8a+ equivalent DCs, -ctrl = *in vitro* Flt3L-cultured CD4+ equivalent DCs. Data are represented as mean +/- standard deviation.

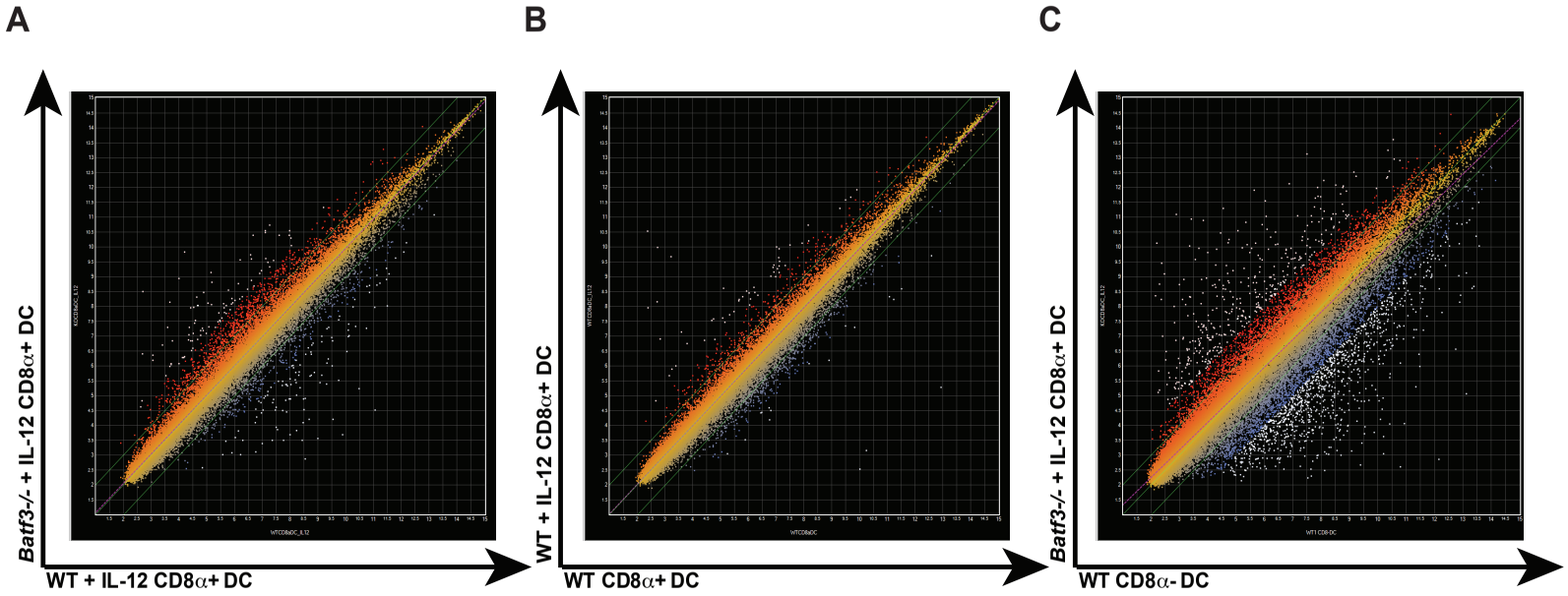

Figure 29. M plots comparing gene expression of IL-12-restored CD8α$^+$ DCs. Genes with a greater than 4-fold difference between the samples are highlighted in white. (A) Comparison of WT IL-12-treated CD8α$^+$ DCs (X-axis) to *Batf3*$^{-/-}$ IL-12-treated CD8α$^+$ DCs (Y-axis), 206 genes being greater than 4-fold different between the samples. (B) Comparison of WT CD8α$^+$ DCs (X-axis) to WT IL-12-treated CD8α$^+$ DCs (Y-axis), with 70 genes being greater than 4-fold different between the samples. (C) Comparison of WT CD8α$^-$ DCs (X-axis) to *Batf3*$^{-/-}$ IL-12-treated CD8α$^+$ DCs (Y-axis), with 1402 genes being greater than 4-fold different between the samples. Performed in collaboration with Wumesh KC.

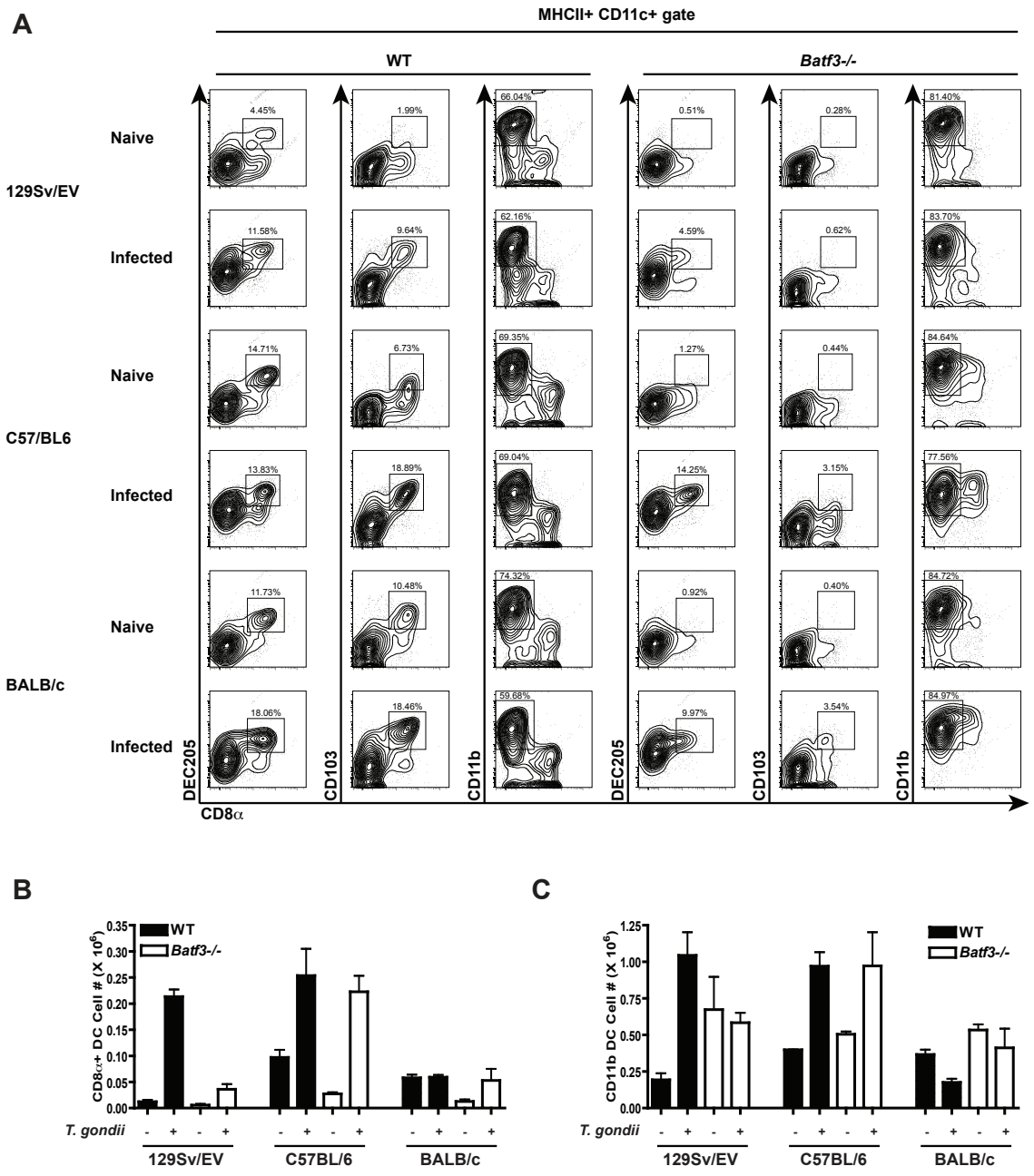

Figure 30. *T. gondii* infection restores CD8α$^+$ DC development in *Batf3*$^{-/-}$ mice. 129S6/SvEV, C57BL/6 and BALB/c wild-type and *Batf3*$^{-/-}$ mice were infected with *T. gondii* tachyzoites ip and harvested 7 days after infection for analysis of the splenic conventional DC compartment. (A) Representative FACS plots of MHCII$^+$ CD11c$^+$ DCs. (B and C) Absolute numbers of CD8α$^+$ DCs (B) and CD11b$^+$ DCs (C). Data are represented as mean +/- standard deviation.

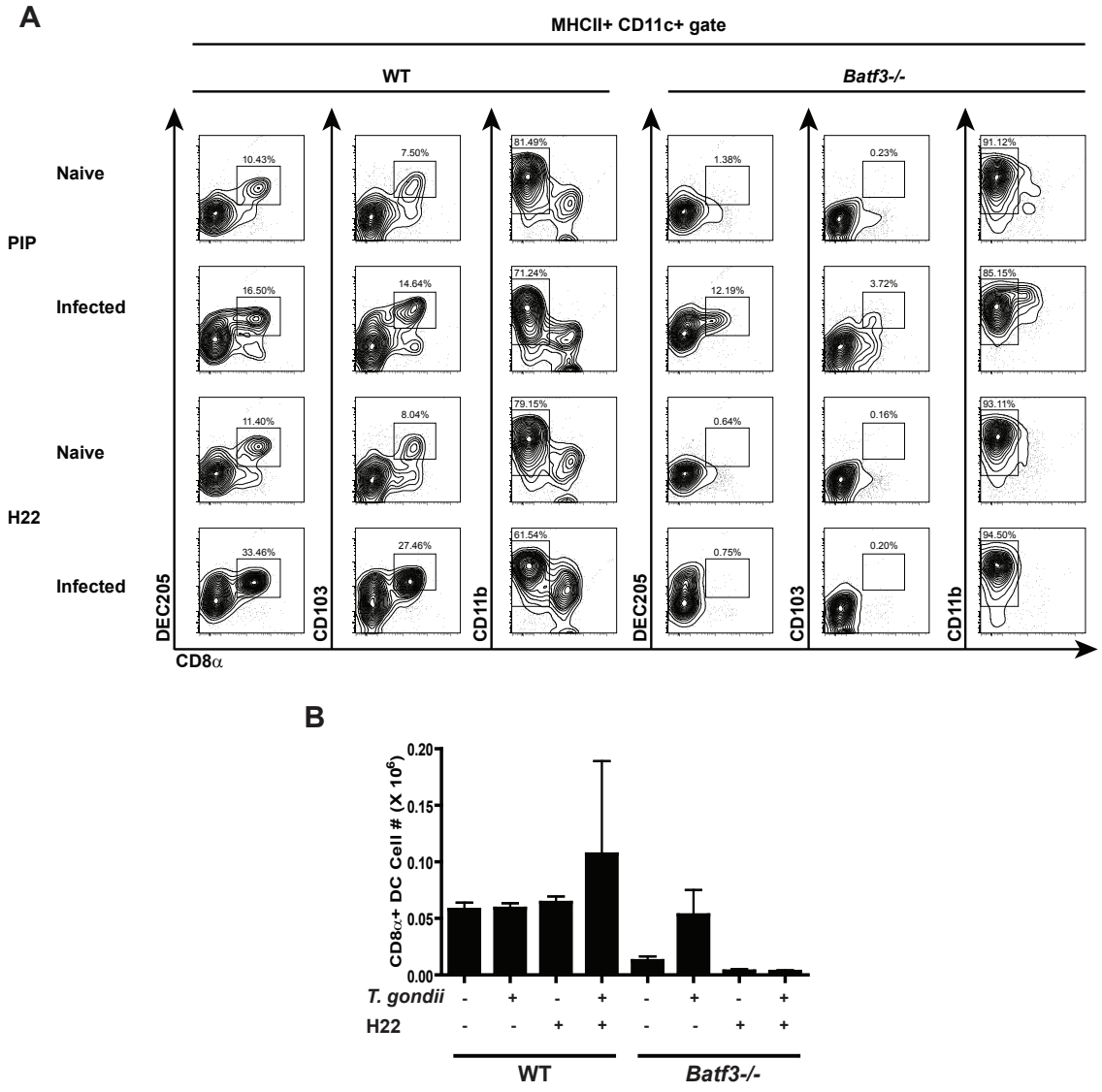

Figure 31. *T. gondii*-mediated restoration of CD8α$^+$ DCs in *Batf3*$^{-/-}$ mice is IFNγ-dependent. BALB/c wild-type and *Batf3*$^{-/-}$ mice were treated with control antibody PIP or anti-IFNγ blocking antibody H22 on days -1 and +2, infected with *T. gondii* on day 0, and sacrificed for analysis on day 7. (A) Representative FACS plots gated on MHCII$^+$ CD11c$^+$ cells are shown. (B) Absolute numbers of CD8α$^+$ DCs are shown. Data are represented as mean +/- standard deviation.

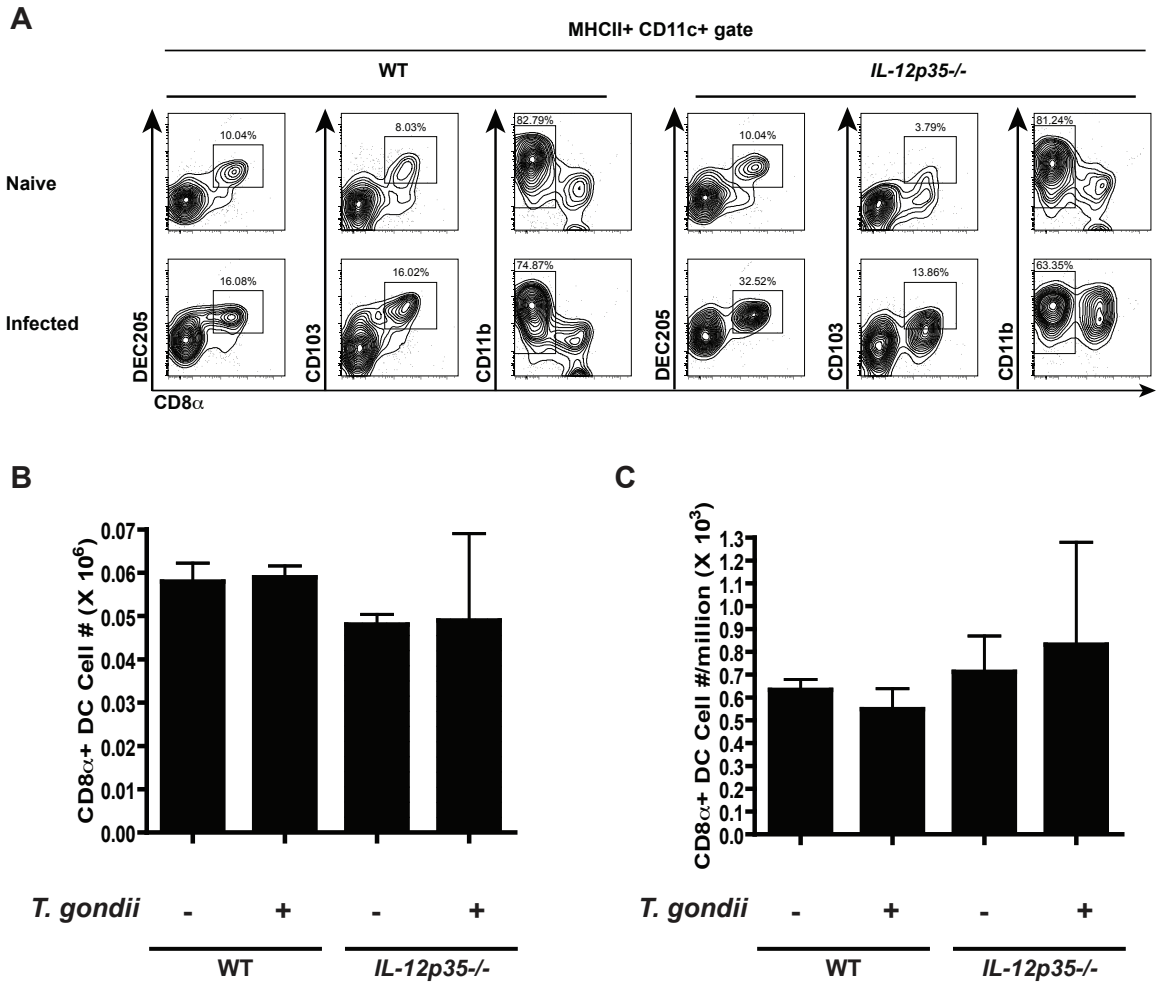

Figure 32. *IL-12p35*$^{-/-}$ CD8α^+ DCs increase in percentage, but not absolute numbers, after *T. gondii* infection. BALB/c wild-type and *IL-12p35*$^{-/-}$ mice were infected with *T. gondii* tachyzoites ip, sacrificed on day 7 after infection, and analyzed for the composition of the conventional DC compartment. (A) Representative FACS plots gated on MHCII$^+$ CD11c$^+$ cells are shown. (B) Absolute numbers of CD8α^+ DCs in the spleen in naïve and infected mice. Data are represented as mean +/- standard deviation.

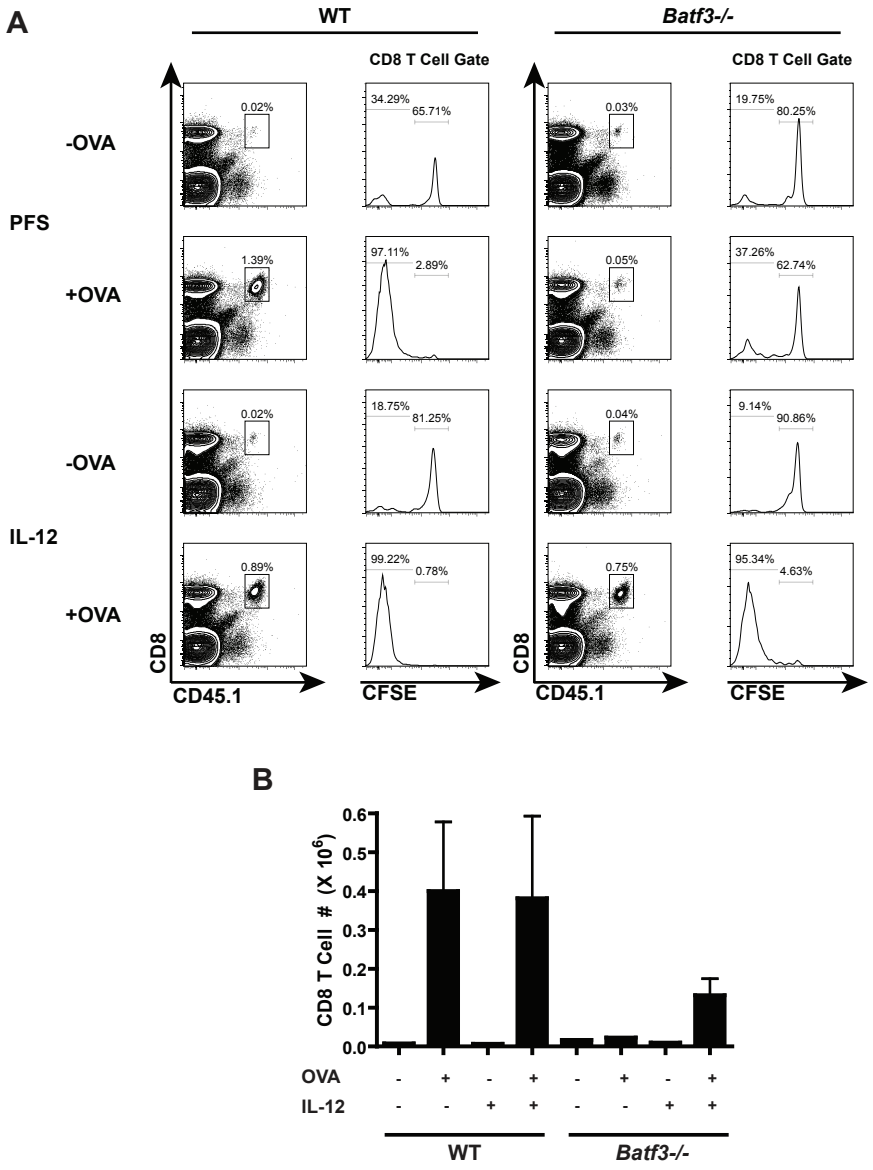

Figure 33. IL-12 treatment restores cross-presentation in *Batf3*$^{-/-}$ mice *in vivo*. C57BL/6 wild-type and *Batf3*$^{-/-}$ mice were analyzed for *in vivo* cross-presentation of necrotic cells. (A) Representative FACS plots gated on CD8^{+} CD45.1^{+} OT-I transgenic T cells in the left panel, followed by analysis of CFSE dilution in OT-I T cells in the right panel. (B) Absolute numbers of OT-I transgenic T cells in the spleen. Data are represented as mean +/- standard deviation.

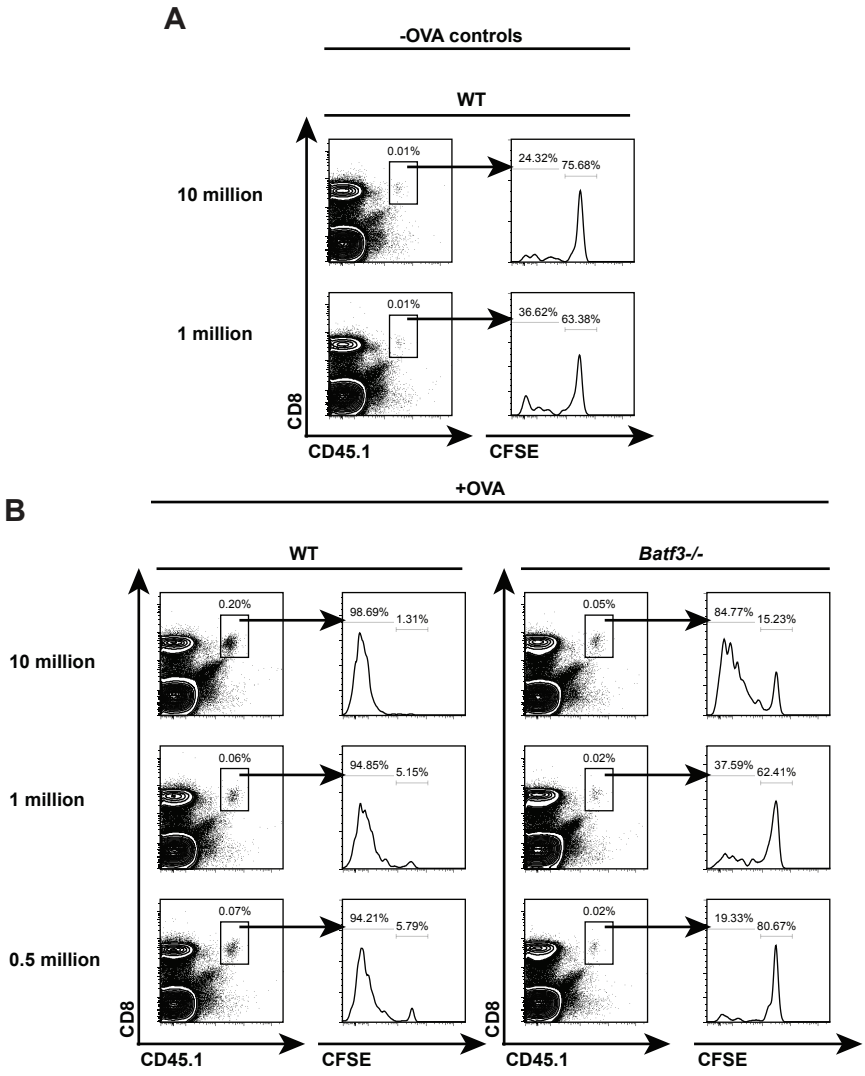

Figure 34. *In vivo* cross-presentation of necrotic cell-associated antigen is severely impaired in *Batf3*$^{-/-}$ mice. C57BL/6 wild-type and *Batf3*$^{-/-}$ mice were tested for cross-presentation of *MHCI*$^{-/-}$ OVA-pulsed splenocytes *in vivo*. Representative FACS plots are shown.

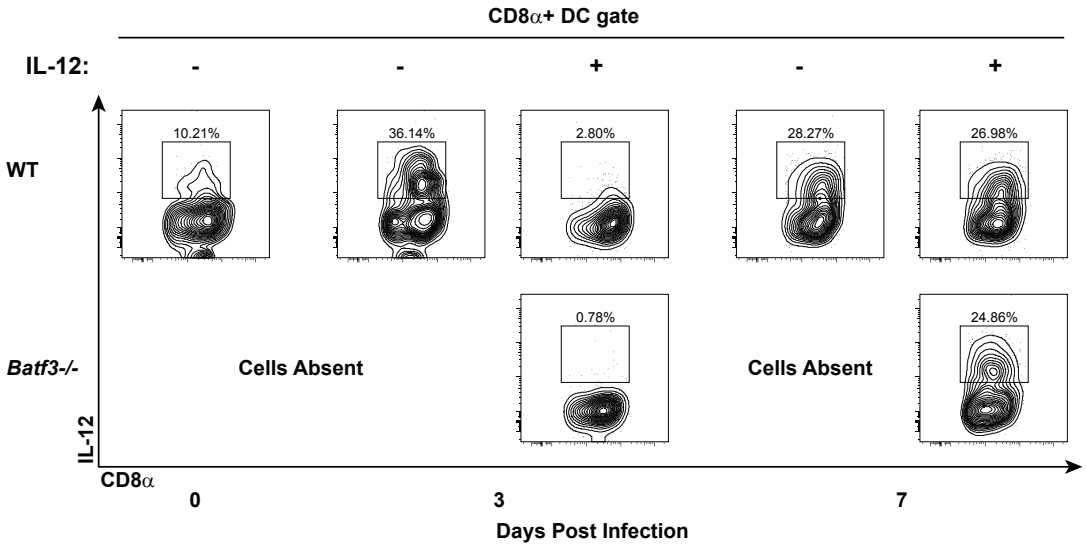

Figure 35. IL-12-restored CD8α$^+$ DCs in *Batf3*$^{-/-}$ mice produce IL-12 in response to *T. gondii* infection *in vivo.* 129S6/SvEv wild-type and *Batf3*$^{-/-}$ mice were infected with *T. gondii* and injected with saline or 0.5μg of recombinant murine IL-12 on days 0, 1, 2, 3, and 4 after infection. Animals were sacrificed on days 3 and 7 after infection, and analyzed by flow cytometry (n=3). Representative FACS plots gated on MHCII$^+$ CD11c$^+$ CD8α$^+$ CD103$^+$ DCs are shown.

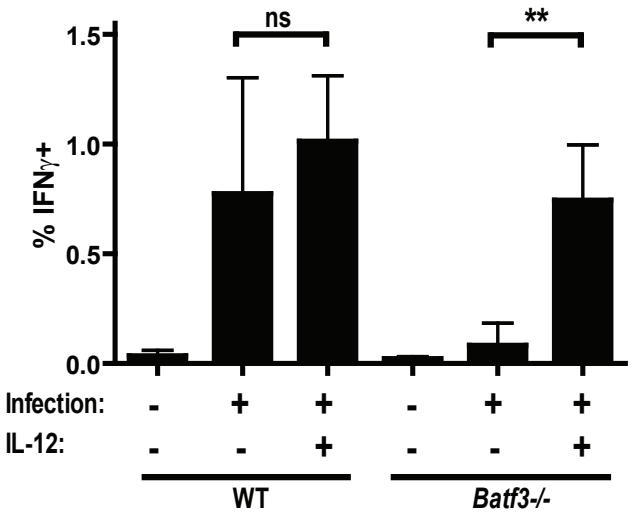

Figure 36. CD8$^+$ T cell priming to *T. gondii*-derived antigen is restored in infected *Batf3*$^{-/-}$ mice given IL-12. Balb/c wild-type and *Batf3*$^{-/-}$ mice were sacrificed on day 7 after infection, and analyzed for CD8$^+$ T cell priming. Shown are absolute numbers of IFNγ-positive CD8$^+$ T cells as measured by intracellular cytokine staining after overnight re-stimulation of whole splenocytes with the GRA4 peptide (n=5). Not significant (ns): $P>0.05$, **: $0.001<P<0.01$. Data are represented as mean +/- standard deviation.

CHAPTER 7

Discussion

CD8α$^+$ DCs are the critical source of IL-12 during T. gondii infection

The present study identifies a second critical activity for the CD8α$^+$ DC subset beyond its recognized role in priming CD8$^+$ T cells responses to viruses. Previously, we demonstrated that the CD8α$^+$ dendritic cell was critical in promoting effective CTL responses against West Nile virus, and was crucial in that setting for cross-presentation of virus-derived antigens involved in immune activation (Hildner et al., 2008). Additionally, priming of Sendai virus-specific CD8$^+$ T cells has been shown to be dependent on the peripheral cross-presenting CD103$^+$ DC, which is also absent in the *Batf3*-deficient mice (Edelson et al., 2010). Here, we show that priming of CD8$^+$ T cells to endogenous *T. gondii* antigen is also defective in *Batf3*-deficient mice early after infection. Additionally, we demonstrate that the same DC subset provides a critical but distinct function by acting as an important early sensor of infection by *T. gondii*. The inability of mixed chimeras generated from bone marrow of *IL-12p35*-deficient and *Batf3*-deficient mice to control *T. gondii* infection demonstrates that the CD8α$^+$ DC is the only cell whose IL-12 production significantly contributes to reducing pathogen burden during acute infection. Thus, in each of these pathogen settings, the CD8α$^+$ DC is unique in its provision of effective defense mechanisms, but the mechanisms by which this cell mediates defenses are different.

The role of CD8α$^+$ DCs in protection against *T. gondii* infection was previously

suggested through the observation that this subset was the major cell type to produce IL-12 in response to intravenous administration of *T. gondii* antigen STAg (Reis e Sousa et al., 1997). Furthermore, $CD8\alpha^+$ DCs express TLR11 at much higher levels than $CD8\alpha^-$ DCs, neutrophils, and monocytes (Yarovinsky et al., 2005) and (Fig. 11). However, pDCs also express TLR11 (Pepper et al., 2008), so that the correlation between sensitivity to activation by *T. gondii* does not exclusively identify the $CD8\alpha^+$ DC as the main responder. Thus, no clear evidence previously was able to uniquely identify the $CD8\alpha^+$ DC as a cell type required for controlling *T. gondii* infection *in vivo*. In addition, while TLR11-deficient mice have impaired IL-12 production following infection by *T. gondii* (Yarovinsky et al., 2005), these mice only show a modest change in susceptibility compared to the dramatic increase seen in MyD88 knockout mice (Scanga et al., 2002), implying that additional sensors for *T. gondii* infection may exist. One group has reported an additional TLR that is responsive to *T. gondii*, TLR12, and has found that mice deficient in both TLR11 and TLR12 are highly susceptible to this infection (A Sher, unpublished). Our data strongly demonstrate that the $CD8\alpha^+$ DC is the main cell induced to produce IL-12 after acute challenge with *T. gondii* tachyzoites, which agrees with selective expression of TLR11, and potentially other uncharacterized *T. gondii*-specific sensors such as TLR12, by this cell type.

Several questions still remain. Once the report on TLR12 has been published, it will be interesting to investigate the expression of this receptor, and determine if it is also highly expressed on $CD8\alpha^+$ DCs. At this time, the nomenclature between TLR11 and TLR12 is extremely muddled, and it is difficult to determine the sequence or location of

TLR12. What was originally described as TLR11, which responds to *T. gondii*-profilin (Yarovinsky et al., 2005), is now listed as TLR12 in NCBI. In addition, the TLR11 ortholog in humans is a pseudogene, and there is still a question of how immune responses to *T. gondii* are initiated in humans (Pifer and Yarovinsky, 2011).

Another unanswered question is the underlying mechanism of the susceptibility of *Batf3*$^{-/-}$ mice to oral infection with *T. gondii*. While intraperitoneal infection with *T. gondii* is considered to be "systemic", oral challenge sets up a local site of infection within the small intestine, where *T. gondii* infects enterocytes in the ileum and also enters the submucosal tissue (Barragan and Sibley, 2003). Intestinal CD103^{+} CD11b^{-} DCs are absent in *Batf3*$^{-/-}$ mice (Edelson et al., 2010), and may serve a critical function in protective immunity to oral *T. gondii* infection. We hypothesize that CD103^{+} DCs in the intestine, similar to CD8α^{+} DCs in the spleen, are early sensors of *T. gondii* and may function as the initial source of IL-12 at the site of infection. Thus, it remains to be determined if CD103^{+} DCs in the gut express high levels of TLR11, and produce IL-12 in response to *T. gondii* infection *in vivo*.

IL-12 bypasses the requirement for Batf3 in CD8α^{+} DC development

In the second part of this work, we describe a novel function of IL-12 in promoting CD8α^{+} DC development independently of *Batf3*. Both exogenous administered IL-12, as well as endogenously generated IL-12 in response to *T. gondii* infection, could restore CD8α^{+} DCs in *Batf3*$^{-/-}$ mice. Furthermore, IL-12-induced restoration of CD8α^{+} DCs was inhibited by the IFNγ blocking antibody H22. Microarray

analysis showed a high degree of similarity between the IL-12-induced CD8α$^+$ DCs in *Batf3*$^{-/-}$ mice and their wild-type counterparts in global gene expression. In addition, restored CD8α$^+$ DCs could produce IL-12 *in vivo* after *T. gondii* infection. Finally, IL-12 treatment restored *in vivo* cross-presentation to necrotic cell-associated antigens as well as *T. gondii*-derived antigens. In summary, IL-12 treatment of *Batf3*$^{-/-}$ mice rescues the CD8α$^+$ DC subset, which is functional for IL-12 production and cross-presentation.

A number of studies are currently ongoing to further characterize the mechanism by which IL-12 restores CD8α$^+$ DCs, and the functional abilities of these restored cells. One possible mechanism is compensation for *Batf3* deficiency by another AP-1 family member, such as *Batf*, after IL-12 treatment. *Batf/Batf3*-double deficient mice are being generated to directly answer this question.

We will also determine if the restored CD8α$^+$ DCs are functional during both *T. gondii* and *Listeria monocytogenes* infection. In each case, *Batf3*$^{-/-}$ mice will be treated with a single dose of IL-12 to restore CD8α$^+$ DCs, and the mice infected 4-6 days later. If restored CD8α$^+$ DCs can respond to *T. gondii* infection, the survival and parasite burden phenotype in *Batf3*$^{-/-}$ mice will be rescued. As a control for this experiment, we will include *IL-12p35*$^{-/-}$ mice to ensure there is no lasting effect of IL-12 treatment at our given time-point, such as increased IFNγ. If there is residual IFNγ after IL-12 treatment, both *Batf3*$^{-/-}$ and *IL-12p35*$^{-/-}$ mice will be protected, since IFNγ has a number of anti-parasitic activities (Yap et al., 2006). However, if there is no residual IFNγ, but restored CD8α$^+$ DCs are still present and functional, then only the *Batf3*$^{-/-}$ mice will be protected. On the other hand, *Batf3*$^{-/-}$ mice are resistant to *L. monocytogenes* infection (BT Edelson,

unpublished). Thus, if CD8α$^+$ DCs are still present and functional in IL-12-treated *Batf3*$^{-/-}$ mice during *L. monocytogenes* infection, the resistance will be abrogated.

Furthermore, to conclusively address the cross-presentation ability of restored CD8α$^+$ DCs, an *in vitro* cross-presentation assay will be performed. CD8α$^+$ DCs from wild-type and IL-12-treated *Batf3*$^{-/-}$ mice will thus be tested on a per cell basis for cross-presentation efficiency. Finally, we will investigate the missing peripheral CD103$^+$ DCs in *Batf3*$^{-/-}$ mice to determine if IL-12 treatment also restores these cells.

It is unclear what role IL-12 plays in DC subset regulation in wild-type mice during physiologic conditions, such as an infection. We hypothesize that IL-12 is important in the context of inflammation to expand the main IL-12-producing cell, the CD8α$^+$ DC, and further increase IL-12 production. However, our attempts to prove the existence of this positive feedback loop using *IL-12p35*$^{-/-}$ mice did not yield a definitive result. Future experiments will address this question using both IL-12-deficient mice, as well as IL-12-blocking antibody.

In conclusion, we demonstrate a requirement for CD8α$^+$ DC production of IL-12 during acute *T. gondii* infection, and describe a novel function of IL-12 in CD8α$^+$ DC development in *Batf3*$^{-/-}$ mice. Future experiments will aim to determine the importance of IL-12 in regulating CD8α$^+$ DC homeostasis in inflammatory settings.

REFERENCES

Aliberti,J., Schulz,O., Pennington,D.J., Tsujimura,H., Reis E Sousa, Ozato,K., and Sher,A. (2003). Essential role for ICSBP in the in vivo development of murine CD8alpha + dendritic cells. Blood *101*, 305-310.

Bar-On,L., Birnberg,T., Lewis,K.L., Edelson,B.T., Bruder,D., Hildner,K., Buer,J., Murphy,K.M., Reizis,B., and Jung,S. (2010). CX3CR1+ CD8alpha+ dendritic cells are a steady-state population related to plasmacytoid dendritic cells. Proc. Natl. Acad. Sci U. S A *107*, 14745-14750.

Barragan,A. and Sibley,L.D. (2003). Migration of Toxoplasma gondii across biological barriers. Trends Microbiol. *11*, 426-430.

Bliss,S.K., Butcher,B.A., and Denkers,E.Y. (2000). Rapid recruitment of neutrophils containing prestored IL-12 during microbial infection. J Immunol *165*, 4515-4521.

Bliss,S.K., Gavrilescu,L.C., Alcaraz,A., and Denkers,E.Y. (2001). Neutrophil depletion during Toxoplasma gondii infection leads to impaired immunity and lethal systemic pathology. Infect. Immun. *69*, 4898-4905.

Bliss,S.K., Zhang,Y., and Denkers,E.Y. (1999). Murine neutrophil stimulation by Toxoplasma gondii antigen drives high level production of IFN-gamma-independent IL-12. J Immunol *163*, 2081-2088.

Brasel,K., De Smedt,T., Smith,J.L., and Maliszewski,C.R. (2000). Generation of murine dendritic cells from flt3-ligand-supplemented bone marrow cultures. Blood *96*, 3029-3039.

CDC. Toxoplasmosis. Centers for Disease Control and Prevention, Division of Parasitic Diseases, http://www.cdc.gov/toxoplasmosis/ . 2008.

Chan,S.H., Perussia,B., Gupta,J.W., Kobayashi,M., Pospisil,M., Young,H.A., Wolf,S.F., Young,D., Clark,S.C., and Trinchieri,G. (1991). Induction of interferon gamma production by natural killer cell stimulatory factor: characterization of the responder cells and synergy with other inducers. J. Exp. Med. *173*, 869-879.

Curtsinger,J.M. and Mescher,M.F. (2010). Inflammatory cytokines as a third signal for T cell activation. Curr. Opin. Immunol *22*, 333-340.

de Brito,C., Tomkowiak,M., Ghittoni,R., Caux,C., Leverrier,Y., and Marvel,J. (2011). CpG promotes cross-presentation of dead cell-associated antigens by pre-CD8alpha+ dendritic dells. J Immunol *186*, 1503-1511.

den Haan,J.M., Lehar,S.M., and Bevan,M.J. (2000). CD8(+) but not CD8(-) dendritic cells cross-prime cytotoxic T cells in vivo. J Exp. Med. *192*, 1685-1696.

Dunay,I.R., Damatta,R.A., Fux,B., Presti,R., Greco,S., Colonna,M., and Sibley,L.D. (2008). Gr1(+) inflammatory monocytes are required for mucosal resistance to the pathogen Toxoplasma gondii. Immunity *29*, 306-317.

Dunay,I.R., Fuchs,A., and Sibley,L.D. (2010). Inflammatory monocytes but not neutrophils are necessary to control infection with Toxoplasma gondii in mice. Infect. Immun. *78*, 1564-1570.

Edelson,B.T., Wumesh,K.C., Juang,R., Kohyama,M., Benoit,L.A., Klekotka,P.A., Moon,C., Albring,J.C., Ise,W., Michael,D.G., Bhattacharya,D., Stappenbeck,T.S., Holtzman,M.J., Sung,S.S.J., Murphy,T.L., Hildner,K., and Murphy,K.M. (2010). Peripheral CD103(+) dendritic cells form a unified subset developmentally related to CD8 alpha(+) conventional dendritic cells. J. Exp. Med. *207*, 823-836.

Frickel,E.M., Sahoo,N., Hopp,J., Gubbels,M.J., Craver,M.P., Knoll,L.J., Ploegh,H.L., and Grotenbreg,G.M. (2008). Parasite stage-specific recognition of endogenous Toxoplasma gondii-derived CD8+ T cell epitopes. J Infect. Dis. *198*, 1625-1633.

Fujigaki,S., Saito,K., Takemura,M., Maekawa,N., Yamada,Y., Wada,H., and Seishima,M. (2002). L-tryptophan-L-kynurenine pathway metabolism accelerated by Toxoplasma gondii infection is abolished in gamma interferon-gene-deficient mice: cross-regulation between inducible nitric oxide synthase and indoleamine-2,3-dioxygenase. Infect. Immun. *70*, 779-786.

Gazzinelli,R.T., Hieny,S., Wynn,T.A., Wolf,S., and Sher,A. (1993). Interleukin 12 is required for the T-lymphocyte-independent induction of interferon gamma by an intracellular parasite and induces resistance in T-cell-deficient hosts. Proc. Natl. Acad. Sci U. S A *90*, 6115-6119.

Gazzinelli,R.T., Wysocka,M., Hayashi,S., Denkers,E.Y., Hieny,S., Caspar,P., Trinchieri,G., and Sher,A. (1994). Parasite-induced IL-12 stimulates early IFN-gamma synthesis and resistance during acute infection with Toxoplasma gondii. J Immunol *153*, 2533-2543.

Goldszmid,R.S., Bafica,A., Jankovic,D., Feng,C.G., Caspar,P., Winkler-Pickett,R., Trinchieri,G., and Sher,A. (2007). TAP-1 indirectly regulates CD4+ T cell priming in Toxoplasma gondii infection by controlling NK cell IFN-gamma production. J Exp. Med. *204*, 2591-2602.

Goldszmid,R.S., Coppens,I., Lev,A., Caspar,P., Mellman,I., and Sher,A. (2009). Host ER-parasitophorous vacuole interaction provides a route of entry for antigen cross-presentation in Toxoplasma gondii-infected dendritic cells. J Exp. Med. *206*, 399-410.

Grohmann,U., Belladonna,M.L., Bianchi,R., Orabona,C., Ayroldi, Fioretti,M.C., and Puccetti,P. (1998). IL-12 acts directly on DC to promote nuclear localization of NF-kappaB and primes DC for IL-12 production. Immunity *9*, 315-323.

Harris,D.P., Goodrich,S., Gerth,A.J., Peng,S.L., and Lund,F.E. (2005). Regulation of IFN-gamma production by B effector 1 cells: essential roles for T-bet and the IFN-gamma receptor. J Immunol *174*, 6781-6790.

Hildner,K., Edelson,B.T., Purtha,W.E., Diamond,M., Matsushita,H., Kohyama,M., Calderon,B., Schraml,B.U., Unanue,E.R., Diamond,M.S., Schreiber,R.D., Murphy,T.L., and Murphy,K.M. (2008). Batf3 deficiency reveals a critical role for CD8alpha+ dendritic cells in cytotoxic T cell immunity. Science *322*, 1097-1100.

Hogquist,K.A., Jameson,S.C., Heath,W.R., Howard,J.L., Bevan,M.J., and Carbone,F.R. (1994). T cell receptor antagonist peptides induce positive selection. Cell *76*, 17-27.

Hou,B., Benson,A., Kuzmich,L., DeFranco,A.L., and Yarovinsky,F. (2011). Critical coordination of innate immune defense against Toxoplasma gondii by dendritic cells responding via their Toll-like receptors. Proc. Natl. Acad. Sci U. S A *108*, 278-283.

Hsieh,C.S., Macatonia,S.E., Tripp,C.S., Wolf,S.F., O'Garra,A., and Murphy,K.M. (1993). Development of TH1 CD4+ T cells through IL-12 produced by Listeria-induced macrophages. Science *260*, 547-549.

Huang,A.Y., Golumbek,P., Ahmadzadeh,M., Jaffee,E., Pardoll,D., and Levitsky,H. (1994). Role of bone marrow-derived cells in presenting MHC class I-restricted tumor antigens. Science *264*, 961-965.

Hunn,J.P., Feng,C.G., Sher,A., and Howard,J.C. (2010). The immunity-related GTPases in mammals: a fast-evolving cell-autonomous resistance system against intracellular pathogens. Mamm. Genome *22*, 43-54.

Hunter,C.A., Subauste,C.S., Van Cleave,V.H., and Remington,J.S. (1994). Production of gamma interferon by natural killer cells from Toxoplasma gondii-infected SCID mice: regulation by interleukin-10, interleukin-12, and tumor necrosis factor alpha. Infect. Immun. *62*, 2818-2824.

Inaba,K., Inaba,M., Romani,N., Aya,H., Deguchi,M., Ikehara,S., Muramatsu,S., and Steinman,R.M. (1992). Generation of large numbers of dendritic cells from mouse bone marrow cultures supplemented with granulocyte/macrophage colony-stimulating factor. J Exp. Med. *176*, 1693-1702.

Ise,W., Kohyama,M., Schraml,B.U., Zhang,T., Schwer,B., Basu,U., Alt,F.W., Tang,J., Oltz,E.M., Murphy,T.L., and Murphy,K.M. (2011). The transcription factor BATF controls the global regulators of class-switch recombination in both B cells and T cells. Nat Immunol *12*, 536-543.

Kamath,A.T., Henri,S., Battye,F., Tough,D.F., and Shortman,K. (2002). Developmental kinetics and lifespan of dendritic cells in mouse lymphoid organs. Blood *100*, 1734-1741.

Kamath,A.T., Pooley,J., O'Keeffe,M.A., Vremec,D., Zhan,Y., Lew,A.M., D'Amico,A., Wu,L., Tough,D.F., and Shortman,K. (2000). The development, maturation, and turnover rate of mouse spleen dendritic cell populations. J. Immunol. *165*, 6762-6770.

Kobayashi,M., Fitz,L., Ryan,M., Hewick,R.M., Clark,S.C., Chan,S., Loudon,R., Sherman,F., Perussia,B., and Trinchieri,G. (1989). Identification and purification of natural killer cell stimulatory factor (NKSF), a cytokine with multiple biologic effects on human lymphocytes. J Exp. Med. *170*, 827-845.

Laliberte,J. and Carruthers,V.B. (2008). Host cell manipulation by the human pathogen Toxoplasma gondii. Cell Mol Life Sci *65*, 1900-1915.

Lertmemongkolchai,G., Cai,G., Hunter,C.A., and Bancroft,G.J. (2001). Bystander activation of CD8+ T cells contributes to the rapid production of IFN-gamma in response to bacterial pathogens. J Immunol *166*, 1097-1105.

Lieberman,L.A., Cardillo,F., Owyang,A.M., Rennick,D.M., Cua,D.J., Kastelein,R.A., and Hunter,C.A. (2004). IL-23 provides a limited mechanism of resistance to acute toxoplasmosis in the absence of IL-12. J Immunol *173*, 1887-1893.

Lin,M.L., Zhan,Y., Villadangos,J.A., and Lew,A.M. (2008). The cell biology of cross-presentation and the role of dendritic cell subsets. Immunol Cell Biol. *86*, 353-362.

Liu,C.H., Fan,Y.T., Dias,A., Esper,L., Corn,R.A., Bafica,A., Machado,F.S., and Aliberti,J. (2006). Cutting edge: dendritic cells are essential for in vivo IL-12 production and development of resistance against Toxoplasma gondii infection in mice. J Immunol *177*, 31-35.

Lybarger,L., Yu,Y.Y., Miley,M.J., Fremont,D.H., Myers,N., Primeau,T., Truscott,S.M., Connolly,J.M., and Hansen,T.H. (2003). Enhanced immune presentation of a single-chain major histocompatibility complex class I molecule engineered to optimize linkage of a C-terminally extended peptide. J Biol. Chem. *278*, 27105-27111.

Ma,X., Chow,J.M., Gri,G., Carra,G., Gerosa,F., Wolf,S.F., Dzialo,R., and Trinchieri,G. (1996). The interleukin 12 p40 gene promoter is primed by interferon gamma in monocytic cells. J. Exp. Med. *183*, 147-157.

Ma,X. and Trinchieri,G. (2001). Regulation of interleukin-12 production in antigen-presenting cells. Adv. Immunol *79*, 55-92.

Mombaerts,P., Iacomini,J., Johnson,R.S., Herrup,K., Tonegawa,S., and Papaioannou,V.E. (1992). RAG-1-deficient mice have no mature B and T lymphocytes. Cell *68*, 869-877.

Mordue,D.G. and Sibley,L.D. (2003). A novel population of Gr-1+-activated macrophages induced during acute toxoplasmosis. J Leukoc. Biol *74*, 1015-1025.

Munder,M., Mallo,M., Eichmann,K., and Modolell,M. (1998). Murine Macrophages Secrete Interferon gamma upon Combined Stimulation with Interleukin (IL)-12 and IL-18: A Novel Pathway of Autocrine Macrophage Activation. J. Exp. Med. *187*, 2103-2108.

Nagineni,C.N., Pardhasaradhi,K., Martins,M.C., Detrick,B., and Hooks,J.J. (1996). Mechanisms of interferon-induced inhibition of Toxoplasma gondii replication in human retinal pigment epithelial cells. Infect. Immun. *64*, 4188-4196.

Naik,S.H., Metcalf,D., van Nieuwenhuijze,A., Wicks,I., Wu,L., O'Keeffe,M., and Shortman,K. (2006). Intrasplenic steady-state dendritic cell precursors that are distinct from monocytes. Nat Immunol *7*, 663-671.

Naik,S.H., Proietto,A.I., Wilson,N.S., Dakic,A., Schnorrer,P., Fuchsberger,M., Lahoud,M.H., O'Keeffe,M., Shao,Q.X., Chen,W.F., Villadangos,J.A., Shortman,K., and Wu,L. (2005). Cutting edge: generation of splenic CD8+ and CD8- dendritic cell equivalents in Fms-like tyrosine kinase 3 ligand bone marrow cultures. J Immunol *174*, 6592-6597.

Norbury,C.C., Chambers,B.J., Prescott,A.R., Ljunggren,H.G., and Watts,C. (1997). Constitutive macropinocytosis allows TAP-dependent major histocompatibility complex class I presentation of exogenous soluble antigen by bone marrow-derived dendritic cells. Eur. J Immunol *27*, 280-288.

Ohteki,T., Fukao,T., Suzue,K., Maki,C., Ito,M., Nakamura,M., and Koyasu,S. (1999). Interleukin 12-dependent interferon gamma production by CD8alpha+ lymphoid dendritic cells. J Exp. Med. *189*, 1981-1986.

Pepper,M., Dzierszinski,F., Wilson,E., Tait,E., Fang,Q., Yarovinsky,F., Laufer,T.M., Roos,D., and Hunter,C.A. (2008). Plasmacytoid dendritic cells are activated by Toxoplasma gondii to present antigen and produce cytokines. J Immunol *180*, 6229-6236.

Pfefferkorn,E.R. (1984). Interferon gamma blocks the growth of Toxoplasma gondii in human fibroblasts by inducing the host cells to degrade tryptophan. Proc. Natl. Acad. Sci U. S A *81*, 908-912.

Pifer,R. and Yarovinsky,F. (2011). Innate responses to Toxoplasma gondii in mice and humans. Trends Parasitol. *27*, 388-393.

Probst,H.C., Tschannen,K., Odermatt,B., Schwendener,R., Zinkernagel,R.M., and Van Den,B.M. (2005). Histological analysis of CD11c-DTR/GFP mice after in vivo depletion of dendritic cells. Clin. Exp. Immunol *141*, 398-404.

Puddu,P., Fantuzzi,L., Borghi,P., Varano,B., Rainaldi,G., Guillemard,E., Malorni,W., Nicaise,P., Wolf,S.F., Belardelli,F., and Gessani,S. (1997). IL-12 induces IFN-gamma expression and secretion in mouse peritoneal macrophages. J Immunol *159*, 3490-3497.

Reis e Sousa,C., Hieny,S., Scharton-Kersten,T., Jankovic,D., Charest,H., Germain, RN, and Sher,A. (1997). In vivo microbial stimulation induces rapid CD40 ligand-independent production of interleukin 12 by dendritic cells and their redistribution to T cell areas [see comments]. J. Exp. Med. *186*, 1819-1829.

Robben,P.M., Mordue,D.G., Truscott,S.M., Takeda,K., Akira,S., and Sibley,L.D. (2004). Production of IL-12 by macrophages infected with Toxoplasma gondii depends on the parasite genotype. J Immunol *172*, 3686-3694.

Saeij,J.P., Boyle,J.P., Grigg,M.E., Arrizabalaga,G., and Boothroyd,J.C. (2005). Bioluminescence imaging of Toxoplasma gondii infection in living mice reveals dramatic differences between strains. Infect. Immun. *73*, 695-702.

Sancho,D., Joffre,O.P., Keller,A.M., Rogers,N.C., Martinez,D., Hernanz-Falcon,P., Rosewell,I., and Reis E Sousa (2009). Identification of a dendritic cell receptor that couples sensing of necrosis to immunity. Nature *458*, 899-903.

Sathe,P., Pooley,J., Vremec,D., Mintern,J., Jin,J.O., Wu,L., Kwak,J.Y., Villadangos,J.A., and Shortman,K. (2011). The acquisition of antigen cross-presentation function by newly formed dendritic cells. J Immunol *186*, 5184-5192.

Satpathy, A., Murphy, K. M., and KC, W. (2011). Transcription Factor Networks in Dendritic Cell Development. Seminars in Immunology *23*, 388-397.

Sayles,P.C. and Johnson,L.L. (1996). Exacerbation of toxoplasmosis in neutrophil-depleted mice. Nat Immun. *15*, 249-258.

Scanga,C.A., Aliberti,J., Jankovic,D., Tilloy,F., Bennouna,S., Denkers,E.Y., Medzhitov,R., and Sher,A. (2002). Cutting edge: MyD88 is required for resistance to Toxoplasma gondii infection and regulates parasite-induced IL-12 production by dendritic cells. J Immunol *168*, 5997-6001.

Scharton-Kersten,T., Contursi,C., Masumi,A., Sher,A., and Ozato,K. (1997a). Interferon consensus sequence binding protein-deficient mice display impaired resistance to intracellular infection due to a primary defect in interleukin 12 p40 induction. J Exp. Med. *186*, 1523-1534.

Scharton-Kersten,T.M., Wynn,T.A., Denkers,E.Y., Bala,S., Grunvald,E., Hieny,S., Gazzinelli,R.T., and Sher,A. (1996). In the absence of endogenous IFN-gamma, mice develop unimpaired IL-12 responses to Toxoplasma gondii while failing to control acute infection. J Immunol *157*, 4045-4054.

Scharton-Kersten,T.M., Yap,G., Magram,J., and Sher,A. (1997b). Inducible nitric oxide is essential for host control of persistent but not acute infection with the intracellular pathogen Toxoplasma gondii. J Exp. Med. *185*, 1261-1273.

Schiavoni,G., Mattei,F., Borghi,P., Sestili,P., Venditti,M., Morse,H.C., III, Belardelli,F., and Gabriele,L. (2004). ICSBP is critically involved in the normal development and trafficking of Langerhans cells and dermal dendritic cells. Blood *103*, 2221-2228.

Schiavoni,G., Mattei,F., Sestili,P., Borghi,P., Venditti,M., Morse,H.C., III, Belardelli,F., and Gabriele,L. (2002). ICSBP is essential for the development of mouse type I interferon-producing cells and for the generation and activation of CD8alpha(+) dendritic cells. J Exp. Med. *196*, 1415-1425.

Schraml,B.U., Hildner,K., Ise,W., Lee,W.L., Smith,W.A., Solomon,B., Sahota,G., Sim,J., Mukasa,R., Cemerski,S., Hatton,R.D., Stormo,G.D., Weaver,C.T., Russell,J.H., Murphy,T.L., and Murphy,K.M. (2009). The AP-1 transcription factor Batf controls T(H)17 differentiation. Nature *460*, 405-409.

Serbina,N.V. and Pamer,E.G. (2006). Monocyte emigration from bone marrow during bacterial infection requires signals mediated by chemokine receptor CCR2. Nat Immunol *7*, 311-317.

Takemoto,N., Intlekofer,A.M., Northrup,J.T., Wherry,E.J., and Reiner,S.L. (2006). Cutting Edge: IL-12 inversely regulates T-bet and eomesodermin expression during pathogen-induced CD8+ T cell differentiation. J Immunol *177*, 7515-7519.

Tamura,T. and Ozato,K. (2002). ICSBP/IRF-8: its regulatory roles in the development of myeloid cells. J Interferon Cytokine Res *22*, 145-152.

Taylor,G.A., Collazo,C.M., Yap,G.S., Nguyen,K., Gregorio,T.A., Taylor,L.S., Eagleson,B., Secrest,L., Southon,E.A., Reid,S.W., Tessarollo,L., Bray,M., McVicar,D.W., Komschlies,K.L., Young,H.A., Biron,C.A., Sher,A., and Vande Woude,G.F. (2000). Pathogen-specific loss of host resistance in mice lacking the IFN-gamma-inducible gene IGTP. Proc. Natl. Acad. Sci U. S A *97*, 751-755.

Trinchieri,G. (2003). Interleukin-12 and the regulation of innate resistance and adaptive immunity. Nat Rev Immunol *3*, 133-146.

Tsujimura,H., Tamura,T., and Ozato,K. (2003). Cutting edge: IFN consensus sequence binding protein/IFN regulatory factor 8 drives the development of type I IFN-producing plasmacytoid dendritic cells. J Immunol *170*, 1131-1135.

Uhlig,H.H., McKenzie,B.S., Hue,S., Thompson,C., Joyce-Shaikh,B., Stepankova,R., Robinson,N., Buonocore,S., Tlaskalova-Hogenova,H., Cua,D.J., and Powrie,F. (2006). Differential activity of IL-12 and IL-23 in mucosal and systemic innate immune pathology. Immunity *25*, 309-318.

Villadangos,J.A. and Schnorrer,P. (2007). Intrinsic and cooperative antigen-presenting functions of dendritic-cell subsets in vivo. Nat Rev Immunol *7*, 543-555.

Vyas,J.M., Van der Veen,A.G., and Ploegh,H.L. (2008). The known unknowns of antigen processing and presentation. Nat Rev Immunol *8*, 607-618.

Xu,Y.K., Zhan,Y.F., Lew,A.M., Naik,S.H., and Kershaw,M.H. (2007). Differential development of murine dendritic cells by GM-CSF versus flt3 ligand has implications for inflammation and trafficking. J. Immunol. *179*, 7577-7584.

Yap,G.S., Shaw,M.H., Ling,Y., and Sher,A. (2006). Genetic analysis of host resistance to intracellular pathogens: lessons from studies of Toxoplasma gondii infection. Microbes Infect. *8*, 1174-1178.

Yarovinsky,F., Zhang,D., Andersen,J.F., Bannenberg,G.L., Serhan,C.N., Hayden,M.S., Hieny,S., Sutterwala,F.S., Flavell,R.A., Ghosh,S., and Sher,A. (2005). TLR11 activation of dendritic cells by a protozoan profilin-like protein. Science *308*, 1626-1629.

Zhao,Y.O., Rohde,C., Lilue,J.T., Konen-Waisman,S., Khaminets,A., Hunn,J.P., and Howard,J.C. (2009). Toxoplasma gondii and the Immunity-Related GTPase (IRG) resistance system in mice: a review. Mem. Inst. Oswaldo Cruz *104*, 234-240.